UCRL 10032

University of California

Ernest O. Lawrence Radiation Laboratory

BIO-ORGANIC CHEMISTRY QUARTERLY REPORT

September through November 1961

TWO-WEEK LOAN COPY

This is a Library Circulating Copy which may be borrowed for two weeks. For a personal retention copy, call Tech. Info. Division, Ext. 5545

DISCLAIMER

This document was prepared as an account of work sponsored by the United States Government. While this document is believed to contain correct information, neither the United States Government nor any agency thereof, nor the Regents of the University of California, nor any of their employees, makes any warranty, express or implied, or assumes any legal responsibility for the accuracy, completeness, or usefulness of any information, apparatus, product, or process disclosed, or represents that its use would not infringe privately owned rights. Reference herein to any specific commercial product, process, or service by its trade name, trademark, manufacturer, or otherwise, does not necessarily constitute or imply its endorsement, recommendation, or favoring by the United States Government or any agency thereof, or the Regents of the University of California. The views and opinions of authors expressed herein do not necessarily state or reflect those of the United States Government or any agency thereof or the Regents of the University of California.

UCRL-10032
UC-4 Chemistry
TID-4500(17th Ed.)

UNIVERSITY OF CALIFORNIA
Lawrence Radiation Laboratory
Berkeley, California

Contract No. W-7405-eng-48

BIO-ORGANIC CHEMISTRY QUARTERLY REPORT

September through November 1961

January 25, 1962

Printed in USA. Price $2.50. Available from the
Office of Technical Services
U. S. Department of Commerce
Washington 25, D.C.

BIO-ORGANIC CHEMISTRY QUARTERLY REPORT

September through November 1961

Contents

1. Molecular Orientation in Quantasomes. I. Electric Dichroism and Electric Birefringence of Quantasomes from Spinach Chloroplasts (Sauer) 1

2. Some Measurements of Magneto-Optic Rotatory Dispersion Spectra (Williams and Andores) 32

3. Oxidation States of Manganese Hematoporphyrin IX in Aqueous Solution (Loach) 45

4. Nuclear Magnetic Resonance of the Methyl Esters of the First and Second Row Inorganic Oxyacids (Hammond) 70

5. Some Observations on Rates of Labeling of Intermediates of the Carbon Reduction Cycle during Steady State Photosynthesis with $C^{14}O_2$ (Kirk and Bassham) 78

6. Methyl Phosphate Formation in Mixtures of P^{32}-Phosphate, Methanol, Water, and Sonically Ruptured Spinach Chloroplasts (Ullrich) 82

7. The Chemical Effect of Ionizing Radiation on Cytosine (Ponnamperuma and Lemmon) 90

8. Experiments on Wilzbach Tritium Labeling Accompanied by Charcoal Absorption and Electric Discharge (Chadha, Woeller, and Lemmon) 94

9. Thermal Transients in Ascites Tumor Suspensions (Lonberg-Holm) 102

10. Further Studies of the Effects of Deuterium and Tritium on Drosophila (Hughes) 118

11. Variation in Environmental Complexity and Brain Measures (Bennett, Morimoto, and Hebert) 120

*Preceding Quarterly Reports: UCRL-9900, UCRL-9772

BIO-ORGANIC CHEMISTRY QUARTERLY REPORT

September through November 1961

M. Calvin, Director

Lawrence Radiation Laboratory and Department of Chemistry
University of California, Berkeley, California

January 25, 1962

1. MOLECULAR ORIENTATION IN QUANTASOMES. I. ELECTRIC DICHROISM AND ELECTRIC BIREFRINGENCE OF QUANTASOMES FROM SPINACH CHLOROPLASTS

Kenneth Sauer*

Summary

Quantasomes isolated from spinach chloroplasts have been shown to exhibit both intrinsic electric birefringence (Kerr effect) and intrinsic electric dichroism. Kerr-constant measurements suggest that the birefringence arises primarily from proteins associated with the preparations, although the results are not unambiguous. The smallest particles studied give rise to relaxation times in the range 20 to 200 μsec. The shortest times may be associated with a particle having a permanent dipole moment. The spherical chromatophore subunits from R. rubrum do not exhibit measurable electric birefringence, as measured in the apparatus of this study.

The dichroic ratio spectrum of spinach quantasomes has been determined through electric dichroism measurements. The measured dichroic ratios of 1.05 to 1.10 throughout most of the spectrum suggest that most of the chlorophyll and carotenoid molecules in the quantasome are largely unoriented. A pronounced peak occurs in the dichroic ratio spectrum at 695 to 700 mμ, about 20 mμ to the long-wavelength side of the strong chlorophyll absorption maximum in this region. The dichroic ratio increment is at least 5 times as great at 698 mμ as at 678 mμ.

The dichroism anomaly is interpreted as resulting from a small fraction (5 to 10%) of the chlorophyll a, which is strongly oriented at some site in the quantasome. It is suggested that an oriented cytochrome is present at this site as well. A mechanism is presented whereby electronic energy resulting from the absorption of light by the pigments of the quantasome is converted at the site of the oriented chlorophyll-cytochrome complex to chemical potential associated with electron transport processes.

---

*U. S. Public Health Service Postdoctoral Fellow, 1960-1962.

The orientation of molecular species in macroscopic materials has frequently been demonstrated by observations of optical properties in polarized light. In particular, birefringence, dichroism, and polarization of fluorescence are commonly used for this purpose by the microscopist. In the case of particles or macromolecules too small to be observed directly in the microscope, various techniques have been applied to orient samples artificially. Certain media exist which orient small amounts of added materials into overall structures characteristic of the medium. In such cases microscopic techniques can be applied to the mixture. In addition, gradients resulting from streaming velocity or from an applied electrostatic field can be used on suspensions of particles that possess asymmetry of shape or electric polarization, respectively. These asymmetries may be either intrinsic to the particle or induced by the gradient itself.

Both flow birefringence and, more recently, electric birefringence have been used extensively in the study of macromolecules of biological origin. The corresponding measurements of dichroism of artificially oriented macromolecules have been relatively much less studied, however. This is due, in part, to the less common occurrence of suitable absorption bands on which to make measurements, and to the substantially greater difficulty of making dichroism measurements than of making birefringence measurements. The ultraviolet dichroism of tobacco mosaic virus (TMV) has been measured on a solution streaming through a small capillary by Butenandt et al.,[1] and DNA solutions have been studied by a similar technique by Ruch and Thorell.[2] The flow dichroism in the infrared of poly-(γ-benzyl-D-glutamate) has been reported by Bird and Blout.[3,4] In electric dichroism the only results reported in the literature, other than a few studies of small molecules like p-nitroso-dimethylaniline,[5] have been the recent ones by Dvorkin on calf thyroid DNA[6] and by Dvorkin and Spirin on RNA from TMV.[7] Aside from these few examples, dichroism measurements have been reported only on relatively large crystals, on material mounted on a microscope slide, etc.

In this work electric dichroism has been used to study the degree of orientation of chlorophyll and carotenoid molecules within the pigment-containing structures of spinach chloroplasts. The suggestion that such orientation occurs first received support from the observations of Menke[8] on the large chloroplasts of Closterium moniliferum. Sections of these

[1] A. Butenandt, H. Friedrich-Freska, St. Hartwig, and G. Scheibe, Z. physiol. Chem., Hoppe-Seyler's 274, 276-84 (1942).

[2] F. Ruch and B. Thorell, Nature 167, 815 (1951).

[3] G. R. Bird and E. R. Blout, J. Chem. Phys. 25, 798-9 (1956).

[4] G. R. Bird, J. Chem. Phys. 28, 1155-8 (1958).

[5] W. Kuhn, H. Duhrkop, and H. Martin, Z. physik. Chem. 45B, 121-55 (1939).

[6] G. A. Dvorkin, Doklady Akad. Nauk. S. S. S. R. 135, 739-42 (1960).

[7] G. A. Dvorkin and A. S. Spirin, Doklady Akad. Nauk. S. S. S. R. 135, 987-90 (1960).

[8] W. Menke, Kolloid-Z. 85, 256-9 (1938); W. Menke and H.-J. Küster, Protoplasma 30, 283-90 (1938); W. Menke and E. Koydl, Naturwissenschaften 27, 29-30 (1939).

chloroplasts, mounted on a microscope slide and stained with noble metals, exhibited both birefringence and dichroism when observed with polarized light. The birefringence was shown to consist of a negative form birefringence superimposed on a positive intrinsic birefringence. (See below for descriptions of these effects.) Dichroism was observed both at 681 and at 540 mμ. These observations were taken as evidence that the chloroplast has a lamellar structure, which at the time was not directly observable. Subsequent investigations by Frey-Wyssling and Wuhrmann used the spectral dispersion of the birefringence of Closterium chloroplasts sectioned "in profile" to suggest that the optical retardation in red light corresponds to $\lambda/2$, whereas that in green light is $\lambda/8$.[9] Form birefringence curves arising from protein interleaved with oriented lipoids were reported by Frey-Wyssling and Steinman;[10] the residual intrinsic birefringence was small, however, indicating that the lipoids were at best imperfectly oriented. A spectral dispersion curve was presented for the birefringence of the large, readily observed, grana-free chloroplasts of Mougeotia sp. by Menke and Menke.[11] Goedheer has used the same chloroplasts (Closterium and Mougeotia) in the most detailed study to date of dichroism and birefringence using the microscope.[12, 13] A weak dichroism was observed between 510 and 700 mμ when the cells were under favorable conditions; however, it could not be decided whether this was form dichroism or intrinsic dichroism. With the small, grana-bearing chloroplasts of Funaria or Elodea no dichroism was observed. The dichroism of Mougeotia could be increased approximately five fold by staining with rhodamine B, as had been observed by Menke. In all cases the dichroism observed was positive. As a consequence of his measurements, Goedheer proposed a model in which a probable orientation of the "red oscillator" of chlorophyll in the direction of the lamellae exists, but in which it is improbable that carotenoid molecules are oriented.

The dichroism of Mougeotia chloroplasts in visible and in ultraviolet light has been reported by Ruch.[14] The dichroism in ultraviolet light was observed to be pure form dichroism, indicating that the proteins within the chloroplast lamellae do not possess a preferred orientation. The dichroism in visible light was also shown to be mainly form dichroism by examination of samples permeated with glycerine, which has a refractive index close to that of protein. These results, coupled with the information that the fluorescence emission of mature chloroplasts is almost completely depolarized, led to the conclusion that the chloroplast pigments in the lamellae cannot be oriented.

---

[9] A. Frey-Wyssling and K. Wuhrmann, Helv. Chim. Acta 30, 20-3 (1947).

[10] A. Frey-Wyssling and E. Steinmann, Biochim. et Biophys. Acta 2, 254-9 (1948).

[11] W. Menke and G. Menke, Z. Naturforsch. 106, 416-19 (1955).

[12] J. C. Goedheer, Biochim. et Biophys. Acta 16, 471 (1955).

[13] J. C. Goedheer, Optical Properties and in vivo Orientation of Photosynthetic Pigments (Thesis), Utrecht, 1957.

[14] F. Ruch, Acta Histochem. 4, 193-6 (1957); Exptl. Cell Research, Suppl. 4, 58-63 (1957).

Menke[15] and Goedheer[13] have reported measurements of the dichroism of isolated photosynthetic pigments oriented artificially in ammonium oleate or in a myelin tube of lecithin. The results showed that the oscillators for all the visible and near-infrared absorption bands of chlorophyll a, chlorophyll b, or bacteriochlorophyll lie in the plane of the porphyrin ring. A high degree of orientation was present, as indicated by the observation of dichroic ratios greater than 6. For chlorophyll a it was suggested that the oscillator responsible for the red absorption band is oriented in the direction of the shortest dimension of the conjugated ring system. Similar studies of artificially oriented carotenoids showed their oscillators to lie along the long molecular axes.

Although unanimous agreement of the published results leads to the conclusion that there is no strong intrinsic dichroism of the chloroplast lamellae pigments, the statement that there is no orientation of pigment molecules is still subject to question. Several situations may arise in practice that would give little or no dichroism from a sample with appreciable pigment orientation. The following not unreasonable examples may be cited.

(a) If pigment molecules were perfectly oriented, but were on a spherical rather than a planar surface, every possible orientation would exist and consequently there would be no intrinsic dichroism. Such an orientation would, however, still lead to appreciable orbital overlap, and energy migration might occur readily from one pigment molecule to another. If the chloroplast lamellae then consisted of sheets made up of spherical units, the surfaces of which are uniformly covered with radially oriented pigment molecules, then no intrinsic dichroism would be expected. It is interesting to note here the model based on electron microscopic studies proposed by Park and Pon,[16] in which the lamellae are considered to be made up of sheets of oblate ellipsoids with their short axes normal to the lamellar plane. Ellipsoids uniformly covered with oriented pigment molecules would, of course, be expected to exhibit some intrinsic dichroism.

(b) It is possible to construct a system wherein pigment molecules are oriented in a plane with their absorption oscillators at 45° to the normal to the plane. If the projections of the oscillators onto the plane give rise to a variety of orientations with respect to an arbitrary direction within the plane, then such a system is not expected to exhibit intrinsic dichroism. A model of pigment structure involving four directions for the projection in the plane has been proposed by Wolken.[17]

(c) The theoretical studies of form dichroism by Wiener[18] have shown that it is a complex phenomenon and can give rise to a variety of experimental results. Wiener has shown that because form dichroism arises from the interaction between the real part of the refractive index and the imaginary part--i.e., spectral absorption coefficient-- it is possible to have for a stacked system of alternately pigmented and nonpigmented lamellae either

[15] W. Menke, Biol. Zentr. 63, 326-49 (1943).

[16] R. B. Park and N. G. Pon, J. Mol. Biol. 3, 1-10 (1961).

[17] J. J. Wolken and F. A. Schwertz, J. Gen. Physiol. 37, 111-120 (1953).

[18] O. Wiener, Kolloidchem. Beih. 23, 189-98 (1926).

positive, negative, or zero form dichroism coupled with positive, negative, or zero difference between the real refractive indices of the two kinds of lamellae. Thus, for those experiments in which chloroplasts were artifically imbedded in a liquid with the same refractive index as protein,[13, 14] in an effort to remove the contribution of form dichroism, it is possible that a form dichroism still existed and may have served to cancel any intrinsic dichroism present. Although this is not held to be a likely occurrence, it is still a possibility to be considered.

In order to remove the consequences of form dichroism from the measurements, the study presented here was undertaken on sonicated chloroplast material in which no grana or other regions of parallel lamellae exist. In fact, for most of the results to be reported here, the sample, as seen in the electron microscope, consisted of aggregates of three to eight of the fundamental particles, or quantasomes,[19] of which the lamellae are made. Since the quantasomes are ellipsoids with major and minor axes of 200 and 100 A, respectively, the particles in this study are disks roughly 500 A in diameter and 100 A thick. There is no evidence for the presence of stacked sheets among these particles; consequently no form dichroism, at least of the type noted previously, can result. Since these small particles are geometrically asymmetric, it is possible in principle to orient them in a velocity or flow gradient. This study shows that they can be oriented by an electric field as well.

Experimental Procedure

Apparatus

Electric birefringence and electric dichroism were studied by means of an apparatus similar to that of O' Konski and Haltner.[20] A schematic diagram of the apparatus is shown in Fig. 1-1. The optical system is designed to produce high-intensity monochromatic light of variable wavelength and relatively high collimation. A 500-watt tungsten projection lamp (General Electric, Type CZX) for measurements in the visible, near-ultraviolet, and near-infrared regions of the spectrum, was powered by a regulated dc supply. It was necessary to remove all the 60-cycle component from the lamp emission. The power supply used accomplished this to better than 1 part in 10,000. The light was focused by an achromatic lens system (L_1) onto the inlet slit of a grating monochromator (Bausch & Lomb, Model 33-86-45-01). The adjustable slits of the monochromator provided wavelength band halfwidths of 3.5 to 7.0 mμ used in this study. A second achromatic lens train (L_2) was used to collimate the monochromatic light emerging from the exit slit. The light was then polarized by means of a rotatable Glan-Thompson prism (P) of 1 cm aperture (Crystal Optics, Chicago, Illinois), and impinged on an adjustable slit (S) in the end of a lighttight box containing the Kerr cell (C) in a first compartment and the photomultiplier in a second.

The Kerr cell assembly used was of the type described by Pytkowicz and O' Konski.[21] All the studies to be reported here were performed using

[19] R. B. Park, Advances in Photosynthesis, J. Chem. Educ. (in press, 1962).

[20] C. T. O' Konski and A. J. Haltner, J. Am. Chem. Soc. 78, 3604-10 (1956).

[21] R. M. Pytkowicz and C. T. O' Konski, Biochim. et Biophys. Acta 36, 466-70 (1959).

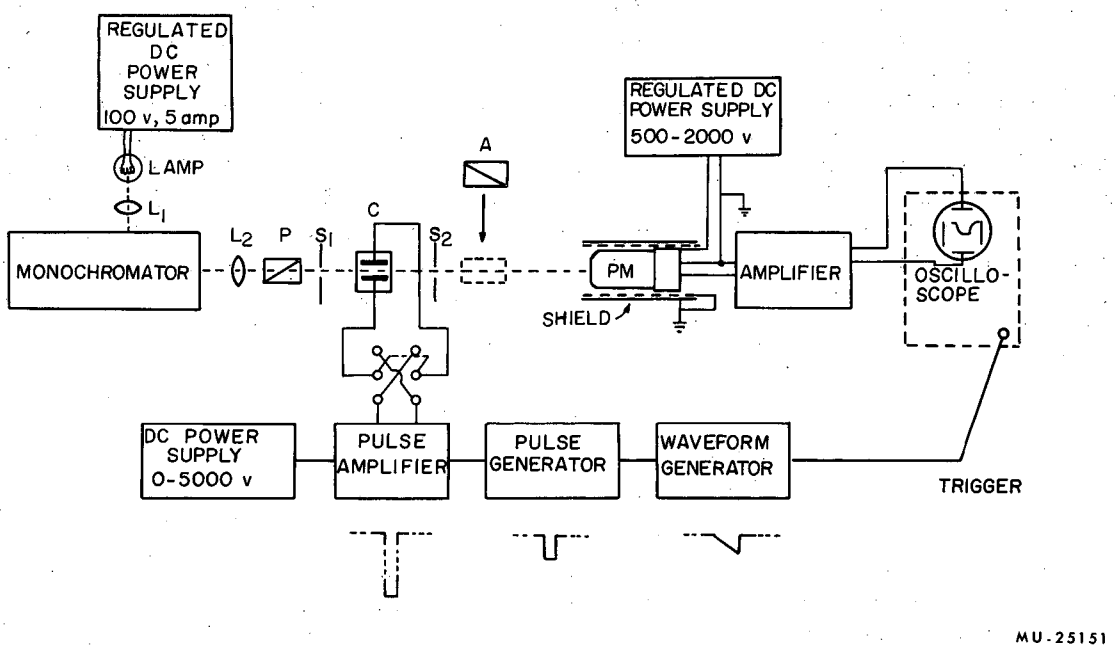

Fig. 1-1. Electric dichroism and birefringence apparatus--schematic diagram of optical and electrical components.

an assembly constructed from fluorethene and teflon. The electrodes were rectangles (1×2.2 cm) cut from 1.5-mm-thick gold plate. They were rigidly held parallel to one another and spaced 3.5 mm apart. Gold wire electrical leads were spot-welded to the tops of the plates and were run out to separate pin-jack connectors mounted on the top of the assembly. The gold electrodes and associated fluorethene spacer fitted snugly inside a standard 1-cm square-cross-section spectrophotometer cuvette. The cuvette, which had four polished transparent sides, was masked on the outside with black tape to define a beam width of 2.5 mm, in order that no interference should result from reflection from the electrodes.

The entrance and exit slits to the cell compartment were used to define a beam of rectangular cross section, approximately 3×9 mm. This served to reduce the effects of unwanted scattered radiation. When birefringence measurements were being made, the beam emerging from the second slit passed through a second Glan-Thompson prism (A) crossed to the First, whereas for dichroism measurements only the first polarizer was in the beam. The final transmitted light intensity was measured by a photomultiplier with a fast-response circuit. Du Mont photomultipliers with flat, 2-in.-diameter end windows were used; tests showed that their sensitivities were independent of the angle of orientation of the incident polarized light. Such is, in general, not the case with side-window or other curved photosurface detectors. The following Du Mont tubes were used: K1292 or 6911 in the red, 6292 in the blue, and 7664 in the ultraviolet. The photomultiplier and its base circuit were mounted inside grounded, coaxial cylinders of mu metal and iron. Without this shield the electrical pickup from the high-voltage Kerr-cell pulse seriously interfered with the measurements. Several base circuits with response time-constants ranging from 2×10^{-4} to 5×10^{-7} sec were used, depending on whether high signal/noise or the accurate measurement of relaxation times was desired from a particular measurement. The detection circuit was completed with a Tektronix Type D or Type Z amplifier associated with a RM35 oscilloscope. The oscilloscope traces were photographed with a Polaroid Land camera.

The square voltage pulse applied to the Kerr cell was initiated manually from a Tektronix Type 162 Waveform Generator coupled with a Type 161 Pulse Generator. The 50-volt output pulse was amplified to a predetermined level, up to 5 kv, by a suitable pulse amplifier, and the amplified square pulse was applied to the Kerr-cell electrodes. A reversing switch was included so that the polarity of the pulse could be changed for alternate measurements. This served to reduce the effects of electrical polarization of the sample being studied. Single pulses of 0.1 to 2 msec duration were used in this study. The Waveform Generator also provided a pulse to trigger the sweep of the oscilloscope, and the Pulse Generator introduced a variable delay into the Kerr-cell pulse in order that a part of the oscilloscope trace preceding the electric pulse could be recorded for each measurement.

Materials

Spinach quantasomes (chloroplast lamellae fragments) were prepared essentially by the procedure of Park and Pon.[16] Chloroplasts isolated from homogenates of spinach leaves were sonically ruptured at 9 kc for 90 sec. The sonicated suspension was centrifuged at 145,000 g for 20 min, giving

rise to a final supernatant containing small aggregates of quantasomes, soluble proteins, and other metabolites, and a precipitate containing larger sheets of quantasomes. The latter was resuspended in deionized water for the electrooptical studies, whereas the former was simply diluted with water to the appropriate optical density. In all cases the final concentration of added electrolytes--i.e., phosphate buffer at pH 7.4--was kept below 10^{-4} M so as to keep the conductivity of the solutions low. In this way the effects due to heating, denaturation of the biological material, formation of gas bubbles on the Kerr cell electrodes, etc. were kept to a minimum.

Chromatophores of Rhodospirillum rubrum were prepared by sonication of a suspension of the bacteria in glycyl glycine buffer, followed by ultracentrifugation to obtain a fraction containing the 100-A-diameter chromatophore subunits.

Nitrobenzene (Eastman 387) was used without additional purification.

Spectra were recorded on a Cary Model 11 or Model 14 spectrophotometer. In all cases the samples were observed to give rise to negligible light scattering. Detailed studies of the spectra of spinach quantasomes were given in a previous report.[22]

Operations

Samples were prepared so that the absorbance was between 0.1 and 0.5 in the region of the spectrum to be studied. In general, measurements were made on the photosynthetic material during the first 8 hours after the preparation, during which time the suspensions were kept in the dark at 0° C. In several cases to be noted in the text, measurements were made on suspensions stored at 5° C for 24 hours or for periods up to 3 weeks. The individual samples were placed in the Kerr cell, and measurements were carried out at room temperature without thermostating.

The magnitude of the electric birefringence or electric dichroism was determined from the amplitude of the change in the photomultiplier signal consequent upon the electric field pulse. The actual values were taken from the photographs of the oscilloscope traces. Decay times were determined by using a fast-response photomultiplier circuit and by replotting on a semilogarithmic basis points taken from the appropriate trace photographs.

Dichroism spectrum measurements were made from a series of measurements on a single sample at different monochromator settings. Wherever possible this was done in such a way as to achieve maximum signal-to-noise ratio. Since nearly all the noise came from the shot effect associated with the emission of photons from the light source, best results were obtained with as high as possible an intensity incident on the photomultiplier; however, care was taken to remain well below intensities that would lead to saturation of the photomultipliers or nonlinear response of the associated circuitry. By use of sufficient measuring-beam intensity, controlled by the position of a wedge stop at the monchromator slit, to give a 4-volt output signal from a

[22] K. Sauer, in Bio-Organic Quarterly Report, UCRL-9900, Oct. 1961, p.1-11.

photomultiplier circuit with 0 to 10 kc band width and 600 v dc applied voltage, a signal/noise ratio of 4000 could be obtained. Often, however, in spectral regions of strong sample absorption, or with low source emission or low detector sensitivity, the signal/noise ratio was considerably less than this. In such cases the wedge was pulled out and the photomultiplier applied voltage raised to as much as 1300 v in order to get an initial measuring-beam signal of 4 v, wherever possible. An excellent discussion of the problems associated with source noise in a system similar to this is given by Witt, Moraw, and Müller.[23]

The considerable labor involved in making point-by-point measurements of the dichroism spectrum was somewhat reduced by taking a series of measurements on the same sample. The effects giving rise to denaturation of the sample are cumulative; however, it was found that reliable results could be obtained with up to 200 pulses of millisecond duration and 6000 volts/cm voltage gradient. At the end of such a series the sample was slightly cloudy. At higher voltage gradients fewer pulses could be applied before denaturation of the sample began to cause irreproducible results. In all cases, the order of measurements for a dichroism spectrum was staggered with respect to wavelength in such a way as to make obvious any consequences of sample decomposition.

Theoretical Considerations

The various effects observed in this study are the result of optical anisotropies consequent upon the orientation of the particles being studied with respect to some space-fixed axes. In birefringence, the anisotropy occurs in the refractive index of the system. If a system is birefringent it has a different refractive index, and consequently a different velocity of light, parallel to an orienting gradient (electric field, velocity, etc.) from that perpendicular to the gradient. The birefringence is defined as $\Delta n = n_{\parallel} - n_{\perp}$, and can have either a positive or a negative sign depending on the relative magnitudes of the two refractive indices. For solids the sign of the birefringence is determined with respect to a given crystal axis, the unique axis of an ellipsoid, etc. For samples mounted on a microscope slide reference is made to some structural feature of the material; e.g., a direction in the planes of lamallae. It is necessary for the measurement that the orienting gradient, crystal axis, etc. of interest be normal to the optic axis of the observation.

Dichroism occurs when the absorption coefficient at a given wavelength is different in directions parallel to or perpendicular to the orienting gradient, crystal axis, structural element, etc. The dichroic ratio D is defined as the direct ratio of the absorbances

$$D = A_{\parallel} / A_{\perp} \qquad (1)$$

when this is greater than unity, and as the reciprocal with a negative sign when the absorbance in the perpendicular direction is the greater.

[23] H. T. Witt, R. Moraw, and A. Müller, Z. physik. Chem. (Frankfurt) 20, 193-205 (1959).

Both the birefringence and the dichroism of materials can be measured with polarized light. The latter phenomenon occurs only in spectral regions where the substance absorbs; however, the former may be present in transparent regions as well.

For dichroism measurements it is usually sufficient to place in the optical path a polarizer which orients the electric vector of the light parallel to or perpendicular to the orienting gradient, and to measure the absorption of the radiation in each case. The dichroic ratio is then just the ratio of the two measured absorbances.

For birefringence two polarizers are used. In general, the first, or polarizing, element is placed between the light source and the sample, and its axis of polarization is oriented at 45° to the field vector. If the polarized radiation is then considered to be the resultant of two electric vector components oriented at 0° and at 90° to the system axis, the birefringence may be thought of as the consequence of the fact that these two radiation components travel at independent velocities through the sample. If the sample is not birefringent the two normal components travel at the same velocity therefore remain in phase with each other. The resultant is always plane-polarized or linearly polarized light. If the second polarizing element, the analyzer, is placed between the sample and the viewer and is oriented at 90° (crossed) with respect to the first, then no light is observed for the non-birefringent sample. If the sample is birefringent, on the other hand, the two vectors travel at different velocities through it and the phase of one is advanced with respect to that of the other. The emergent light is, in general, elliptically polarized and now has a component in the direction of the optic axis of the analyzer. The intensity of this light is related to the path length through the sample and to the magnitude of its birefringence. It should be noted that the production of circularly polarized light and of linearly polarized light by a phase advance of $n\pi$ radians by a birefringent specimen are merely special cases of the above result.

A number of general discussions of birefringence, dichroism, and related phenomena are in the literature.[24-27] Furthermore, the principles discussed here apply to the ultraviolet, the infrared, and other regions of the radiation spectrum as well as to the visible. A number of observations of phenomena in these other regions have been reported.

In many cases dichroism or birefringence in a system is a direct consequence of spatial orientation at the molecular level--what is frequently

---

[24] H. A. Scheraga and R. Signer, in Technique of Organic Chemistry, Vol. I, part 3, Physical Methods of Organic Chemistry, 3rd Edition, A. Weissberger, Editor (Interscience Publishers, Inc., New York, 1960), pp. 2387-2457.

[25] C. G. LeFèvre and R. J. W. LeFèvre, ibid., pp. 2459-2496.

[26] G. Oster, in Physical Techniques in Biological Research, G. Oster and A. W. Pollister, Editors (Academic Press, Inc., New York, 1955) pp. 439-60.

[27] W. E. Seeds, Progr. in Biophys. and Biophys. Chem. 3, 27 (1953).

referred to as the secondary structure. If the molecular unit responsible for an absorption band is not totally symmetric, then, in general, the oscillator responsible for the absorption has one or more fixed orientations with respect to a molecule-fixed coordinate system. If the sample is illuminated with polarized light such that the direction of its electric vector coincides with that of the absorption oscillator, absorption occurs. On the other hand, if the polarizer axis is rotated 90° to the absorption oscillator, no absorption results. It is readily seen that in a sample of randomly oriented absorption oscillators, an average absorption occurs which is independent of polarizer orientation. Such a sample, of course, is not dichroic. In real systems one frequently encounters overlapping absorption bands arising from oscillators oriented in different directions; or--particularly in polymers with secondary structure or when studying vibrational transitions in the infrared--a single absorption band may arise from oscillators with a number of fixed orientations within the system. These samples, in general, exhibit some dichroism, however. Thus there is frequently found to be a relationship between the presence of dichroism and the existence of regular ordering of molecules or monomeric units. Similar conclusions can often be drawn from the observation of birefringence in a material; however, the derivation of the relationship is somewhat more involved.

Situations may arise, particularly in systems of biological origin, in which birefringence and dichroism occur even in the absence of secondary structure. These phenomena are known as "form" birefringence and "form" dichroism, as opposed to the corresponding "intrinsic" properties discussed above. The theory has been worked out by Wiener for both form birefringence[28] and form dichroism.[18] Two models of structures frequently found in nature have been commonly used to illustrate these phenomena.[18, 26, 28] The one consists of flat disks or lamellae stacked in a parallel arrangement and imbedded in a second medium. The other consists of an array of long rods of one material oriented parallel to one another and permeated by the second medium. Neither the lamellae, the rods nor the imbedding medium need have any secondary substructure in order to give rise to birefringence or dichroism; furthermore, the repeating units are frequently of sufficient extent to be observable under the optical microscope. It is merely sufficient that the ordered elements have a different refractive index from that of the imbedding medium to give rise to form birefringence. The equations defining the resultant form birefringence have been dealt with in a particularly graphic fashion by Oster,[26] using electric circuit analogies.

If the rods or lamellae also absorb at the wavelength of the observation and are imbedded in a medium which is transparent at the same wavelength, both form dichroism and anomalies in the form birefringence result in general. As mentioned previously, however, Wiener[18] has shown that tertiary structure of the types being considered may not give rise to form dichroism or form birefringence anomalies, even though the necessary conditions would appear to obtain. Although the exact, if complicated, equations for these situations have been worked out by Wiener, it is usually not possible

[28] O. Wiener, Abhandl. sächs. Ges. Wiss., math.-phys. Kl. 33, 507 (1912).

to determine in advance when such situations will prevail. The equations involve terms related to the tertiary structure and, in particular, to the real parts of the refractive indices of the individual components of the system, which are seldom known independently, especially in the wavelength regions of interest. Furthermore, the models for which these equations have been worked out--examples of which are the lamellae of the grana in the chloroplasts of higher plants and the myofibrils of striated muscle, respectively--are oversimplifications of the real in vivo situations.

The experimental test of whether observed birefringence is intrinsic or due to tertiary structure is usually accomplished by altering the refractive index of the imbedding medium. When the imbedded structures are proteins, for example, the medium is changed by imbibition of glycerine or of solutions of soluble protein. As the refractive index of the imbedding medium approaches that of the oriented components, any form birefringence tends to disappear whereas intrinsic birefringence is unaffected. In practice, situations are commonly encountered in which both types contribute simultaneously to the observed birefringence of the untreated material.

The presence of form dichroism is usually tested for in the same way--i. e., by altering the refractive index of the imbedding medium. In this case, however, the absence of any residual dichroism in the treated specimen does not necessarily prove the absence of secondary structure of the chromophoric groups, as is made clear from the theory of Wiener. Thus, statements based on such experiments to the effect that a given substance possesses only form dichroism must be noted with reservation.

A more definitive test of the source of observed dichroism is to break up the tertiary structure while leaving the secondary structure intact. In no case is it possible to retain form dichroism or form birefringence in the absence of appreciable parallel ordering of the component elements. In its absence any residual dichroism or birefringence can be due only to the intrinsic effects. The method of breaking up the tertiary structure has seldom, if ever, been used as a criterion for assignment of the origin of the optical effects, usually for the lack of suitable methods of doing it completely without altering the secondary structure and in the absence of adequate tests for the desired extent of disruption. In this study sonication followed by ultracentrifugation has been used to obtain concentrated suspensions of the basic units, the quantasomes, which make up spinach chloroplast lamellae. The absence of stacks of lamellae or grana in the preparations used has been demonstrated by electron microscopy.[16] The retention of the secondary structure is apparent from the electron micrographs; however, the most convincing evidence to this point is the ability of these particles to carry out Hill oxidation upon illumination and, upon addition of the soluble enzymes, to accomplish photosynthetic carbon dioxide fixation. Furthermore, it has been shown that the visible absorption spectra of these quantasome preparations are essentially identical with those of intact chloroplasts or leaves and appreciably different from those of extracts or otherwise denatured material.[22]

In order to calculate dichroic ratios from the immediate observables, it has been advantageous to recast the associated equations. The definition of the dichroic ratio at a given wavelength is

$$D = \frac{A_{\parallel}}{A_{\perp}} = \log \frac{I_0}{I_{\parallel}} / \log \frac{I_0}{I_{\perp}} , \qquad (1)$$

where D is the dichroic ratio; $A_{\parallel}$ and $I_{\parallel}$ are the absorbance and the transmitted intensities, respectively, when the polarizer axis is oriented parallel to the field; $A_{\perp}$ and $I_{\perp}$ are the corresponding quantities when the perpendicular orientation obtains, and I_0 is the intensity of polarized light incident on the sample. This is not, however, a particularly useful form when the dichroic ratios are close to unity, as in this study. The numerator and denominator of Eq. (1) can be separately expanded according to the scheme

$$A_{\parallel} = \log \frac{I_0}{I_{\parallel}} = \log \frac{(I_0 \cdot I_*)}{(I_* \cdot I_{\parallel})} = \log \frac{I_0}{I_*} - \log \frac{I_{\parallel}}{I_*} , \qquad (2)$$

where I_* is the intensity of light that would be transmitted by the sample for an incident intensity I_0 of unpolarized light. Defining

$$(\delta I)_{\parallel} = I_{\parallel} - I_* ,$$

substitution in (2) yields

$$A_{\parallel} = A_* - \log \frac{I_* + (\delta I)_{\parallel}}{I_*} = A_* - \frac{1}{2.3} \ln \left[1 + \frac{(\delta I)_{\parallel}}{I_*} \right] , \qquad (3)$$

where A_* is the absorbance in unpolarized light as measured in a conventional spectrophotometer. When $(\delta I)_{\parallel} / I_*$ is small compared with unity, the logarithmic expression in Eq. (3) can be written as a series of terms,

$$A_{\parallel} = A_* - \frac{1}{2.3} \left\{ \frac{(\delta I)_{\parallel}}{I_*} - \frac{1}{2} \left[\frac{(\delta I)_{\parallel}}{I_*} \right]^2 + \frac{1}{3} \left[\frac{(\delta I)_{\parallel}}{I_*} \right]^3 - \cdots \right\} , \qquad (4)$$

$$\Delta_{\parallel} = \frac{A_{\parallel}}{A_*} - 1 = - \frac{1}{2.3 A_*} \left\{ \frac{(\delta I)_{\parallel}}{I_*} - \frac{1}{2} \left[\frac{(\delta I)_{\parallel}}{I_*} \right]^2 + \cdots \right\} , \qquad (5)$$

where $\Delta_{\parallel}$ represents the increment measured from unity of a partial dichroic ratio with light polarized with its electric vector parallel to the field gradient. A similar equation can be written for light polarized perpendicular to the field gradient,

$$\Delta_{\perp} = \frac{A_{\perp}}{A_*} - 1 = - \frac{1}{2.3 A_*} \left\{ \frac{(\delta I)_{\perp}}{I_*} - \frac{1}{2} \left[\frac{(\delta I)_{\perp}}{I_*} \right]^2 + \cdots \right\} . \qquad (6)$$

The true dichroic ratio is then

$$D = \frac{A_{\parallel}}{A_{\perp}} = \frac{1 + \Delta_{\parallel}}{1 + \Delta_{\perp}} , \qquad (7)$$

where the values for $\Delta_{\parallel}$ and $\Delta_{\perp}$ have opposite signs. Again, since $\Delta_{\parallel}$ and $\Delta_{\perp}$ are both small compared with unity, Eq. (7) can be written as

$$D = 1 + \frac{\Delta_{\parallel} - \Delta_{\perp}}{1 + \Delta_{\perp}} \cong 1 + \Delta_{\parallel} - \Delta_{\perp} = 1 + \Delta, \tag{8}$$

where $\Delta = \Delta_{\parallel} - \Delta_{\perp}$. By substituting from Eqs. (5) and (6), the expression

$$D \approx 1 + \frac{(\delta I)_{\parallel} - (\delta I)_{\perp}}{2.3 A_{*} I_{*}} = 1 + \Delta \tag{9}$$

is obtained. Finally, Δ, the increment of the total dichroic ratio measured from unity, is given by

$$\Delta = D - 1 = \frac{(\delta I)_{\perp} - (\delta I)_{\parallel}}{2.3 A_{*} I_{*}} = \frac{(\delta I)}{2.3 A_{*} I_{*}} . \tag{10}$$

In the study of electric dichroism $(\delta I)_{\parallel}$ and $(\delta I)_{\perp}$ are measured from the magnitudes of the pulses obtained from the photomultiplier during the application of the electric field; I_{*} is equal to the intensity of polarized light transmitted by the unoriented sample, and A_{*} is the absorbance at the same wavelength, as determined from a spectrophotometer recording. These quantities are all directly and readily observable by the techniques described above. It is significant to note that, in order to determine the spectrum of the dichroic ratio, the relative change in transmission of the sample caused by the field pulse must be divided at each wavelength by the absorbance of the sample at that wavelength.

Test calculations show that Eq. (9) gives dichroic ratios up to 1.15 with an accuracy better than 0.1%, and even at D = 1.30, the highest value actually observed in this study, the result calculated from Eq. (9) is too high by only 1%. Corrections utilizing the second and further terms of the series expressions could be used to reduce this error; however, this operation was not carried out for any of the results reported here. The errors introduced from signal noise and the wavelength bandwidth of the light from the monochromator were, in general, somewhat greater in any case.

Results

Electric Birefringence

Measurements on a number of preparations of spinach quantasomes demonstrated the presence of a pronounced electric birefringence (Kerr effect). These measurements were made by using the apparatus described above with crossed polarizer and analyzer and with monochromatic light at 560 mμ, at the point of minimum absorbance in the visible spectrum of the spinach quantasomes. An applied voltage gradient of 2500 v/cm was required for the signal to be clearly distinguishable; gradients between 4000 and 15,000 v/cm produced a large electric birefringence signal with excellent discrimination.

The times required for particles to orient in the electric field, or to become disoriented when the field is turned off, are known as the orientation time and the relaxation time, respectively. These times depend on the size and shape of the particle, on the viscosity of the medium, and on the temperature, in a manner described by Perrin,[29] Benoit,[30] and others. These times are especially easy to determine when a square voltage pulse is used, as in this work. For a square pulse the relaxation time at the end of the pulse is independent of the magnitude of the voltage gradient applied. At low fields, the orientation time is also not dependent on the magnitude of the voltage gradient; however, fields strong enough to lead to birefringence saturation (strong alignment of the particles) are associated with progressively shorter orientation times.[31] At voltage gradients below saturation, the orientation and relaxation times are equal if the particles under investigation possess only an induced polarizability; however, the orientation time is longer than the relaxation time if they possess a permanent dipole moment as well. This phenomenon has been used frequently to distinguish between the two electrical situations.[20, 30] It should be noted that polydisperse systems generally give rise to complex orientation and relaxation curves characterized by time constants associated with each of the species involved.

Relaxation times were measured for the birefringence of a number of samples prepared in different ways. In general, only the longer relaxation times were accurately observed, because relatively slow time constants were chosen for the detection system in order to reduce the noise. In these cases only an upper limit can be given for the shortest relaxation times. In one series of experiments, however, a detection circuit with an inherent time constant of about 0.5 μsec was employed. The measuring system was tested with nitrobenzene, which has a relaxation time of the order of 10^{-9} sec. The results showed that the observed birefringence accurately followed the shape of the applied voltage pulse. The limiting factor in this case is the rise and decay of the applied voltage pulse, the time constant for which was observed to be 2 μsec. This fast circuit was used to study the relaxation time for a sample containing small chloroplast quantasome sheets and small, colorless particles present in the supernatant liquid following centrifugation of the sonicate for 20 min at 145,000 g (maximum acceleration). The shortest relaxation time observed was 26 ± 4 μsec, and arose from about 80% of the birefringence signal. The remainder of the signal appeared to have a relaxation time of 180 ± 20 μsec; less than 1% of the signal was associated with time constants appreciably longer than 200 μsec. The data were not good enough to ascertain whether there were materials giving rise to intermediate relaxation times. It does show conclusively, however, that there is negligible contribution to the electric birefringence from species with relaxation times shorter than 20 μsec.

---

[29] F. Perrin, J. phys. radium 5, 497-511 (1934); 7, 1-11 (1936).

[30] H. Benoit, Ann. Phys. 6, 561-609 (1951).

[31] C. T. O'Konski, K. Yoshioka, and W. H. Orttung, J. Phys. Chem. 63, 1558-65 (1959).

The quantasome sheets which remained in suspension after centrifugation for 10 min at 35,000 g, but which precipitated during 20 min at 145,000 g, gave rise to signals with roughly equal parts having decay times less than 0.7 msec and between 0.7 and 6 msec, respectively. If this material is subsequently treated to a second sonication, the resuspended fragments exhibit electric birefringence of which 80% has a time constant of less than 0.4 msec and 20% a relaxation time of about 2 msec. Again, the intermediate relaxation pattern may be more complicated than this cursory summary would indicate. Owing to the complex nature of the systems being studied, assignments for these relaxation times cannot be made at present. The experimental findings do serve, however, to delimit the ranges of particle sizes encountered in these samples and give some feeling as to the effectiveness of the sonication and separation procedures.

Orientation times were measured for the small supernatant particles with the fast-response apparatus. With an applied field gradient of 10,000 v/cm these particles exhibit nearly identical orientation and relaxation times. This gradient, however, is beyond the saturation limit for the quantasomes, as is shown below. At lower gradients, down to 5,000 v/cm, the electric birefringence transients appeared to have longer orientation than relaxation times. This would indicate the presence of a permanent dipole moment for the particles. The transients were not of sufficient magnitude to justify accurate time-constant determinations from a semilogarithmic plot, however, and the presence of a dipole moment must remain a tentative conclusion for the time being.

From an appropriate plot of the magnitude of the birefringence versus the electric field it is possible to derive values for the Kerr constants for these particles. Using the notation of O'Konski and Haltner,[32] one can state a summary of the conclusions of the relevant theoretical equations. The optical retardation, δ, in radians is given by

$$\delta = 2\pi l \Delta n / \lambda_0 \quad , \tag{11}$$

where l is the path length of the birefringent medium; $\Delta n = n_{\parallel} - n_{\perp}$, and $n_{\parallel}$ and $n_{\perp}$ are the refractive indices for linearly polarized radiation with electric vectors lying parallel and perpendicular, respectively, to the direction of the electric field; and λ_0 is the wavelength of the radiation *in vacuo*. The Kerr law can be written

$$\Delta n = KnE^2, \tag{12}$$

where K is the Kerr constant for the system, n is the refractive index, as measured in a conventional refractometer, of the solution at wavelength λ_0; and E is the electric field. For the particular optical system utilized here, the optical retardation, for small values, is given by

$$\frac{\Delta I_\delta}{I_0} \approx \delta^2 \quad , \tag{13}$$

[32] C. T. O'Konski and A. J. Haltner, J. Am. Chem. Soc. 79, 5634-49 (1957).

where ΔI_δ is the magnitude of the change in light intensity at the photomultiplier for an optical retardation δ and where I_0 is the intensity at the photomultiplier when the polarizer axes are turned parallel to each other. This relationship was demonstrated experimentally to be valid for all the results to be reported below. It can be seen from these equations that a plot of δ versus E^2 will permit the calculation of the Kerr constant. In cases such as this one, in which the solvent makes negligible contribution to the observed birefringence, the Kerr constant is directly proportional to the concentration c of the macromolecular species. Thus it is useful to define a specific Kerr constant

$$K_{sp} = \frac{K}{c} . \tag{14}$$

Plots of δ vs E^2 for two samples are shown in Fig. 1-2. The middle curve shows the results for the small quantasome sheets and colorless particles present in the final supernatant fraction; the lower curve is for the final quantasome precipitate, which has been resonicated. This second material is relatively free of soluble colorless macromolecules. Both materials exhibit saturation effects above applied voltage gradients of about 5000 v/cm, so that the curves approach horizontal asymptotes at higher gradients. In the regions of saturation the particles are almost completely oriented by the applied field. The difference between the two curves in the upper part of the figure demonstrates the consequence of irreversible changes which frequently occur following application of several pulses with gradients of 10,000 v/cm and higher. The effects are frequently even more pronounced.

Kerr constants for these systems can be calculated from the limiting slopes at low fields. Calculations based on Eqs. (11) and (12) yield values of 1.9×10^{-9} cm^2/statvolt^2 for the small particles (middle curve) and 1.5×10^{-9} cm^2/statvolt^2 for the twice sonicated fragments (lower curve). In the absence of measured values for the total concentrations in terms of protein, the major constituent, specific Kerr constants were calculated on the basis of chlorophyll content, as determined from the absorptions at 678 mμ for the two suspensions. Assuming the extinction coefficient to be 9×10^4 l/mole-cm, as is observed in acetone extracts,[33] specific Kerr constants of 2.3×10^{-7} and 0.7×10^{-7} cm^2/statvolt^2-(g Chl/l) are obtained for the small fragments and for the twice sonicated material, respectively. It is interesting to note that the chlorophyll/nitrogen ratios reported by Park and Pon[16] lead to the conclusion that, relative to chlorophyll, one might expect about four times as much protein in the supernatant fraction as in the precipitated quantasome aggregates. The fact that in this study the specific Kerr constants, based on chlorophyll concentration, for the comparable fractions are in the ratio 3.3 to 1 suggests that the observed birefringence arises predominantly from the protein present. This would be the expected result, in fact. On the other hand, the saturation levels of optical retardation would be expected to yield about the same ratio. When normalized to the amount of chlorophyll present, however, the corresponding ratio of specific saturation limits is only 1.23 to 1. These discordant results

[33] J. H. C. Smith and A. Benitez, in Modern Methods of Plant Analysis, Vol. 4 (Springer, Berlin, 1955), pp. 143-196.

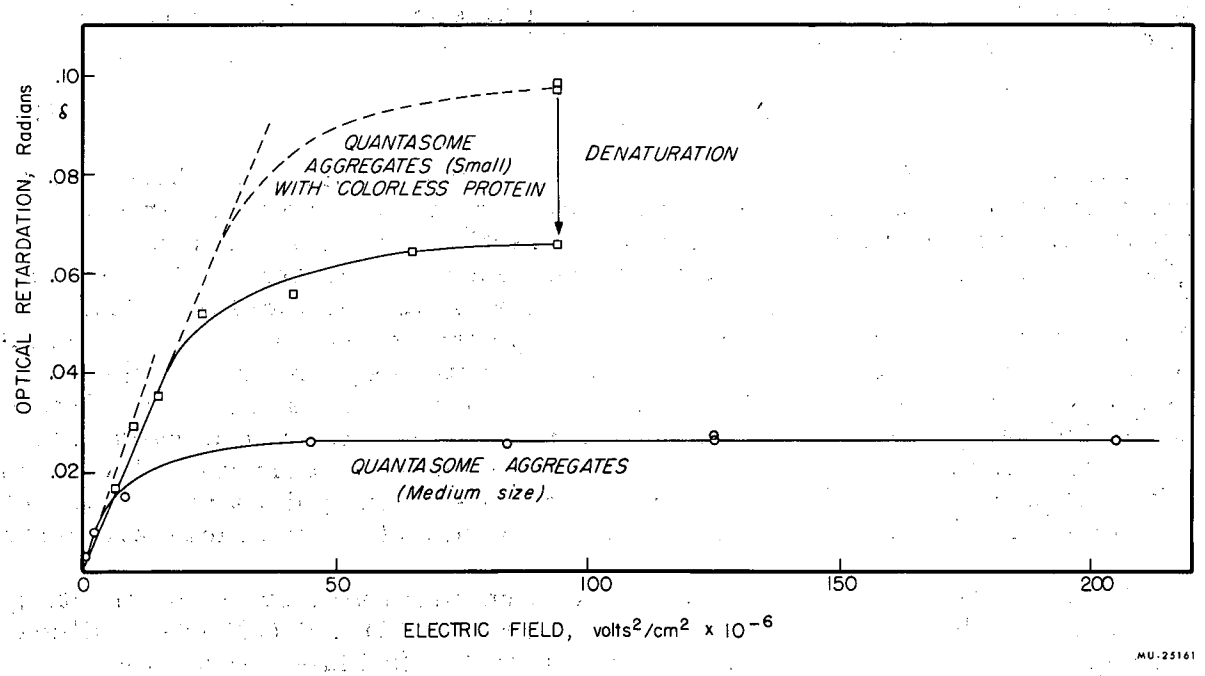

Fig. 1-2. Birefringence versus electric field for spinach quantasome preparations.

very likely result from the fact that the sample of small aggregates was stored considerably longer before the measurements than was the other preparation. Reconciliation of the lack of agreement must await further investigation.

An attempt was made to observe electric birefringence in chromatophore subunits isolated from Rhodospirillum rubrum. In this case measurements were made at 640 mμ on a suspension which possessed an absorbance of 4.9 at 890 mμ. No electric birefringence was observed at applied fields up to 15,000 v/cm. The sensitivity was such that an optical retardation greater than 0.015 radian would have been observed. This failure to observe a Kerr effect is not surprising, as the chromatophore subunits appear to be spherical as seen in the electron microscope.

Electric Dichroism

Preparations of spinach quantasomes of the type described above were observed to possess uniformly a marked electric dichroism at the same applied voltage gradients as gave rise to electric birefringence. The observed dichroic ratio, although always positive in sign, had a magnitude which depended on the wavelength of radiation used. Figure 1-3 gives a composite curve for the dichroic ratio spectrum between 340 and 734 mμ. Although the results within either (a) the ultraviolet, (b) the blue, or (c) the yellow, red, and near infrared regions of the spectrum are reproducible, the magnitudes of one region do not necessarily accurately relate to those in another, as is discussed further below. The dichroic ratio spectrum has relatively little structure compared with the absorption spectrum light (dashed curve in Fig. 1-3), with the exception of the very pronounced peak centering at 695 to 700 mμ. This peak, however, is of considerable interest with respect to its possible significance in the mechanism of photosynthesis.

With a single exception, all experiments were carried out on suspensions prepared from the final supernatant liquid following centrifugation of the spinach chloroplast sonicate at 145,000 g for 20 min. In one experiment the precipitate from this centrifugation was resuspended and sonicated a second time, and the supernatant from centrifugation at 45,000 g for 10 min was examined for electric dichroism. No signal was observed from this sample of larger fragments, for reasons which are unknown; therefore, all the results reported are for suspensions containing small quantasome aggregates (3 to 8 quantasome units) together with the colorless stroma proteins and metabolites. Most of the studies were carried out on the quantasomes within a few hours after their isolation from fresh spinach leaves. In several cases measurements were made on quantasome suspensions stored for 24 hours at 5° C. The results of these experiments were quantitatively identical with those carried out on the corresponding fresh preparations. In all, six preparations from different sources of spinach gave rise to the dichroism effects to be discussed. In one additional case, the effect was observed only weakly, probably owing to an artifact in the quality of the material prepared. In general, however, the dichroism of the small quantasome aggregates is uniformly observed.

As mentioned previously, the measurement of small electric dichroism effects is much more difficult than for comparable electric birefringence,

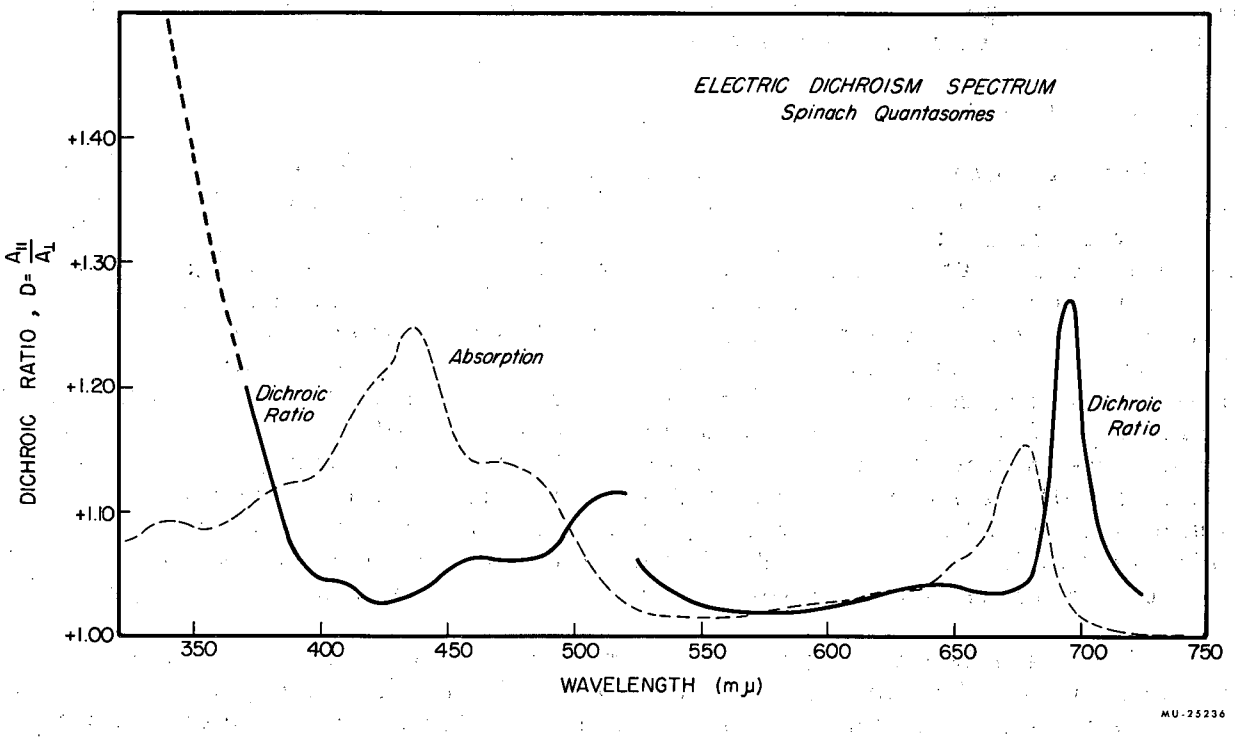

Fig. 1-3. Electric dichroism spectrum from 340 to 734 mμ for spinach quantasomes (small aggregates) (heavy curve). Absorption spectrum of spinach quantasomes (light curve, dashed).

owing to the high noise level in the transmitted light intensity. Consequently, in regions where instrument sensitivity is low, where the sample absorbance is either particularly small or particularly large, and where the dichroic ratio itself is small, the level of noise becomes a serious limitation on the measurements. In general, however, the signals to be reported were quite well defined, and in some cases signal/noise ratios in excess of 100 were obtained. This situation obtained only at the expense of decreased time resolution (system band pass); therefore, measurements of orientation and relaxation times for electric dichroism in these systems were virtually impossible. The one series of measurements carried out with a fast-response system gave an upper limit of about 100 μsec for the dichroism relaxation time for small particles; however, no data have been obtained so far that will permit meaningful comparison with relaxation times for the electric birefringence.

The pulse shapes in about half the measurements were superficially what would be expected from an exponential rise to a saturation level, followed by an exponential decay. This is normal when the time constant of the measuring circuit is limiting. In the remaining cases the observed pulses appeared to be superimposed on a curving baseline. Instead of rising to a horizontal asymptote, the traces approached an ascending or descending limit, depending on the sign of the transient (i.e., on the direction of the polarizer). The decay after turning off the applied field then either did not reach the initial baseline or overshot it. Similar effects have been noted in other systems by O'Konski (private communication). These effects were quite regular for the series of measurements in which they occurred; however, their source has not been ascertained. In most cases it was still possible to get a good value for the magnitude of the field-induced transients by correcting for these superimposed slower transients.

In general, the absolute magnitudes of the observed signals due to the electric dichroism were not the same when the polarizer was oriented with its axis parallel to the field as when it was perpendicular to the field. This might at first seem surprising; however, there is some theoretical justification for such observations. This theory would indicate that a transient should be observed even in the absence of any polarizing element in the measuring beam. Such transients have, in fact, been observed experimentally in connection with this study. The transient in unpolarized light always has the same sign as the transient of greatest magnitude in polarized light, and roughly accounts for the difference in pulse magnitudes resulting from the two polarizer orientations. Furthermore, when the polarizing prism was oriented at intermediate angles, between 0° and 90° with respect to the field gradient, the signal did not decrease to zero at an angle of 45°, but at an angle displaced by 10° or more in the direction of the normal orientation giving rise to the smaller magnitude transient. Which orientation this was depended solely on the wavelength of the measurement. Throughout most of the spectrum the perpendicular orientation gave rise to a signal of roughly twice the absolute magnitude of that in the parallel orientation. In the near ultraviolet the ratio increased to around 3. Between 660 and 715 mμ, however, the parallel orientation gave the transient of larger magnitude. The ratio of the transients in this spectral region has a maximum of about 2 at 695 to 700 mμ. It is undoubtedly of significance that this is the region in which the pronounced peak in the dichroic ratio spectrum occurs; however, the basis for the former effect is not yet clearly understood.

Two series of experiments on different preparations were carried out to determine the voltage gradient required for saturation of the electric dichroism. In the first case, no measurable difference in the magnitude of the dichroic ratio was observed when the voltage gradient was increased from 6000 v/cm to 9000 v/cm. Thus, as in electric birefringence, the effect appeared to be saturated at fields of 6000 v/cm and greater. Consequently, voltage gradients in this range were uniformly utilized for the determination of the dichroic ratio spectru, with the expectation that measurements would thereby be made only on essentially completely oriented particles. In the second series of experiments, however, the dichroism transients increased linearly with applied fields up to gradients as high as 16,000 v/cm. Furthermore, measurements on this sample with a gradient of 6000 v/cm gave values of Δ that were smaller by roughly an order of magnitude than those observed in the same wavelength region for other samples under apparently identical conditions. This discrepancy is discussed further below. In view of this latter result, however, some uncertainty remains as to the saturation level of the electric dichroism of the small quantasome aggregates.

In one experiment an attempt was made to determine whether the dichroism disappeared following denaturation of the sample. A sample was heated in a small tube for 2 min in a water bath at 70° C. The electric dichroism observed afterwards at 435 mμ was identical ($\Delta \pm 5\%$) with that observed before the heat treatment. After the first field pulse the heat-treated material rapidly coagulated in the Kerr cell, however. The effect of denaturation has not been studied at other wavelengths.

Measurements on three preparations gave dichroic ratios of 1.025, 1.025, and 1.026 at 435 mμ and 1.060, 1.070, and 1.060 at 480 mμ. On a fourth preparation, values of 1.0038 and 1.008, respectively, were obtained at the same two wavelengths. Measurements at seven other wavelengths between 400 and 510 mμ also gave values for Δ which were eightfold lower for this fourth preparation than for one of the earlier three. The fourth preparation is also the one, described above, which did not exhibit saturation at 6000 v/cm applied field gradient. Since this sample was the one on which the most detailed study was made of the dichroic ratio spectrum in the blue and near-ultraviolet regions, its values of Δ have been uniformly multiplied by a factor of 8 to bring them in line with the other results. These corrected results are compared with those determined from the first three preparations in Fig. 1-4. It is seen that there are now fairly good internal consistency and reproducible spectral features in those regions where both sets of data correspond. The partially corrected spectrum shown should correspond to nearly complete orientation of the quantasome aggregates.

Equation (10) shows that the dichroic ratio is independent of concentration. This requirement was tested at six wavelengths in the region 410 to 450 mμ with solutions differing twofold in concentration. Agreement of the calculated dichroic ratios was obtained within the accuracy of the measurements ($\Delta \pm 10\%$).

In general, the dichroic ratio spectrum, as seen in Fig. 1-3, proceeds from relatively large values in the near ultraviolet through a minimum near

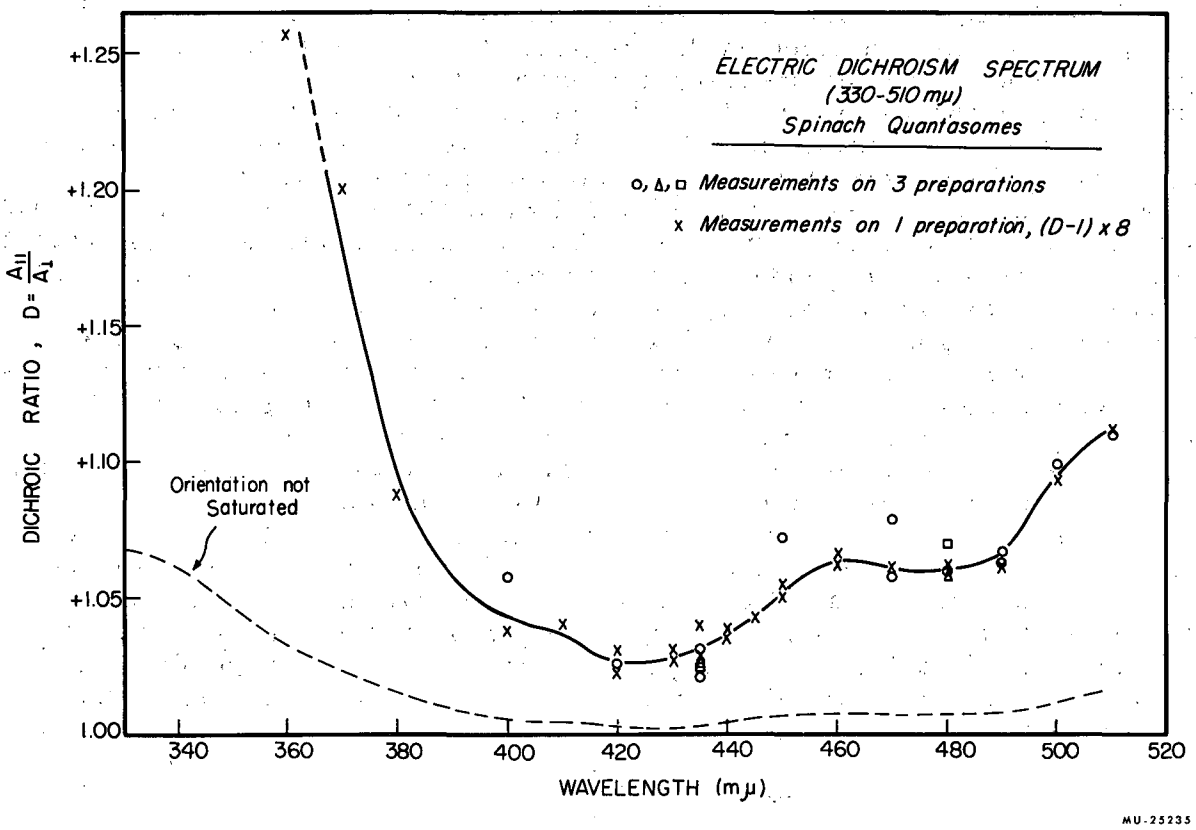

Fig. 1-4. Electric dichroism spectrum from 330 to 510 mμ for spinach quantasomes (small aggregates). Lower curve represents observed results for the preparation studied in greatest detail, but the orientation was not saturated. Symbol X refers to the corresponding data multiplied eight-fold. Symbols O, Δ, and □ refer to directly measured dichroic ratios for three other preparations. Upper curve probably represents the dichroic ratio spectrum for nearly saturated orientation.

435 mμ (corresponding to the maximum in the absorption spectrum), and rises again to an apparent maximum, which has not yet been well studied, near 525 mμ. At longer wavelengths no pronounced features are encountered until the very strong peak which begins at 675 mμ and reaches a maximum at 695 to 700 mμ. This peak is by far the most striking feature in the dichroic ratio spectrum and has been made the subject of detailed investigations.

The strong maximum near 700 mμ has been observed for each of the three preparations examined in this region. In no case was it not observed. Figure 1-5 shows the results from one preparation measured at three concentrations, in the ratio 1:3:7.5, and a second preparation corresponding to the lowest of the first three. The influence of the concentration on the magnitude of the observed dichroic ratio may, perhaps, be accounted for in this particular case. As seen in Fig. 1-3, the absorption in the region from 680 to 700 mμ is decreasing rapidly with increasing wavelength. In order to make accurate measurements of the dichroic ratio in such a region, it is necessary to have highly monochromatic radiation and accurately reproducible wavelength settings. The first of these criteria, at least, did not obtain sufficiently well in the present study. The measurements shown in Fig. 1-5 were made using a monochromator slit width corresponding to a spectral band half width of 5 mμ. Over the range of 10 mμ included in each measurement, there occurs as much as a threefold variation in the absorbance of the sample in the region 680 to 700 mμ. It is not sufficient simply to use the absorbance at the center of spectral band and expect to obtain a good "average" value of Δ from the calculations using Eq. (10). In order to evaluate the consequences of using radiation with a finite bandwidth in the spectral region corresponding to a strongly changing absorption coefficient, it is worth while considering the hypothetical example of a situation in which the dichroic ratio is a constant, independent of wavelength, throughout an absorption band. Rewriting Eq. (10) in the form

$$A_* = \frac{1}{2.3\Delta} \times \frac{(\delta I)}{I_*} , \qquad (15)$$

one can see that the relative change in transmitted intensity during the field pulse at any wavelength is directly proportional to the absorbance.

If the transmitted intensity were inversely proportional to the absorbance, then the values of the dichroic ratio calculated by using the absorbance at the center of the band of wavelengths from the monochromator and the observed values of (δI) and I_* would be approximately correct. Since the relationship between the transmitted intensity and the absorbance is an exponential one, however, wavelengths corresponding to relatively low-absorbance regions make disproportionately large contributions to the transmitted intensity in comparison with wavelengths in regions of high absorbance. Since regions of low absorbance, according to Eq. (15), contribute low values of $(\delta I)/I_*$, the observed signal is weighted heavily in that direction. It can readily be seen that if one uses in Eq. (15) the value of the absorbance at the center of the wavelength band, as read from the monochromator, and values of $(\delta I)/I_*$ which are too low because they are weighted in the direction away from the maximum of the absorption band, then the calculated values for D will be <u>less</u> than the true value in such a region.

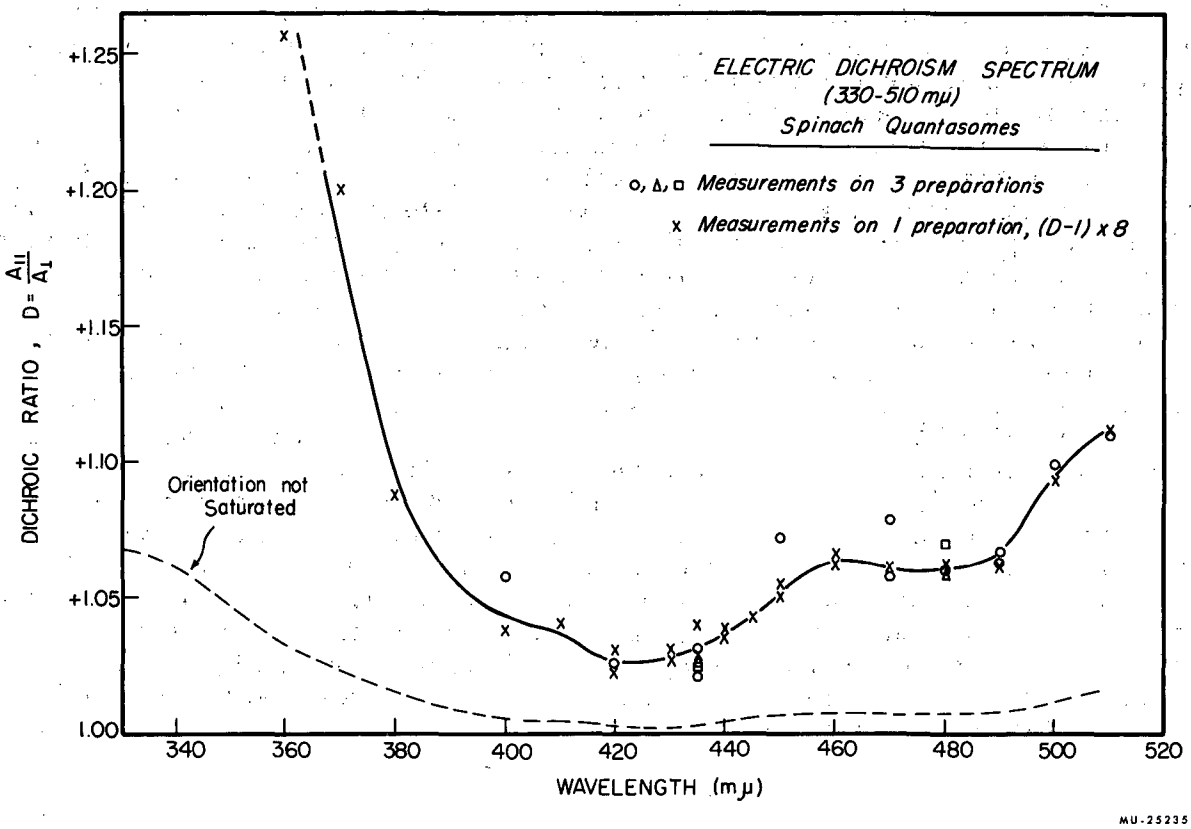

Fig. 1-4. Electric dichroism spectrum from 330 to 510 mμ for spinach quantasomes (small aggregates). Lower curve represents observed results for the preparation studied in greatest detail, but the orientation was not saturated. Symbol X refers to the corresponding data multiplied eight-fold. Symbols O, Δ, and □ refer to directly measured dichroic ratios for three other preparations. Upper curve probably represents the dichroic ratio spectrum for nearly saturated orientation.

435 mμ (corresponding to the maximum in the absorption spectrum), and rises again to an apparent maximum, which has not yet been well studied, near 525 mμ. At longer wavelengths no pronounced features are encountered until the very strong peak which begins at 675 mμ and reaches a maximum at 695 to 700 mμ. This peak is by far the most striking feature in the dichroic ratio spectrum and has been made the subject of detailed investigations.

The strong maximum near 700 mμ has been observed for each of the three preparations examined in this region. In no case was it not observed. Figure 1-5 shows the results from one preparation measured at three concentrations, in the ratio 1:3:7.5, and a second preparation corresponding to the lowest of the first three. The influence of the concentration on the magnitude of the observed dichroic ratio may, perhaps, be accounted for in this particular case. As seen in Fig. 1-3, the absorption in the region from 680 to 700 mμ is decreasing rapidly with increasing wavelength. In order to make accurate measurements of the dichroic ratio in such a region, it is necessary to have highly monochromatic radiation and accurately reproducible wavelength settings. The first of these criteria, at least, did not obtain sufficiently well in the present study. The measurements shown in Fig. 1-5 were made using a monochromator slit width corresponding to a spectral band half width of 5 mμ. Over the range of 10 mμ included in each measurement, there occurs as much as a threefold variation in the absorbance of the sample in the region 680 to 700 mμ. It is not sufficient simply to use the absorbance at the center of spectral band and expect to obtain a good "average" value of Δ from the calculations using Eq. (10). In order to evaluate the consequences of using radiation with a finite bandwidth in the spectral region corresponding to a strongly changing absorption coefficient, it is worth while considering the hypothetical example of a situation in which the dichroic ratio is a constant, independent of wavelength, throughout an absorption band. Rewriting Eq. (10) in the form

$$A_* = \frac{1}{2.3\Delta} \times \frac{(\delta I)}{I_*} , \qquad (15)$$

one can see that the relative change in transmitted intensity during the field pulse at any wavelength is directly proportional to the absorbance.

If the transmitted intensity were inversely proportional to the absorbance, then the values of the dichroic ratio calculated by using the absorbance at the center of the band of wavelengths from the monochromator and the observed values of (δI) and I_* would be approximately correct. Since the relationship between the transmitted intensity and the absorbance is an exponential one, however, wavelengths corresponding to relatively low-absorbance regions make disproportionately large contributions to the transmitted intensity in comparison with wavelengths in regions of high absorbance. Since regions of low absorbance, according to Eq. (15), contribute low values of $(\delta I)/I_*$, the observed signal is weighted heavily in that direction. It can readily be seen that if one uses in Eq. (15) the value of the absorbance at the center of the wavelength band, as read from the monochromator, and values of $(\delta I)/I_*$ which are too low because they are weighted in the direction away from the maximum of the absorption band, then the calculated values for D will be <u>less</u> than the true value in such a region.

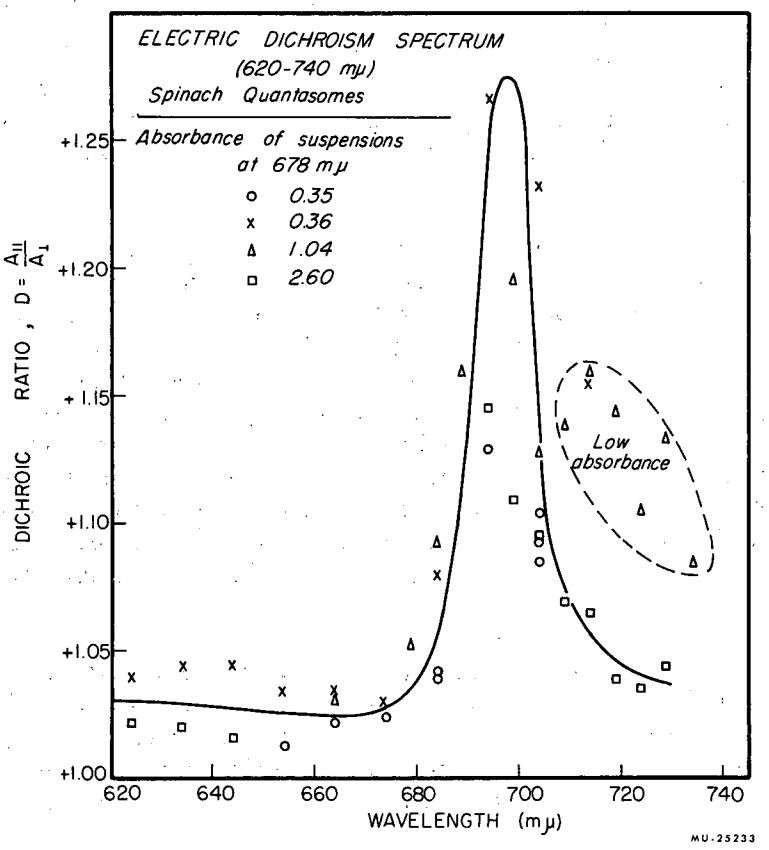

Fig. 1-5. Electric dichroism spectrum from 620 to 730 mμ for spinach quantasomes (small aggregates); effect of sample concentration on the dichroic ratio measurements.

A somewhat more detailed analysis shows that in such a situation as that discussed above, the apparent dichroic ratio will exhibit minima on either side of the absorption band. Through the use of an appropriate model for the wavelength distribution of light intensity, it is possible to estimate that, if the true dichroic ratio were 1.05 throughout the red absorption band of the quantasomes, then the value obtained with use of a 10-mμ bandwidth from measurements at the steepest part of the absorption band (at 686 mμ) would be down only to 1.04, even for the most concentrated solution whose results are shown in Fig. 1-5.

The most important conclusion to be gained from this discussion is that the finite spectral bandwidth can in no way account for the maximum observed in the dichroic ratio spectrum on the long-wavelength side of the red absorption band. The effect expected is in the opposite direction, and is small in magnitude.

Conclusive evidence that this dichroic ratio maximum is not an experimental aritifact is obtained from measurements at higher resolution. Figure 1-6 shows that when the spectral band half width of the monochromator is reduced from 5 to 3.5 mμ, by closing the monochromator slits, the magnitude of the dichroic ratio in the vicinity of 700 mμ is essentially unchanged. This consequence of higher resolution would be expected only if the peak corresponds to a real maximum in the dichroic ratio of the quantasomes in this region of the spectrum; an experimental artifact would lead to a decrease in the measured dichroic ratios with decreasing bandwidth. Further increase in resolution could not be achieved with the present apparatus, owing to the serious loss in light intensity which accompanies narrowing of the monochromator slits.

The dichroic ratio at wavelengths longer than 710 mμ was difficult to measure because of the small magnitude of the field-induced transients in this region. The points in Fig. 1-5 corresponding to the highest concentration are the most reliable at the longest wavelengths. They probably give the dichroic ratio spectrum fairly accurately out as far as 725 mμ.

Discussion

The measurements of dichroic ratio made in this study show conclusively that it is an intrinsic rather than a form effect. The nature of the sample preparation precludes the existence of a structure of parallel lamellae, as occurs in the intact chloroplast. It might be argued that the quantasome itself contains a network of planes or lines of otherwise randomly oriented pigment molecules; however, such a model is incapable of explaining the observed wavelength dependence of the dichroic ratio--especially the strong anomaly at 700 mμ, which does not coincide with the maximum in the absorption spectrum in that region.

The preferred explanation is based on a model which assumes a small fraction of the chlorophyll molecules in the quantasome relatively highly oriented with respect to one another. Furthermore, this orientation must be approximately the same in each quantasome, with respect to a set of identical coordinate axes associated with the quantasome. The other

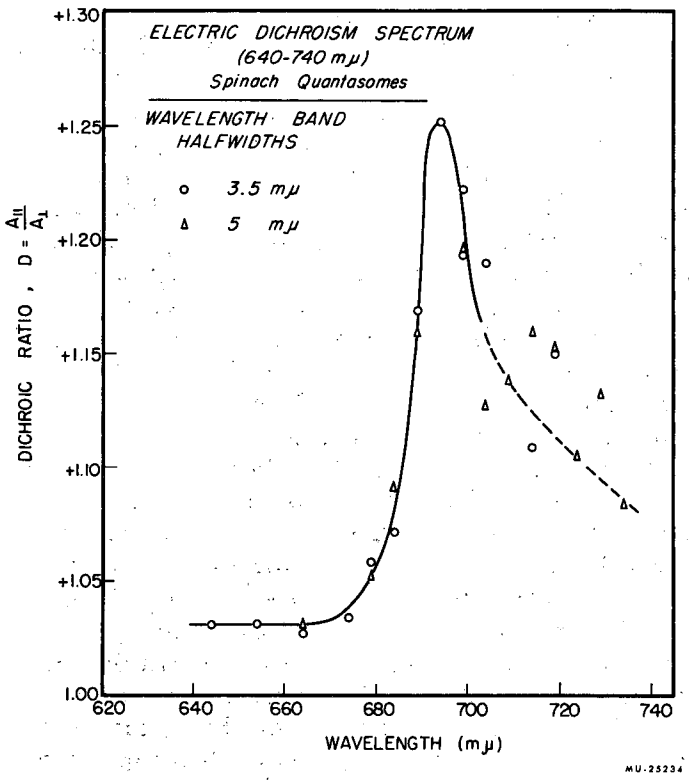

Fig. 1-6. Electric dichroism spectrum from 640 to 740 mμ for spinach quantasomes (small aggregates); effect of spectral band width on the dichroic ratio measurements.

chlorophyll molecules and all the carotenoid molecules are very likely nearly unoriented in the quantasome; however, it is possible they possess a relatively high degree of orientation on a nonplanar surface. It is known that aggregation of chlorophyll shifts its absorption maximum appreciably to longer wavelengths,[34, 35, 36, 37] even to 740 mμ in crystalline chlorophyll. Thus, the fact that the highly oriented molecules present in quantasomes possess absorption on the long wavelength side of the main band is consistent with what is known about the spectral properties of chlorophyll.

It is possible to make a rough estimate of the fraction of the total chlorophyll that has this strong orientation. Assuming that all the absorption at 695 mμ is due to oriented molecules, one can calculate from the dichroic ratio spectrum their contribution to the absorption at other wavelengths in the red absorption band. Such a calculation produces a value in the neighborhood of 15%. If all the chlorophyll absorption at 695 were due to oriented molecules, however, one would expect a pronounced shoulder in the measured absorption band in this region. This is not observed in the spectrum, undoubtedly because the tail of the main chlorophyll absorption extends to these long wavelengths and contributes to the absorption. Therefore, a figure of about 5 to 10% is probably a more realistic representation of the fraction of the total chlorophyll that has high orientation. It is possible to estimate that a quantasome from a mature spinach chloroplast contains about 300 chlorophyll molecules. About 20 of these, then, are especially oriented. It is clear that the number cannot be much smaller than this, or the effect would not be observable--i. e., one or two "oriented" pigment molecules would not be noticed in a sea of unoriented ones. In fact, the only reason the anomaly is observable at all in this case is that the absorption maximum of the oriented chlorophyll absorption is shifted 20 mμ from that of the main band. Undoubtedly the reason that a corresponding dichroism anomaly arising from the Soret band of the oriented chlorophyll molecules is not observed in the blue region of the spectrum is the much broader absorption bands of the bulk of the unoriented chlorophyll and carotenoid molecules, which overwhelm it. It is curious to note at this point that Goedheer,[13] in his studies on the dichroism of Mougeotia chloroplasts, made observations at 680 mμ and at 715 mμ, but not at wavelengths in between. From Fig. 1-5 it is evident that these wavelengths are just at the edge on either side of the maximum in the dichroism spectrum. Presumably, one more measurement at the midpoint of this interval would have led to the discovery of the anomaly five years earlier.

---

[34] E. E. Jacobs, A. E. Vatter, and A. S. Holt, Arch. Biochem. Biophys. 53, 228-38 (1954).

[35] K. B. Serebrovskaya and A. I. Oparin, Doklady Akad. Nauk S. S. S. R. 135, 1532-5 (1960).

[36] G. Colmano, Biochim. et Biophys. Acta 47, 454-457 (1961).

[37] J. A. Lippincott, J. Aghion, and W. F. Bertsch, Plant Physiol. 36, iv (1961).

The general shape of the dichroic ratio spectrum (Fig. 1-3) suggests that the carotenoids (445 to 490 mμ) exhibit greater dichroism than does the major fraction of chlorophyll a (420 to 440, 670 to 680 mμ) or of chlorophyll b (650 mμ). The dichroic ratios of 1.05 to 1.10 are all quite small, however, in comparison with the value of 6 obtained by Goedheer for artificially oriented chlorophyll.

It is possible to speculate as to the role of this oriented chlorophyll and to its significance in the overall mechanism of photosynthesis. It is well known that the energy absorbed in the Soret band of chlorophyll and also that absorbed by many accessory pigments can be utilized efficiently in photosynthesis. Apparently this can be done only through a transfer of excitation to the state corresponding to that resulting from the direct absorption of radiation by the red band of chlorophyll a. Since, for the "organized" chlorophyll observed in this study, this band is shifted to the long-wavelength side of the main red band, it represents the bottom of the hill in terms of the flow of electronic energy, at least so far as we now know. It is a consequence of this fact that, once the electronic energy produced anywhere in the quantasome has migrated to the organized chlorophyll, it cannot then return or move away in any manner without conversion to fluorescence or some new form of energy. Thus, these molecules serve as an energy trap to localize or concentrate the poly-ergonic absorbed radiation. It is proposed that the normal fate of this "trapped" electronic energy is in the initiation of electron-transfer reactions, thereby converting it directly to chemical potential.

Witt and co-workers,[38, 39, 40] through the study of absorption changes in photosynthetic systems induced by brief flashes of illumination, have mapped the outlines of a scheme whereby the successive processes are thought to be carried out. Of particular interest to this study are the earliest of these processes--i.e., those which occur most rapidly following the exciting flash. In brief, these may be stated in the equations

$$\mathrm{Chl} \xrightarrow[(680\ m\mu)]{h\nu} \mathrm{Chl}^{\bullet}\ ; \tag{16}$$

$$\mathrm{Chl}^{\bullet} \longrightarrow \mathrm{Chl}^{+} + e\ ; \qquad \tau \leq 10^{-5}\ \mathrm{sec} \tag{17}$$

$$\mathrm{Chl}^{+} + \mathrm{Cyt} \longrightarrow \mathrm{Chl} + \mathrm{Cyt}^{+}\ ; \qquad \tau = 2\times10^{-5}\ \mathrm{sec} \tag{18}$$

$$\mathrm{Cyt}^{+} + \mathrm{X} \longrightarrow \mathrm{Cyt} + \mathrm{X}^{+}\ ; \qquad \tau_{20^{\circ}\mathrm{C}} \approx 10^{-2}\ \mathrm{sec} \tag{19}$$

[38] H. T. Witt, R. Moraw, A. Müller, B. Rumberg, and G. Zieger, Z. Elektrochem. 64, 181-7 (1960).

[39] G. Zieger, A. Müller, and H. T. Witt, Z. physik. Chem. (Frankfurt) 29, 13-24 (1961).

[40] H. T. Witt, A. Müller, and B. Rumberg, Nature 191, 194-5 (1961); Angew. Chem. 73, 507-8 (1961).

The first three reactions all occur within 2×10^{-5} sec following the flash of illumination and are essentially temperature-independent from 60° C to -200° C. The fourth reaction has a time constant of about 10^{-2} sec, is temperature-dependent from 30° to 0° C, and does not occur at all at -200° C. In view of these experimental results, one is led necessarily to the conclusion that the first three cannot be chemical reactions in the usual sense. It is highly unlikely in a system such as this that any rapid reaction which possesses a temperature-independent time constant and occurs at -200° C is due to species that require any appreciable migration in the medium in order to react. Therefore, it is proposed that the organized chlorophyll is intimately contiguous with the site at which a cytochrome (probably an f-type cytochrome, according to Witt) is bound to the quantasome. The interaction of the cytochrome with the chlorophyll may, in fact, be the initial determinant of the chlorophyll orientation.

In this model, the exciton trapped by the organized chlorophyll is able to lose an electron eventually to an as yet unknown acceptor, and to abstract an electron from the nearby cytochrome molecule. Whether these events occur simultaneously or--if not--which of them is prior, is as yet unanswered. The important consequence of the scheme is that such an event could occur even at -200° C, since in principle it involves no migration of independent chemical species. The next reaction in the sequence, the oxidation of X in Reaction (19) by the oxidized cytochrome produced in Reaction (18), is a true chemical process in the sense that it does not occur at -200° C. X may be an independent species in the stroma liquid or it may be attached to some flexible part of the quantasome; the essential point is that it appears to require migration through the medium to the activated organized site in order for a reaction to occur. The time constant for this process is about 2×10^{-2} sec at 20° C. Once the cytochrome has abstracted an electron from X, it is ready to carry out the cycle of Reactions (18) and (19) again. It is worth noting at this point the discovery by Emerson and Arnold that two successive brief pulses of saturating light are efficient in producing photosynthesis only if they are spaced at least 20 to 30 msec apart.[41] At shorter intervals the efficiency of the second pulse is markedly reduced. This is just the effect expected from the cycle above, in which there is a limited number of cytochrome sites, not more than one or two per quantasome, which then cannot accept a second electron from the substrate X less than about 20 msec following the initial excitation.

Independent evidence has been reported which suggests that a form of chlorophyll absorbing near 700 mμ participates in the light reaction of photosynthesis. Using an apparatus involving a specially-designed rotating sector, Kok has studied transients in the absorption of photosynthetic systems following a millisecond pulse of illumination.[42, 43] The difference spectra resulting from these measurements are complex and suggest the

[41] R. Emerson and W. Arnold, J. Gen. Physiol. 15, 391-420; 16, 191-205 (1932).

[42] B. Kok, Biochim. et Biophys. Acta 22, 399-401 (1956); 48, 527-33 (1961).

[43] B. Kok and G. Hoch, in Light and Life, W. D. McElroy and B. Glass, Editors (Johns Hopkins Press, Baltimore, 1961), pp. 397-416.

participation of several factors. Nevertheless, the most prominent feature in the difference spectra, not only of chloroplasts from higher plants but also in algae (Porphyra, Nitzschia, Nostoc, Anacystis, Scenedesmus), is a decrease in absorbance at 700 to 705 mμ induced by the light pulse. The effect is reversible, and the back reaction was reported to have a time constant of 10 msec, under the conditions of the experiment. In Anacystis one of the most prominent of the other absorption changes was a photoinduced increase in absorbance at 520 mμ.[44] In Chlorella the time constant associated with the reversal of the change at 520 mμ following the light pulse was found to be identical with that for the decay of the change at 700 mμ.[45] A number of cytochromes have an absorption band in the region 500 to 550 mμ, in addition to strong Soret bands between 400 and 450 mμ.[46] Both the change at 520 mμ and, recently, the change at 700 mμ have been observed by Witt.[38, 40, 47, 48]

In this study the cytochrome Soret bands are located in the region of very strong absorption by the much larger amounts of chlorophyll and carotenoid present. At 520 mμ, however, the absorption of these other pigments is substantially reduced, and that due to cytochrome would represent a much larger fraction of the total absorption. It is interesting to note in Fig. 1-3 that the dichroic ratio spectrum exhibits a small, but pronounced, maximum in this region. If our hypothesis that the cytochrome is located at the site of the organized chlorophyll molecules is correct, then an increase in the overall dichroism due to cytochrome absorption would be expected if the cytochrome molecule were oriented at the site. The maximum in the dichroic ratio near 520 mμ is highly suggestive that this is the case, although this region of the spectrum has not been studied sufficiently well for one to be certain of the precise nature of the maximum.

---

[44] B. Kok, Nature 179, 583-4 (1957).

[45] B. Kok, Acta Botanica Neerland. 6, 316 (1957).

[46] H. Lundegardh, Nature 192, 243-8 (1961).

[47] R. Moraw and H. T. Witt, Z. physikal. Chem. (Frankfurt) 29, 1-12 (1961).

[48] H. T. Witt, A. Müller and B. Rumberg, Nature 192, 967-9 (1961).

2. SOME MEASUREMENTS OF MAGNETO-OPTIC ROTATORY DISPERSION SPECTRA

Robley C. Williams, Jr., and Gaylord M. Androes

Introduction

In 1845 Michael Faraday discovered that a beam of polarized light passed through a material in a magnetic field undergoes rotation of its plane of polarization. This magneto-optic rotation is not dependent upon the presence of asymmetric carbon atoms in the material, but is directly proportional to the strength of the applied magnetic field, to the concentration of the material, and to the length of the light path in the material. A specific rotation of the form

$$[\alpha]_m^\lambda = \theta/c\,l\,H\cos\phi$$

may thus be assigned to a given substance, where $[\alpha]_m^\lambda$ is the specific magnetic rotation of the material at a given wavelength, θ is the rotation of the plane of polarization due to the sample, H is the magnetic field strength, ϕ is the angle between the direction of the field and the direction of the light beam, c is the concentration of the sample, and l is the length of the sample through which the light travels.

Specific magnetic rotation is found to vary with wavelength, outside of optical absorption bands, in a manner given approximately by the relation

$$[\alpha]_m = A\nu^2/[\nu_0^2 - \nu^2]^2,$$

where $[\alpha]_m$ is the specific magnetic rotation, ν is the frequency at which the specific rotation is calculated, ν_0 is the frequency at which the peak of the nearest electronic transition occurs, and A is a constant of the material. Thus, for a material with a strong absorption band in the blue or ultraviolet, specific magnetic rotation is expected to increase in the direction of shorter wavelengths.[1]

In late 1960 some results appeared which indicated that a number of compounds having singlet → triplet excitation states exhibit peaks in their magneto-optic rotation spectra at wavelengths corresponding closely to the wavelengths at which triplet → singlet emission bands are seen in their flash-photolysis spectra.[2] This effect was said to be particularly pronounced in azobenzene, phenazine, and benzophenone in solution, and in polystyrene films.

In this study an attempt is made to verify this observation. We have repeated several of the experiments described by Shashoua.[2] The triplet → singlet transitions in the homologous series benzene-naphthalene-anthracene-pyrene have been the subject of considerable study.[3] Thus, the magneto-optic

[1] Irwin Tobias and Walter Kauzmann, J. Chem. Phys. 35, 538 (1961).

[2] Victor E. Shashoua, J. Am. Chem. Soc. 82, 5505 (1960).

[3] G. Porter and M. Windsor, Discussions Faraday Soc. 17, 178 (1954).

rotation spectra of the members of this series have also been measured and compared with their known triplet → singlet transitions.

Equipment

In order to investigate this effect a Rudolph High Precision polarimeter was equipped with a monochromator and an electromagnetic solenoid producing a uniform field parallel to the light beam. A Beckman Model DU monochromator with a tungsten lamp is used to produce light in a band of wavelengths of theoretical half-intensity band width between 0.6 mμ and 5 mμ at 350 mμ and 700 mμ, respectively. This beam is collimated, passed through a fixed Nicol prism (polarizer), and then through the sample, which is mounted in the solenoid in an accurately reproducible position. The beam is then passed through a Nicol prism (analyzer), mounted so that it may be rotated about its optic axis and its angular displacement from an arbitrary zero measured. The beam then strikes a photomultiplier tube whose response registers on a voltmeter.

Measurement

In a solution, measurements are made by finding the analyzer setting at which a minimum intensity of light is transmitted through the analyzer with the solution in place, finding the corresponding setting with the solvent in place, and then taking the difference of these two settings as the rotation of the plane of polarization of the incident light due to the solute.

The light intensity striking the photomultiplier varies as the cosine squared of the angle through which the analyzer is rotated (see Fig. 2-1). Since this variation is symmetric about the angle θ_0 of minimum transmission, measurements are made by finding two angles, θ_1 and θ_2, where the transmitted intensity has convenient and equal values; θ_0 is then given by the mean of θ_1 and θ_2.

Considerable mechanical, electronic, and optical difficulty was experienced with the apparatus. When finally operating correctly, the instrument was found to exhibit a rms deviation of $\pm 0.01^{\circ}$ in the range 450 to 650 mμ, and a somewhat larger imprecision near the limits of the visible spectrum. This imprecision is, of course, doubled in the calculation of θ_0 for the solute.

When possible, the visible range of the spectrum was examined for each compound investigated, points were taken at 10-mμ intervals, and two or three complete measurements were made at each spectral point considered. Sample temperature was $30 \pm 5^{\circ}$ C, due to heating of the solenoid, and the sample was allowed to come to thermal equilibrium with its surroundings before measurements were attempted.

Magnetic rotation spectra were measured in solutions containing azobenzene, benzophenone, phenazine, benzene, naphthalene, anthracene, and pyrene. Results, except as otherwise noted, are expressed as specific magnetic rotation: degrees of rotation per molar concentration of solute,

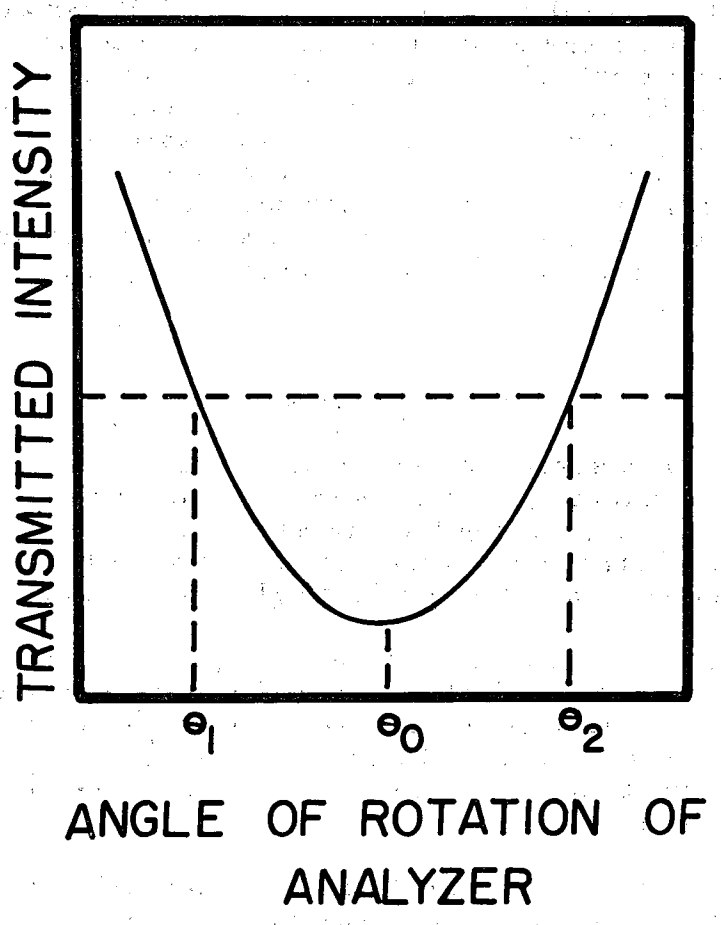

MU-24774

Fig. 2-1. Intensity transmitted through the polarimeter as a function of the angle through which the analyzer is rotated.

per centimeter of path length, per 1,000 gauss of magnetic field. Except where noted, the measurements were made in a 10-cm tube and at a field strength of 1,450 gauss. Each magnetic rotation spectrum is accompanied by an optical absorption spectrum showing absorption of 1 cm of the solution used in the rotation measurements.

Experimental Results

Previously Measured Compounds

Attempts were made, without success, to reproduce the results reported by Shashoua[2] for the compounds azobenzene, benzophenone, and phenazine.

Azobenzene

The magnetic rotation spectrum of azobenzene at a concentration of of 5.5×10^{-3} molar in isooctane was measured in tubes of different lengths in order to provide measurable light intensities in the absorption region (see Fig. 2-2). The concentration and field strength matched closely those used by Shashoua, and path lengths were longer than or equal to his. Measurements were made in a 1-cm tube in the absorption region, and in 2-, 5-, and 10-cm tubes outside this region. In no case was a rotation observed that was unequivocally greater than the estimated experimental imprecision. A comparison of Fig. 2-2 with the azobenzene spectrum in Ref. 2, which has a reported experimental imprecision of $\pm 0.01^{\circ}$ indicated by the vertical lines, shows that they bear no relation to each other.

Phenazine

An attempt was made to duplicate the experiment of Shashoua by using iodomethane as a solvent for this compound. The results are of dubious value, since the solvent either decomposed or reacted with the solute during the course of the measurements, as indicated by an obvious discoloration of the solution. None of the sharp peaks reported at 680, 625, and 578 mμ were seen. Measurements were then made with benzene as a solvent (see Fig. 2-3), but only small rotations were seen. The possibility of peaks at 625 and 680 mμ is not ruled out by these data, but the nature of the magnetic rotation spectrum of phenazine must be considered as doubtful at this time. It is suggested that this magnetic rotation spectrum be remeasured, with iodoethane used as a solvent.

Benzophenone

The magnetic rotation spectrum of benzophenone showed a peak (Fig. 2-4), but this is probably an artifact owing to absorption which increases strongly at wavelengths less than 400 mμ. The position of the apparent rotation peak may be shifted by variation of the spectral purity of the light beam. As can be seen in Fig. 2-4, the optical absorption of benzophenone increases very sharply below 400 mμ, thereby decreasing the intensity of light transmitted through the instrument at shorter wavelengths. Thus, at the 390-mμ setting on the monochromator, any stray light of wavelength

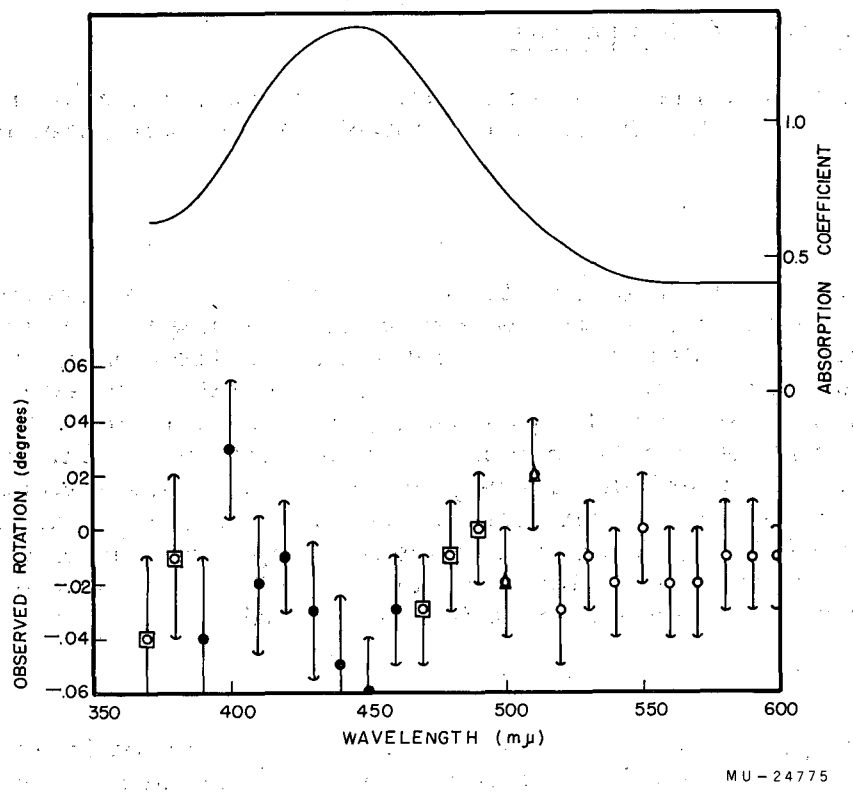

Fig. 2-2. Observed magnetic rotation of azobenzene solution. Rotation of 10 cm of solution is represented by open circles, rotation of 5 cm by triangular points, of 2 cm by square points, and of 1 cm by filled circles. In this and subsequent figures the vertical lines represent estimated (r. m. s) experimental uncertainty.

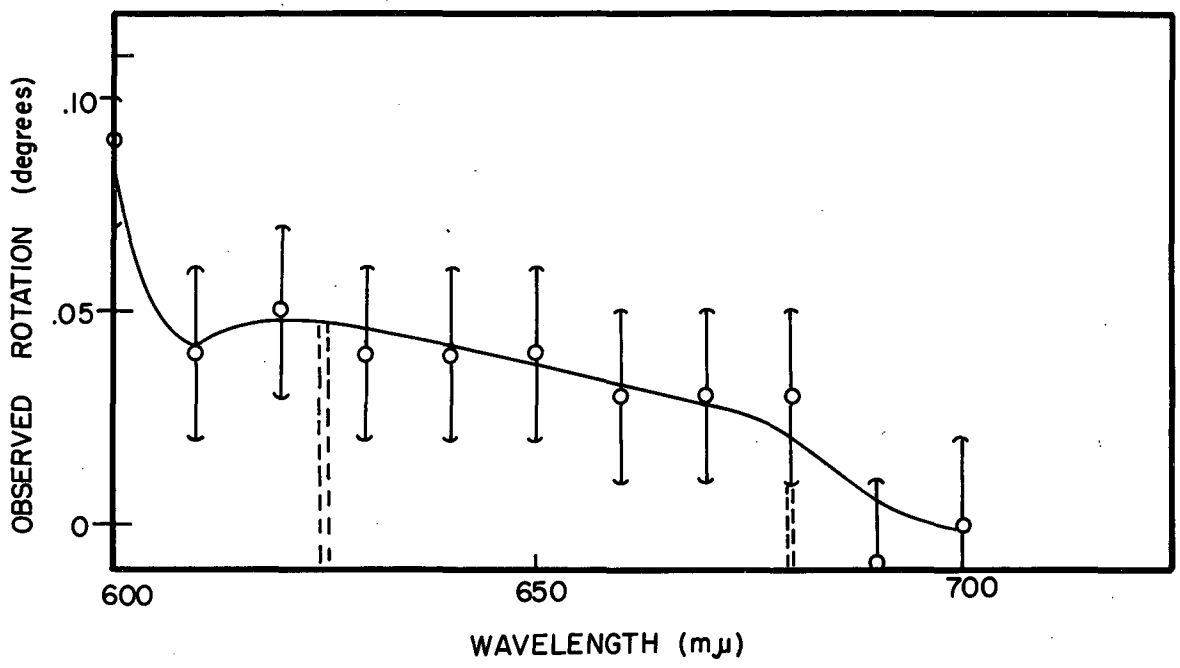

MU-24776

Fig. 2-3. Observed magnetic rotation of 10 cm of a saturated solution of phenazine in benzene. The positions of rotation maxima reported in Ref. 2 are indicated by double dashed lines. Optical absorption is essentially zero through the range of wavelengths measured.

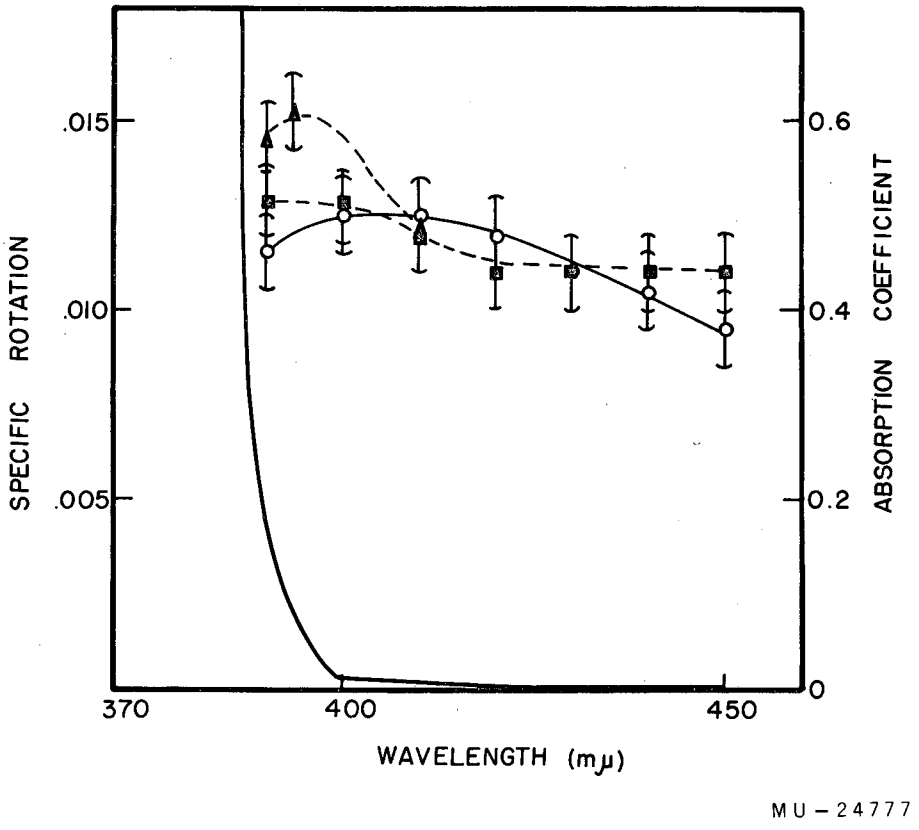

Fig. 2-4. Specific magnetic rotation of benzophenone. Measurements made with a 10-cm path length are represented by open circles, with a 5-cm path length by square points, and with a 5-cm path length and interference filters by triangular points.

above 400 mμ that may be present in the beam from the monochromator becomes a large fraction of the total light striking the photomultiplier. The magnetic rotation corresponding to these longer wavelengths is smaller than that corresponding to 390 mμ, and thus the presence of stray light of long wavelength causes an apparent peak in the rotation spectrum.

This effect is shown by keeping the solute concentration constant and repeating the measurements in a 5-cm tube. In the shorter tube more of the incident monochromatic light is transmitted and hence the long-wavelength stray light is a smaller fraction of the total transmitted light than it is in a 10-cm tube. The result is that the apparent rotation peak now occurs at a shorter wavelength. This effect is shown more strikingly by using a 5-cm tube and placing interference filters in the beam to increase spectral purity. As can be seen, this method shifts the peak still farther toward shorter wavelengths than the measurements in the 5-cm tube without filters.

Although the experimental imprecision and the small specific rotation of benzophenone make this shifting of the apparent rotation peak somewhat equivocal, the same effect has been seen much more strikingly in pyrene (see below), and it is quite probable that the magnetic rotation peak at 425 mμ observed by Shashoua in the benzophenone rotation spectrum is an artifact of this kind.

Benzene Homologues

Flash-photolysis investigations by Porter and Windsor of the emission spectra of a number of benzene homogues in solution[3] have indicated the presence of emission bands from long-lived excited states, almost certainly triplets. The magnetic rotation spectra of naphthalene, anthracene, and pyrene were measured in order to investigate the possibility that one or more of these compounds might show magnetic rotation peaks corresponding in position to the positions of their triplet emission bands. No such peaks were found. The spectra are reproduced in graphs below, and the position of their triplet → singlet emission bands are indicated by double broken lines.

Naphthalene

The magnetic rotation spectra of naphthalene, 3.12 M in benzene and 0.763 M in n-hexane, are shown in Fig. 2-5, and it is noted that the specific magnetic rotation of naphthalene is affected somewhat by the nature of the solvent. This may be due to a partial complexing of naphthalene with the benzene solvent, which does not occur with the n-hexane solvent.

Anthracene

Measurements were made of the magnetic rotation spectrum of 0.089 M anthracene in benzene. The sample used in this set of measurements was not pure, as indicated by the fact that it had a slight yellow color and an absorption spectrum unlike that commonly found for pure anthracene (Fig. 2-6). The small dip in the rotation spectrum at 480 mμ may well be due to impurities, since it occurs at an absorption maximum of the impurity, where an ordinary Cotton-effect inversion is to be expected in the impurity. At any rate, it does not occur near either of the two triplet → singlet emission

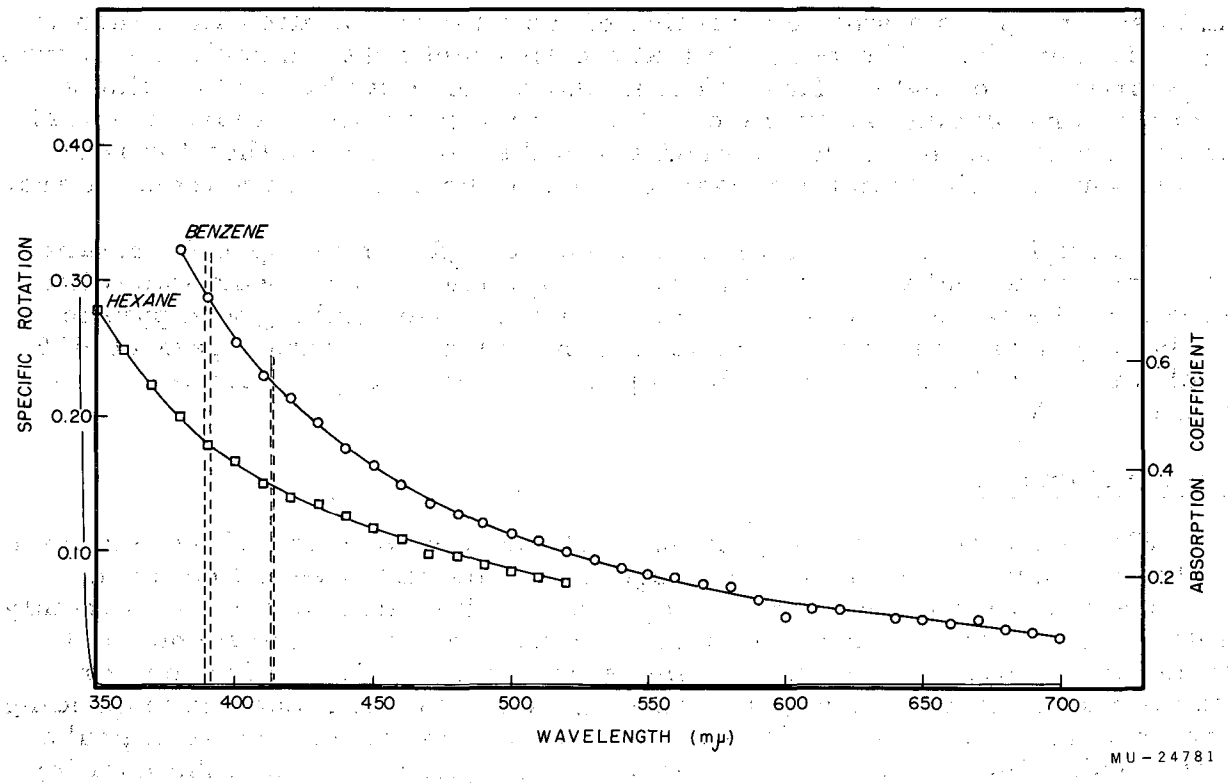

Fig. 2-5. Specific magnetic rotation of naphthalene. Measurements made in n-hexane are indicated by square points, those made in benzene by round points. The experimental error is indicated by the size of the points.

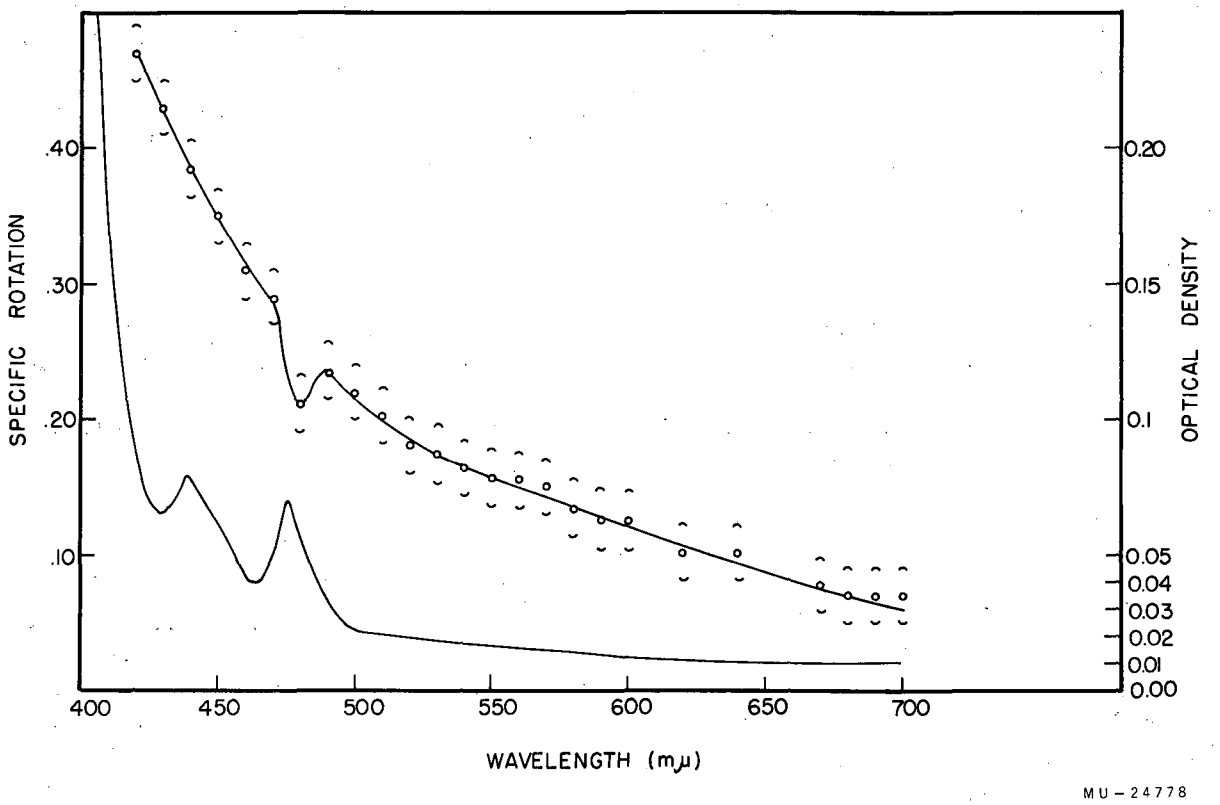

Fig. 2-6. Specific magnetic rotation of anthracene. The peak in the optical absorption spectrum at 475 mμ is due to an impurity.

bands in the visible. Unfortunately, no measurements could be made at the triplet band at 420 mμ because of high optical absorption below this wavelength.

Pyrene

The magnetic rotation spectrum of pyrene, measured at 0.276 M concentration in benzene, shows quite clearly the artifact peak due to the absorption band (Fig. 2-7). The specific magnetic rotation and solubility of this compound are high enough that an unequivocal check could be made on the apparent peak. The specific magnetic rotation computed from the 5-cm cell quite clearly continues to rise through the region where a maximum is observed for the 10-cm cell, and appears to approach a new maximum near 390 mμ. As in the benzophenone spectrum presented above (Fig. 2-4), the apparent leveling of the curve as the absorption band is entered may or may not be meaningful. The important fact is that a peak that occurs at the shoulder of an absorption band is suspect.

Benzene

The rotation spectrum of benzene was measured, and its specific rotation is included in Fig. 2-8 for the purposes of comparison with its higher homologues. The molar concentration of liquid benzene at 30° C is taken to be 10.1. It is to be noted that in this series, the specific magnetic rotation increases as the molecular weight of the compound increases.

Conclusions

The measurements seem to indicate that under the stated conditions, in the compounds previously examined by Shashoua and in the benzene homologues investigated, there is no peak of measurable magnitude in the magneto-optic rotation spectrum at the wavelengths of the triplet → singlet emission bands.

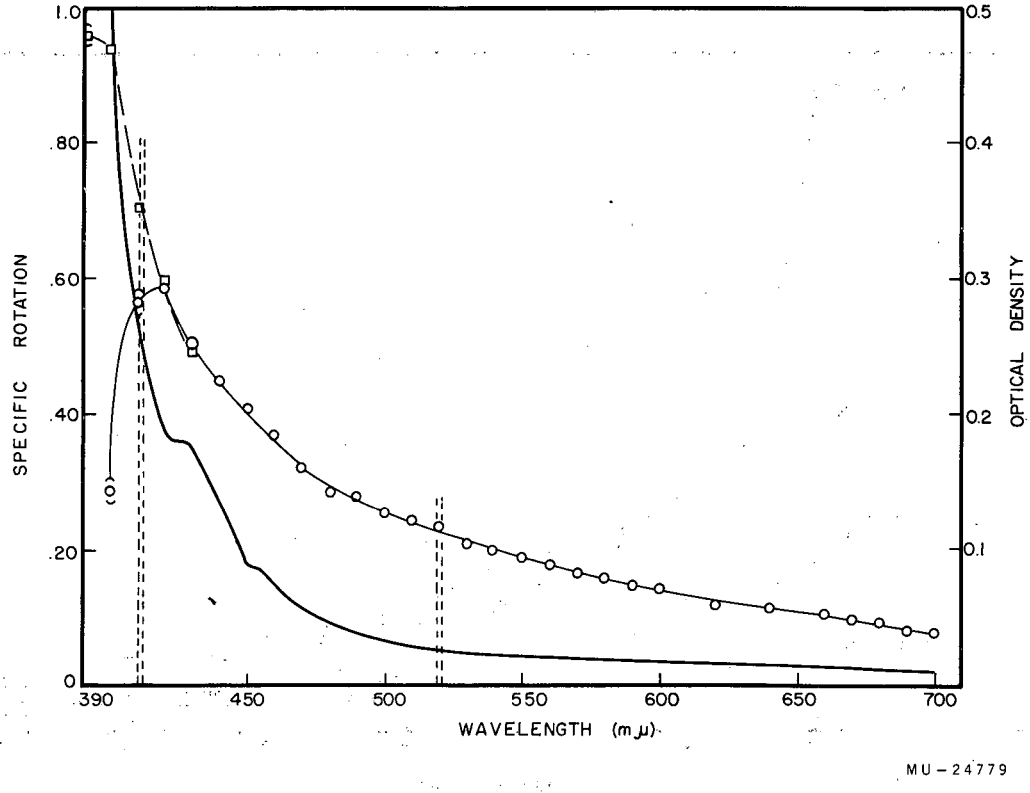

Fig. 2-7. Specific magnetic rotation spectrum of pyrene.
O 10-cm path length
□ 5-cm path length
Where experimental error is not shown it may be taken as indicated by the sizes of the experimental points.

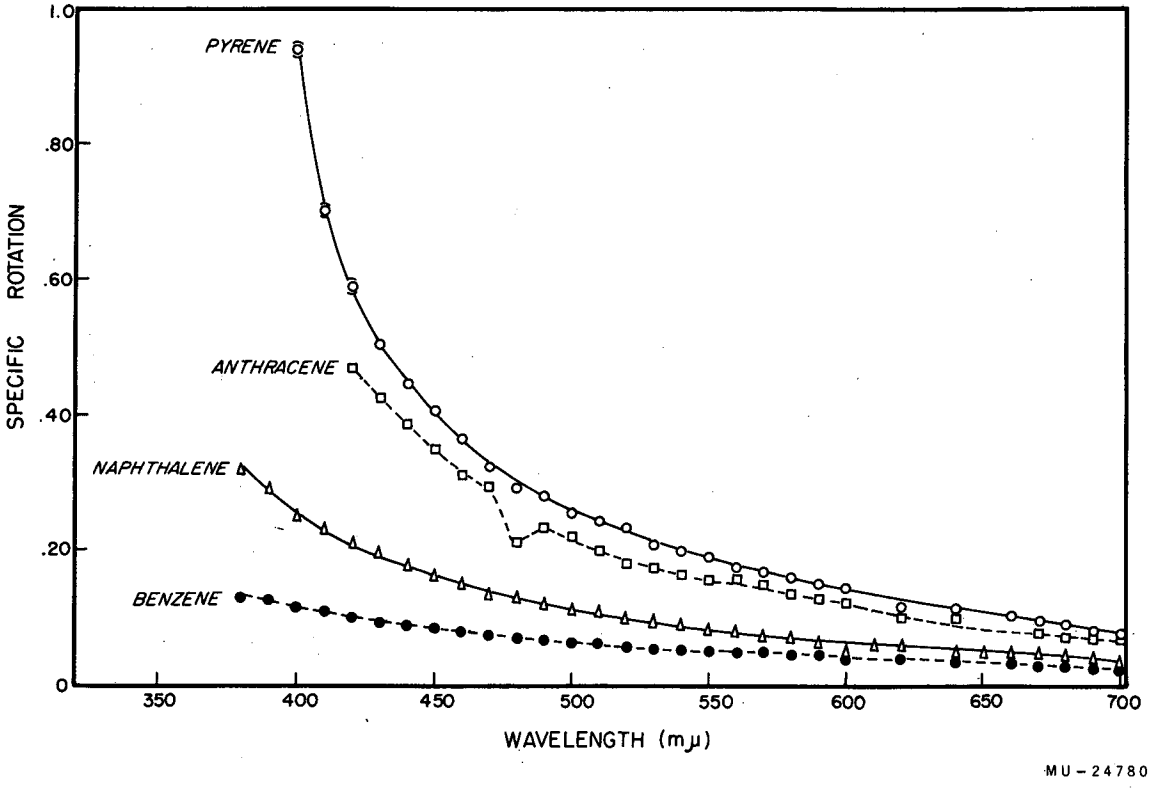

Fig. 2-8. Specific magnetic rotation of benzene and its homologues, naphthalene, anthracene, and pyrene.

3. OXIDATION STATES OF MANGANESE HEMATOPORPHYRIN IX IN AQUEOUS SOLUTION

Paul Loach

Summary

Manganese hematoporphyrin IX and its dimethyl ester have been prepared. The most stable form of these complexes was shown to be one in which manganese exists in the 3+ oxidation state. Magnetic susceptibility measurements yielded values in agreement with the presence of four unpaired electrons for both the free acid and its dimethyl ester in the solid state and in aqueous solution.

Two other oxidation states were demonstrated to be reversibly obtainable in aqueous alkaline solution. Oxidation-reduction potentials are reported for the system Mn^{III}/Mn^{II} hematoporphyrin IX between pH 8.3 and 12.9, and also for the system Mn^{IV}/Mn^{III} hematoporphyrin IX between pH 11 and 13. Both systems show evidence for an oxidation-linked proton function in Mn^{III} hematoporphyrin IX with a pK' value of 12. The presence of this proton function was also demonstrated by its spectrophotometric determination, and it is suggested that this pK'_a reflects the loss of a proton by a coordinated water molecule. Data for the Mn^{IV}/Mn^{III} hematoporphyrin IX system indicate the presence of two oxidation-linked proton functions in Mn^{IV} hematoporphyrin IX having pK'_a values below 10. It is suggested that these reflect the loss of a proton by each of two water molecules, one in coordination position 5 and the other in coordination position 6.

Mn^{IV} hematoporphyrin IX was found to be a very strong oxidizing agent and its reduction to Mn^{III} hematoporphyrin IX in aqueous alkaline solution was observed to occur without the addition of reducing agents. The results are discussed in relation to existing data on metalloporphyrin systems and also with respect to primary events in photosynthesis.

A study has been in progress in this Laboratory concerned with the light-catalyzed reactions of manganese phthalocyanine.[1,2] In addition, manganese etioporphyrin I has been prepared and a light-catalyzed reduction in pyridine solution is suggested by the data.[3] Both these manganese complexes are readily soluble in solvents such as pyridine or α-chloronaphthalene, but are almost totally insoluble in water. In an extension of these studies this report deals with two water-soluble manganese prophyrin systems, manganese hematoporphyrin IX and its dimethyl ester.

---

[1] E. Markham, in Bio-Organic Chemistry Quarterly Report, UCRL-9041, Dec. 1959, p. 55; UCRL-9208, June 1960, p. 40

[2] A. Yamamoto, in Bio-Organic Chemistry Quarterly Report, UCRL-9652, April 1961, p. 55.

[3] E. Markham and G. Engelsma, in Bio-Organic Chemistry Quarterly Report, UCRL-9652, April 1961, p. 43. Also, G. Engelsma, private communication.

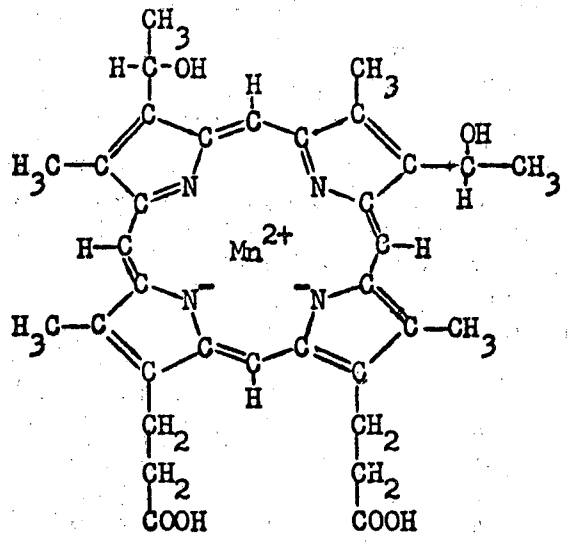

(The oxidation state of manganese is arbitrarily written as 2.)

As one of the many studies of metalloporphyrin systems carried out in the laboratory of W. M. Clark,[4-6] Taylor prepared manganese mesoporphyrin IX and studied its properties in water containing 20% pyridine.[4] From potentiometric data he found that two oxidation states of manganese mesoporphyrin IX can exist. These were assumed to be the complexes in which manganese has the oxidation states of 2+ and 3+. All efforts to examine a reversible system in the absense of added ligand molecules were without success. Large amounts of aggregation were suspected as the cause of the problems encountered. In the study presented here, manganese hematoporphyrin IX was found to be sufficiently soluble in water that difficulty of this sort was not a limiting factor even in the absence of added ligand molecules.

Materials

Hematoporphyrin IX dihydrochloride was obtained from the California Corporation for Biochemical Research and was purified in the following manner. The dimethyl ester was first prepared by dissolving 1 g hematoporphyrin IX dihycrochloride in absolute methanol previously saturated with

[4] W. M. Clark, J. F. Taylor, T. H. Davies, and C. S. Vestling, J. Biol. Chem. 135, 543 (1940).

[5] J. Shack and W. M. Clark, J. Biol. Chem. 171, 143 (1947).

[6] R. W. Cowgill and W. M. Clark, J. Biol. Chem. 198, 33 (1952).

dry hydrogen chloride. The mixture was stoppered, stirred magnetically, and allowed to react for 6 hours at 0° C. At the end of this time the pigment was extracted with 200 ml of a 1:1 mixture of chloroform and water. Some pigment remaining in the aqueous phase was further extracted with 100 ml chloroform and this material combined with the rest of the chloroform fraction, which was subsequently washed with five 200-ml portions of glass-distilled water followed by three 300-ml portions of 0.05 N NH_4OH. After evaporation of the chloroform solvent, the pigment was taken up in 5 ml of a 1:1 mixture of chloroform and ligroin (petroleum ether, bp = 120 to 135° C) and applied to a silica gel column. The preparation of the silica gel for the column and its use for purification of porphyrins has been described by Orten.[7,8] The column used in this work was prepared with 50 g of silica gel and was 2 cm in diameter by 30 cm long. About 200 ml of a 1:4 mixture of chloroform and ligroin was first used to develop the column. With this solvent a fast-running band containing 1 to 2% of the pigmented material came off the column. At this point, the developing solvent was changed to a 7:3 mixture of chloroform and ligroin. The hematoporphyrin IX dimethyl ester band moved down the column, broadening considerably as it went, and was collected in about 300 ml of eluent. A very narrow band, which was presumably composed of unesterified porphyrin and metal-complexed prophyrin, remained at the top of the column. Throughout the procedure care was taken to protect the pigment from light.

The fraction containing hematoporphyrin IX dimethyl ester was evaporated to dryness and the residue taken up in 50 ml of glacial acetic acid; 2 g of manganese diacetate was pulverized and added to the solution of pigment in a 250-ml Erlenmeyer flask. The system was loosely stoppered and stirred magnetically in the dark, and the course of the reaction was followed spectrophotometrically. The temperature was about 20° C. According to the absorption spectrum, 99+% of hematoporphyrin IX dimethyl ester had been converted to a manganese complex in the first 6 hours (see Fig. 3-1). After 22 hr total reaction time, the acetic acid was evaporated at about 15° C under reduced pressure and the residue was taken up with a small amount of water. After drying over P_2O_5 and KOH, the pigment was separated from excess manganese diacetate by dissolving it in benzene, evaporating the solvent in vacuum, and redissolving the residue in benzene. This procedure was repeated four times. After the last benzene solution was evaporated to dryness, the manganese hematoporphyrin IX complex was taken up in a small amount of water and evaporated to dryness over P_2O_5 and KOH. A carbon-hydrogen-manganese analysis is given in Table 3-I together with calculated values for possible complexes. It is apparent from Table 3-I that several complexes would satisfy the analysis.

As a further step in purification, the manganese hematoporphyrin IX dimethyl ester complex was dissolved in water and then precipitated from solution by the addition of enough potassium chloride to make the system half-saturated with this salt. Such precipitation was repeated a total of three times, and the solid was dried and extracted with benzene to separate the

[7] L. M. Marshall, J. M. Orten, and A. H. Smith, J. Biol. Chem. 179, 1127 (1949).

[8] J. Lucas and J. M. Orten, J. Biol. Chem. 191, 287 (1951).

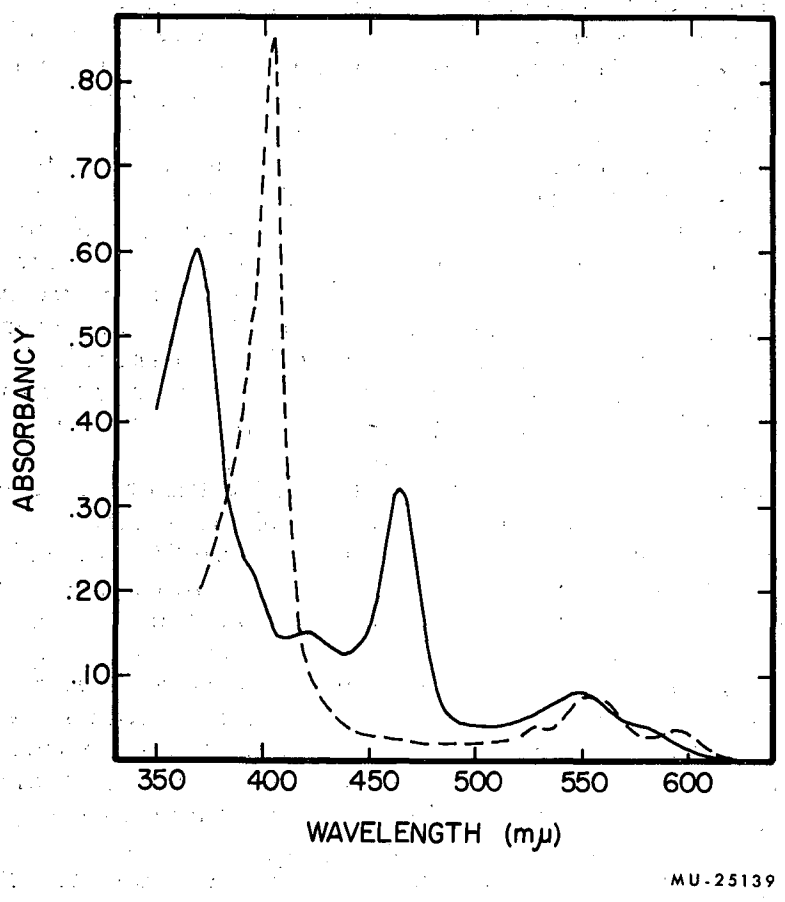

Fig. 3-1. Spectra of hematoporphyrin IX dimethyl ester (dashed curve) and manganese hematoporphyrin IX dimethyl ester (solid curve) in glacial acetic acid. Concentrations are not equivalent although both are near 5×10^{-6} M; 1-cm cuvette; room temperature.

Table 3-I. Elemental analysis of manganese hematoporphyrin IX dimethyl ester

Element	Found	Composition calculated for complex a	b	c	d
carbon	60.5	60.3	61.8	60.4	60.5
hydrogen	6.0	6.0	5.9	5.8	6.1
manganese (determined as Mn_3O_4)	7.5	7.3	7.5	6.9	7.7

a. Mn^{III} hematoporphyrin IX dimethyl ester monoacetate monohydrate.

b. Mn^{III} hematoporphyrin IX dimethyl ester monoacetate.

c. Mn^{IV} hematoporphyrin IX dimethyl ester diacetate.

d. Mn^{III} hematoporphyrin IX dimethyl ester monohydroxide monohydrate.

manganese hematoporphyrin IX dimethyl ester complex from KCl. After four such benzene extractions the material was dissolved in a small amount of water and dried over KOH and P_2O_5 in vacuum. Analysis of this chloride derivative may be found in Table 3-II along with theoretical values for possible complexes. The data of Tables 3-I and 3-II suggest that the metal complexes formed are Mn^{III} hematoporphyrin IX dimethyl ester monoacetate monohydrate and Mn^{III} hematoporphyrin IX dimethyl ester monochloride monohydrate.

Table 3-II. Elemental analysis of manganese hematoporphyrin IX dimethyl ester

Element	Found	Composition calculated for complex a	b	c	d
carbon	58.9	59.0	59.0	60.5	57.5
hydrogen	5.8	5.8	5.6	5.6	5.4
chloride	5.0	4.9	4.9	5.0	9.5
manganese (determined as Mn_3O_4)	8.0	7.5	7.5	7.7	7.3

a. Mn^{III} hematoporphyrin IX dimethyl ester monochloride monohydrate.

b. Mn^{IV} hematoporphyrin IX dimethyl ester monochloride monohydroxide.

c. Mn^{III} hematoporphyrin IX dimethyl ester monochloride.

d. Mn^{IV} hematoporphyrin IX dimethyl ester dichloride.

Not given in either Table 3-I or 3-II are the results of nitrogen determinations. In each case low values were obtained, and identical samples failed to give consistent values, whereas carbon and hydrogen determinations were quite reproducible. Typical results were between 6.0 and 7.5% when the amount expected was 7.6 to 7.8%. It is possible that stable nitrogen-manganese complexes are formed during preparation of the sample for analysis so that not all the nitrogen is released for assay.

In addition to these two dimethyl ester derivatives, the free acid complex was prepared. One g of hematoporphyrin IX dihydrochloride was dissolved in 50 ml of glacial acetic acid and 2 g of manganese diacetate added as before. The reaction mixture was loosely stoppered, stirred in the dark, and its progress followed by spectrophotometry for 24 hours. The acetic acid was evaporated and the pigment dried over KOH and P_2O_5. This complex was then dissolved in 0.1 N KOH half saturated with KCl, and precipitated from solution by dropwise addition of concentrated HCl. Such precipitation was repeated five times and the final dried solid extracted with a minimum amount of absolute methanol. The methanol extraction and evaporation was repeated six times to separate manganese hematoporphyrin IX from KCl, and the material was dried in a vacuum over P_2O_5 and KOH. Analysis of this compound is given in Table 3-III together with theoretical values for possible complexes. It is immediately apparent that one chloride per molecule is not present. If it is assumed that this complex is Mn^{III} hematoporphyrin IX, as its absorption spectrum indicates, then the net positive charge on the molecule must be balanced by an anion; if it is not chloride, it must be either hydroxide or a carboxylate group of one of the propionate side chains. The former is not likely, since the chloride derivative of the dimethyl ester was easily prepared. The latter is in keeping with a generally hypothesized polymerization of metalloporphyrin systems having free carboxyl groups. Thus, it is assumed that the solid material has the structure shown on the facing page, where the net charge of the manganese hematoporphyrin

Table 3-III. Elemental analysis of manganese hematoporphyrin IX

Element	Found		Composition calculated for complex		
	1	2	a	b	c
carbon	64.4	61.2	62.6	59.5	61.0
hydrogen	5.7	5.7	5.4	5.3	5.6
chloride	0.9	3.9	0	5.2	0
manganese (determined as Mn_3O_4)	8.1	8.0	8.4	8.0	8.2

a. Mn^{III} hematoporphyrin IX.

b. Mn^{III} hematoporphyrin IX monochloride.

c. Mn^{III} hematoporphyrin IX monohydrate.

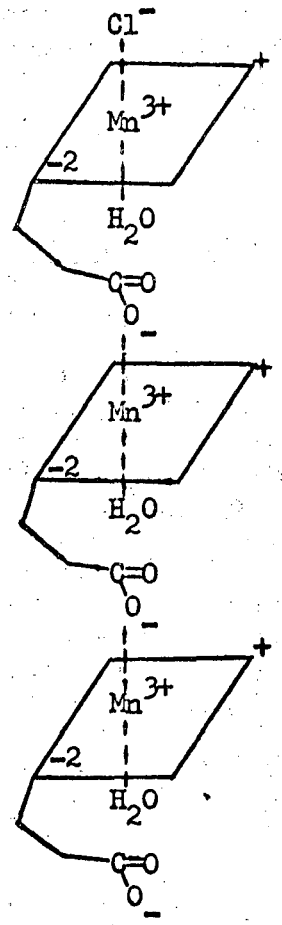

etc.

complex is written outside the rhombus. The rhombus represents the porphyrin ring and side chains, with the exception of one propionic acid chain involved in salt linkage to another molecule. The "-2" written inside the rhombus represents the charge distributed on the pyrolle nitrogen atoms of the prophyrin ring, and the "3+" indicates the oxidation state of manganese. Other molecules in coordination positions 5 and 6 are written above and below the plane of the porphyrin.

In the studies described, the compound whose analysis is given in Table 3-III, as well as the two dimethyl ester derivatives (analyses given in Tables 3-I and 3-II), were used as sources of Mn^{III} hematoporphyrin IX. The dimethyl ester derivatives were first saponified at alkaline pH.

Methods

The procedures and apparatus used in oxidation-reduction potentiometry were essentially those described by Harbury.[9] Absorption spectra were

[9] H. A. Harbury, J. Biol. Chem. 225, 1009 (1957).

recorded with a Cary Model 14 M spectrophotometer. A Beckman Model 76 expanded-scale pH meter and a Beckman Glass Electrode with Type E2 glass were used for making pH measurements. The apparatus used for making magnetic susceptibility measurements on small amounts of solid samples has been described by Cunningham.*[10]

Results and Discussion

Simple metalloporphyrin compounds are known to exhibit large aggregation effects in aqueous solution.[4, 5, 11, 12] One of the first needs in this study was to determine whether or not monomeric manganese hematoporphyrin IX could exist in aqueous solution at concentrations that would permit its physical properties to be studied. In Fig. 3-2 is shown a plot of the molar absorbancy index versus log concentration for Mn^{III} hematoporphyrin IX dimethyl ester monoacetate monohydrate in methanol and in water. Behavior similar to that in methanol has also been observed for ethanol and chloroform solutions. The lack of dependency of a_m upon concentration could mean that Mn^{III} hematoporphyrin IX dimethyl ester is monomeric in alcohol and chloroform solutions. It is of course possible that aggregates could be forming without effect upon the absorption spectrum, but this is not likely for such a highly conjugated system as a metalloporphyrin complex. Another possibility is that a distinct polymeric unit, such as a dimer, exists and is very stable. However, molecular-weight determinations in ethanol and chloroform, in which Mn^{III} hematoporphyrin IX dimethyl ester was 4×10^{-3} M, have ruled out the existence of aggregates.

The results shown in Fig. 3-2 for water solutions of Mn^{III} hematoporphyrin IX dimethyl ester indicate that at concentrations above 5×10^{-6} M aggregation occurs. From these data, at a concentration of 10^{-5} M in water solution, over 90% of Mn^{III} hematoporphyrin IX dimethyl ester may be monomeric. Molecular weight determinations with this material, at a concentration of 4×10^{-3} M, also give evidence that aggregation is occurring.

From the elemental analyses, it would appear that the stable form of these manganese hematoporphyrin complexes is one in which the oxidation state of the manganese is 3+. If this is so, the magnetic susceptibility of these compounds should agree with an even number of unpaired electrons, four for a square-planar configuration of the dsp^2 type or two for an octahedral complex of the d^2sp^3 type. The experimental value found at 25° for both solid Mn^{III} hematoporphyrin IX dimethyl ester monochloride monohydrate and solid Mn^{III} hematoporphyrin IX was 4.4 ± 0.1 B. M. The values of 4.5 and 4.8 ± 0.3 B. M. were found for aqueous solutions of each form at a concentration of 3×10^{-2} M. The experimental values given have been corrected for the minor diamagnetic contribution of the porphyrin ring, but the temperature dependence of the susceptibility has not been determined. Since the theoretical value for four unpaired electrons is 4.9 B. M., the

*I wish to thank Dr. Cunningham for the use of this equipment.

[10] B. D. Cunningham, Microchem. J. Symposium, 69 (1961).

[11] A. C. Maehly and A. Åkeson, Acta Chem. Scand. 12, 1259 (1958).

[12] F. Haurowitz, Z. physiol. Chem. 254, 266 (1938).

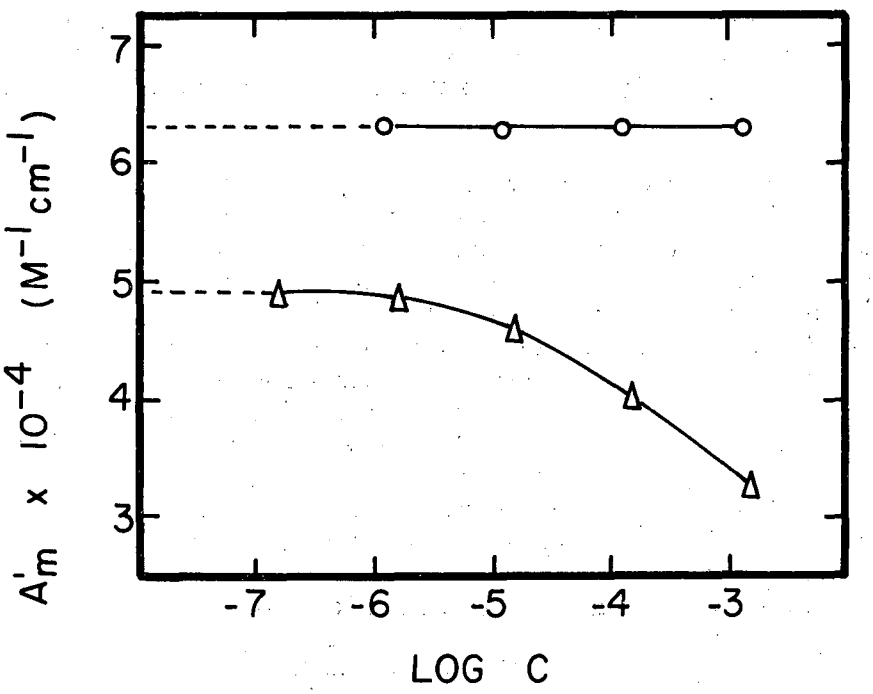

MU-25140

Fig. 3-2. Apparent molar absorbancy index values at 460 mμ for Mn^{III} hematoporphyrin IX dimethyl ester monoacetate monohydrate in methanol (circles) and in water (triangles). No buffer or salt present; room temperature; cuvettes having 0.1-mm to 10-cm path lengths.

experimental results are in support of the conclusion, based upon elemental analysis, that manganese is in the 3+ oxidation state in each complex prepared.

A method used to further test the latter conclusion is paper electrophoresis. In this experiment it would be expected that Mn^{III} hematoporphyrin IX dimethyl ester, having a net positive charge, would move toward the cathode. This was found to be the case for the material whose analysis is in Table 3-I, at both pH 7.5 and 10.0. On the other hand, Mn^{III} hematoporphyrin IX has a net of one negative charge at alkaline pH and would be expected to move toward the anode. The experimental results at pH 10.0 showed this was true for the material whose assay is shown in Table 3-III. Thus, the results are compatible only if the oxidation state of manganese is 3 in each case.

Reductive titration of Mn^{III} hematoporphyrin IX with sodium dithionite solution resulted in the formation of a Mn^{II} hematoporphyrin IX complex. Figure 3-3 shows a representative set of absorption curves recorded in the course of such a titration requiring one equivalent of reducing agent. The normality of the sodium dithionite solution was determined before-hand by titrating a standard potassium ferricyanide solution. All values of E_m are based on complete titrations carried out with concurrent measurement of potentials and spectra. Figure 3-4 shows the potentials corresponding to the absorption spectra of Fig. 3-3. Dilute samples were used in order to favor the monomeric state; the concentration in different titrations ranged from 5×10^{-6} to 2×10^{-5} M. Equilibrium between the electrodes and solutions was established rapidly, usually in a matter of seconds along the central portion of a titration curve, and the results obtained agree well with those predicted for a reversible one-electron oxidation-reduction system:

$$E_h = E_m + \frac{RT}{F} \ln \frac{(Ox)}{(Red)}, \qquad (1)$$

where E_m is the potential of the half-reduced system; at pH 0, $E_m = E_0$.

Potentials for the system Mn^{III}/Mn^{II} hematoporphyrin IX have been determined over a range of pH from 8.2 to 12.9 and the results are summarized in Table 3-IV. The simplest relationship between E_m and pH consistent with the data at hand[13] is

$$E_m = E_x + \frac{RT}{F} \ln \frac{(H^+)}{(H^+) + K_0'}, \qquad (2)$$

where K_0' is an apparent equilibrium constant for an oxidation-linked proton function[14] in Mn^{III} hematoporphyrin IX. E_x is the potential which the half-reduced system would have at pH 0, were there no net oxidation-linked proton functions at values of pH below those covered in this study. In Fig. 3-5 the experimentally determined values of E_m are plotted against pH and are compared with the curve described by Eq. (2) upon assignment of the constants $E_x = -0.346$ volt, $K_0' = 1.26\times10^{-12}$. Differences in observed and calculated values of E_m are given in Table 3-IV.

[13] W. M. Clark and B. Cohen, Public Health Repts. (U.S.) 38, 666 (1923).

[14] J. Wyman, Advances in Protein Chem. 4, 408 (1948).

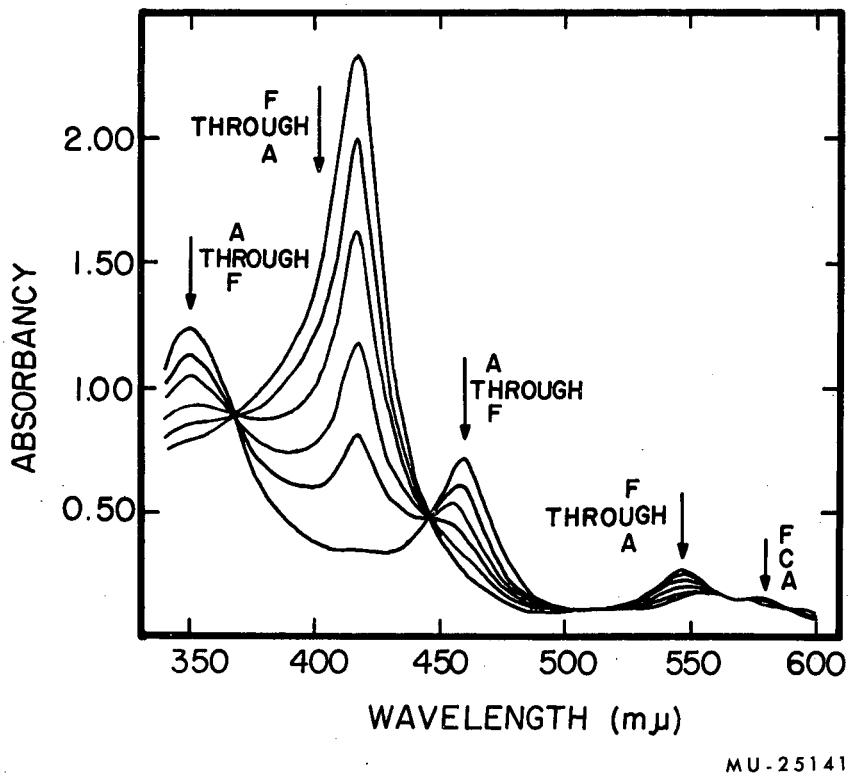

Fig. 3-3. Spectra of Mn^{III} hematoporphyrin IX recorded in the course of a reductive titration. Mn^{III} hematoporphyrin IX, 1.5×10^{-5} M; pH 12.88; temp $22 \pm 2^{\circ}$ C; 1-cm cuvette. Percentage of reduction: A, 0%; B, 24.1%; C, 42.6%; D, 66.4%; E, 84.9%; F, 100%.

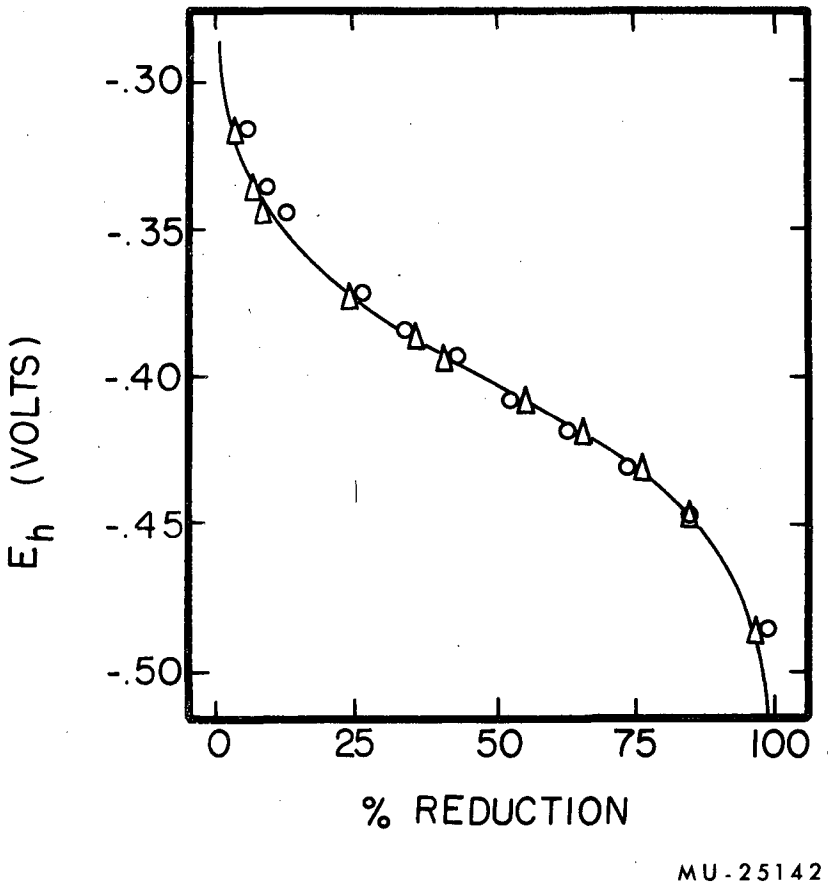

Fig. 3-4. Reductive titration of Mn^{III} hematoporphyrin IX. Mn^{III} hematoporphyrin IX, 1.5×10^{-5} M; pH 12.88; temp $22 \pm 2^{\circ}$ C; reducing agent, sodium dithionite. Solid line, theoretical curve for n = 1, E_m = -0.400 v; o, experimental points with percentage of reduction calculated from volume of reducing agent added; Δ, experimental points with percentage of reduction calculated from spectra shown in Fig. 3-3.

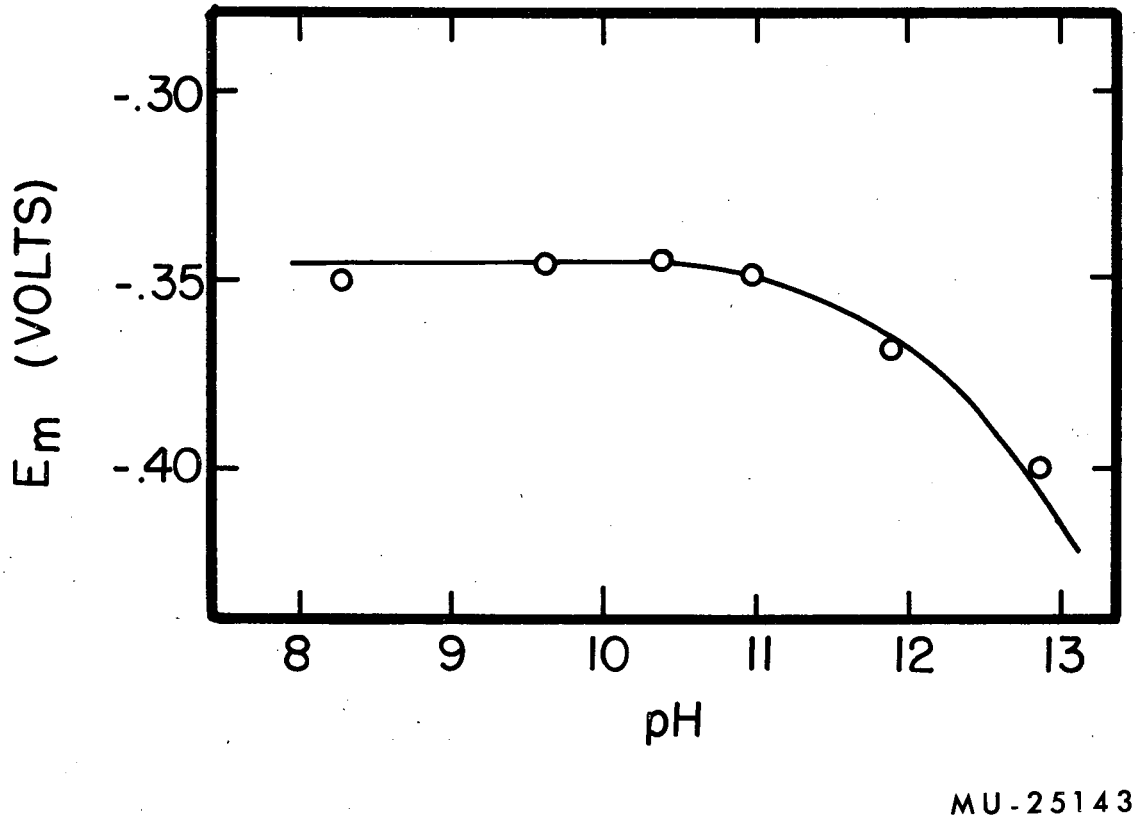

Fig. 3-5. pH dependence of the oxidation-reduction potentials of half-reduced Mn^{III} hematoporphyrin IX. Temp $22 \pm 2^{\circ}$ C; o, experimental values; the solid line represents Eq. (2) with $K_b = 1.26 \times 10^{-12}$ and $E_x = -0.346$ v.

Table 3-IV. E_m values for Mn^{III}/Mn^{II} hematoporphyrin IX system.[a]

pH	Buffer[b]	Titrating agent[c]	E_m observed (v)	E_m calculated (v)	E_m observed $-E_m$ calculated (v)
8.24[d]	I	A	-0.350	-0.346	-0.004
9.62	I	A	-0.346	-0.346	0
10.38	I, II	A	-0.345	-0.346	+0.001
10.97	II	A	-0.349	-0.349	0
11.90	II	A	-0.368	-0.364	-0.004
12.88	II, III	A	-0.400	-0.406	+0.006

a. The temperature for these experiments was $22 \pm 2^{\circ}$ C.

b. I, H_3BO_3-KH_2BO_3; II, K_2HPO_4-K_3PO_4; III, KOH

c. A, sodium dithionite.

d. The concentration of Mn^{III} hematoporphyrin IX in this experiment was 1×10^{-3} M.

Examination of the change with pH in absorption spectrum of Mn^{III} hematoporphyrin IX also reveals the function with $pK_0' = 12$. Figure 3-6 shows these changes, and a plot of pH versus absorbancy at 370 mμ is found in Fig. 3-7. The results obtained agree well with those predicted for a reversible one-proton dissociation,

$$pH = pK_a' + \log \frac{(Ac^-)}{(HAc)} , \qquad (3)$$

where (Ac^-) is the concentration of the conjugate base and (HAc) is the concentration of the conjugate acid. In analogy to Fe^{III} porphyrin systems, the proton equilibrium underlying this pK_0' is assigned to the reaction

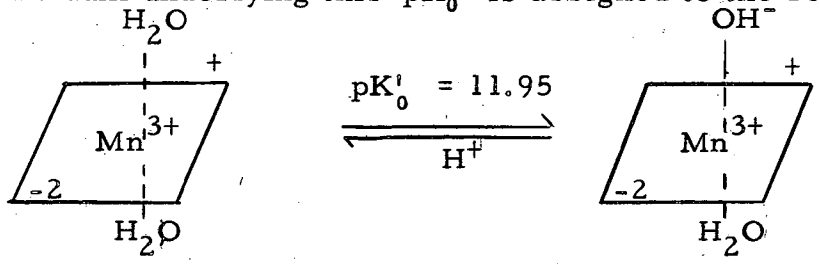

It is of interest that in comparison with most Fe^{III} porphyrin systems, for which pK_0' is usually near 10, hydroxide is bound more weakly to Mn^{III} hematoporphyrin IX by a factor of about 100.

Examination of the change with pH in the absorption spectrum of Mn^{III} hematoporphyrin IX dimethyl ester reveals changes completely analogous to those found with the free acid. However, in this case the pK_0' was found to be 11.3 (Fig. 3-8), and the role of the negative carboxylate groups is apparent in making the metal less attractive to hydroxide, or perhaps competing for coordination positions 5 and 6.

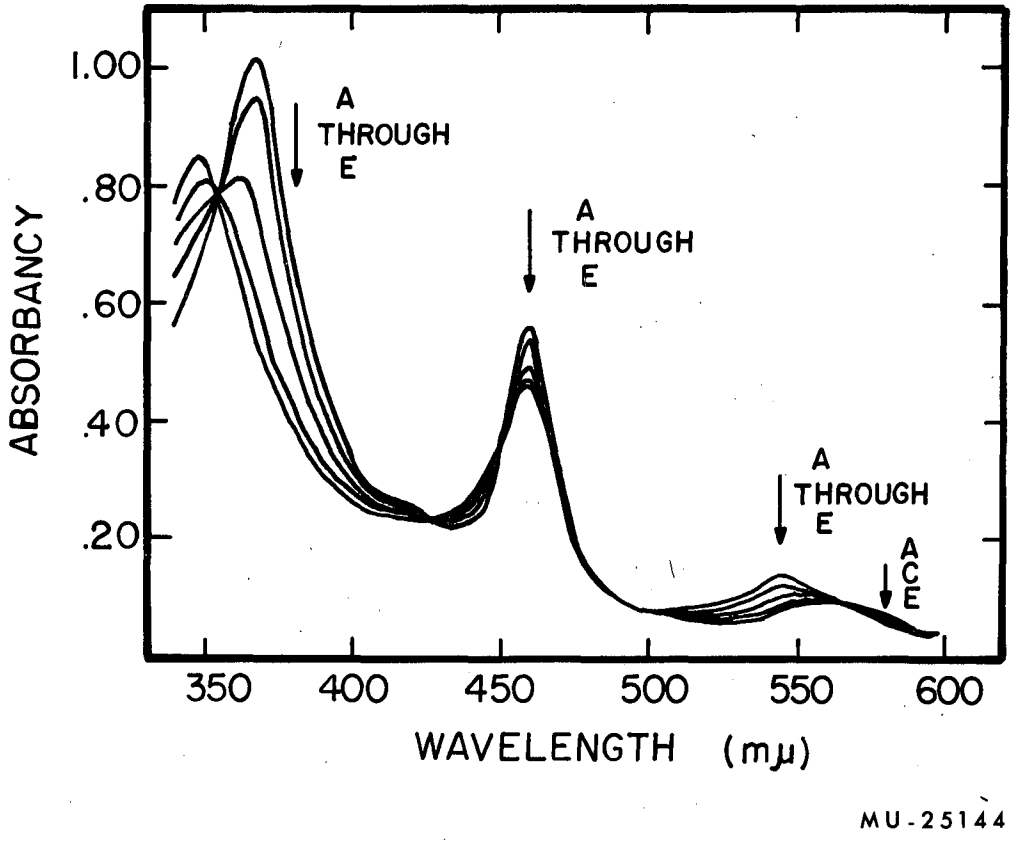

Fig. 3-6. Change with pH in the absorption spectrum of Mn^{III} hematoporphyrin IX. Mn^{III} hematoporphyrin IX, 2×10^{-5} M; 0.05 M borate and phosphate buffers employed; ionic strength adjusted to 0.30 with KCl in all cases; 1-cm cuvette. A, pH 7.38 and 10.00; B, pH 11.49; C, pH 11.95; D, pH 12.48; E, pH 13.42.

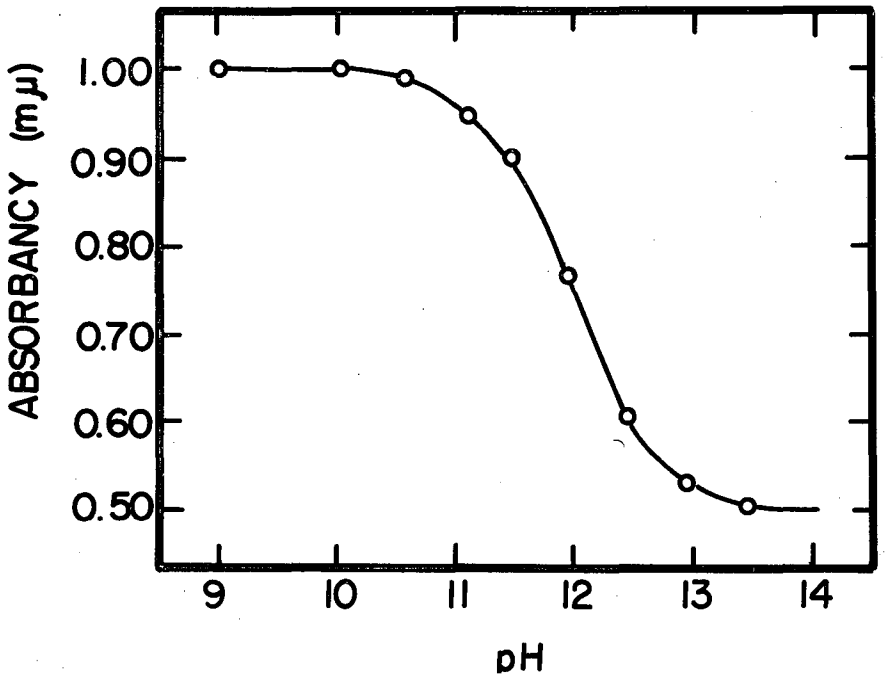

MU-25145

Fig. 3-7. Spectrophotometric determination of pK'_a for Mn^{III} hematoporphyrin IX. Mn^{III} hematoporphyrin IX, 2×10^{-5} M; 0.05 M borate and phosphate buffers employed; ionic strength adjusted to 0.30 with KCl in all cases; temp $22\pm2^{\circ}$ C; absorbancy measured at 370 mμ; 1-cm cuvette. Solid line, theoretical curve for $pK'_a = 11.95$ in Eq. (3); o, experimental values.

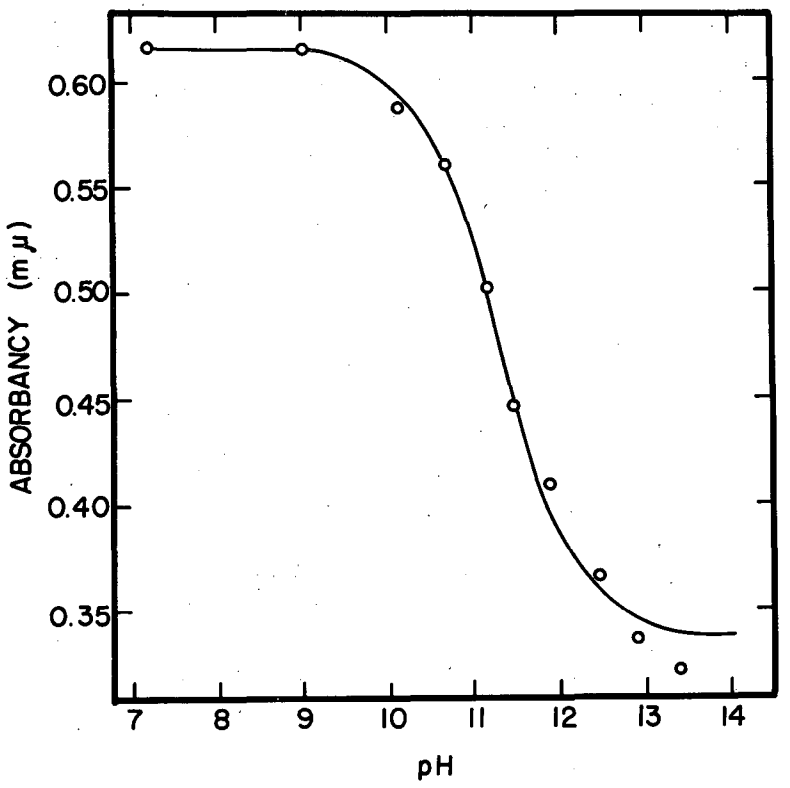

MU-25146

Fig. 3-8. Spectrophotometric determination of pK'_a for Mn^{III} hematoporphyrin IX dimethyl ester. Mn^{III} hematoporphyrin IX dimethyl ester, 2×10^{-5} M; 0.05 M borate and phosphate buffers employed; ionic strength adjusted to 0.30 with KCl in all cases; temp $22 \pm 2^{\circ}$ C; absorbancy measured at 370 mμ; 1-cm cuvette. All spectra were taken within 5 min after preparation of solution. Those at values of pH above 11 are subject to undetermined amounts of hydrolysis of the methyl ester. Solid line, theoretical curve for $pK'_a = 11.3$ in Eq. (3); o, experimental values.

A similar study of the change with pH in the absorption spectrum of Mn^{II} hematoporphyrin IX gives some indication that here, too, hydroxide may interact. However, the change occurs at such alkaline values of pH that the pK'_r would have a value near 14. The presence of this pK'_r would explain the failure of the $\Delta E_m/\Delta pH$ to reach a slope of -0.060 v per pH unit above pH 13.

Taylor, in his potentiometric studies of manganese mesoporphyrin IX in the presence of excess pyridine,[4] did not see a pK'_b similar to those consistently found for other metalloporphyrin systems under the same conditions. The presence of these pK'_b values in systems containing pyridine or pyridine analogues has been difficult to explain, since evidence indicates that pyridine is not displayed by hydroxide from coordination positions 5 and 6. In keeping with a suggestion made earlier for Fe^{III} porphyrin complexes in the presence of excess pyridine,[15] it is suggested that, here too, Mn^{III} hematoporphyrin IX in the presence of excess pyridine would react with hydroxide to form an addition or charge-transfer complex, but the pK'_0 of the reaction would be above 12. Thus, such a pK'_0 might not be readily detectable.

Oxidative titration of Mn^{III} hematoporphyrin IX with one equivalent of sodium hypochlorite resulted in the formation of a higher oxidation state. Figure 3-9 shows a representative set of absorption curves obtained by the addition of sodium hypochlorite. The normality of the hypochlorite solution was periodically determined by titration with sodium dithionite solution previously standardized by titration against potassium ferricyanide. The hypochlorite-chloride couple is not electromotively active, but the end point may be detected as a sudden negative surge in potential, or by following the spectrophotometric change concurrent with the conversion of potassium ferricyanide to potassium ferrocyanide which occurs after the hypochlorite has been titrated. Addition of more than one equivalent of oxidizing agent had no immediate effect, but a large excess brought about spectrophotometric changes which were found to be irreversible and eventually resulted in total loss of absorption in the visible regions of the spectrum. The relative stability of this manganese porphyrin to such strong oxidants as hydrogen peroxide and sodium hypochlorite is quite striking, since most simple iron-porphyrin systems are rapidly bleached in the presence of these oxidants.

Attempts to measure E_m values for this transition to a higher oxidation state are complicated by a number of factors. First, the material exhibiting curve F of Fig. 3-9 returns spontaneously to Mn^{III} hematoporphyrin IX by just standing in a cuvette for 1 or 2 hours in the dark. This indicates that something in solution must be oxidized, since the pigment has been reduced. Any destructive oxidation of manganese hematoporphyrin IX complex at concentrations as low as 10^{-5} M can be ruled out, since the absorbancy of the material before and after its oxidation by hypochlorite is unchanged. In these simple systems other possible interactants are sodium hypochlorite derivatives and contaminating materials in the bleach used, together with the water and KOH present as solvent. However, the compounds present in bleach are not essential for restoring the higher oxidation state to

[15] H. A. Harbury and P. A. Loach, J. Biol. Chem. 235, 3646 (1960).

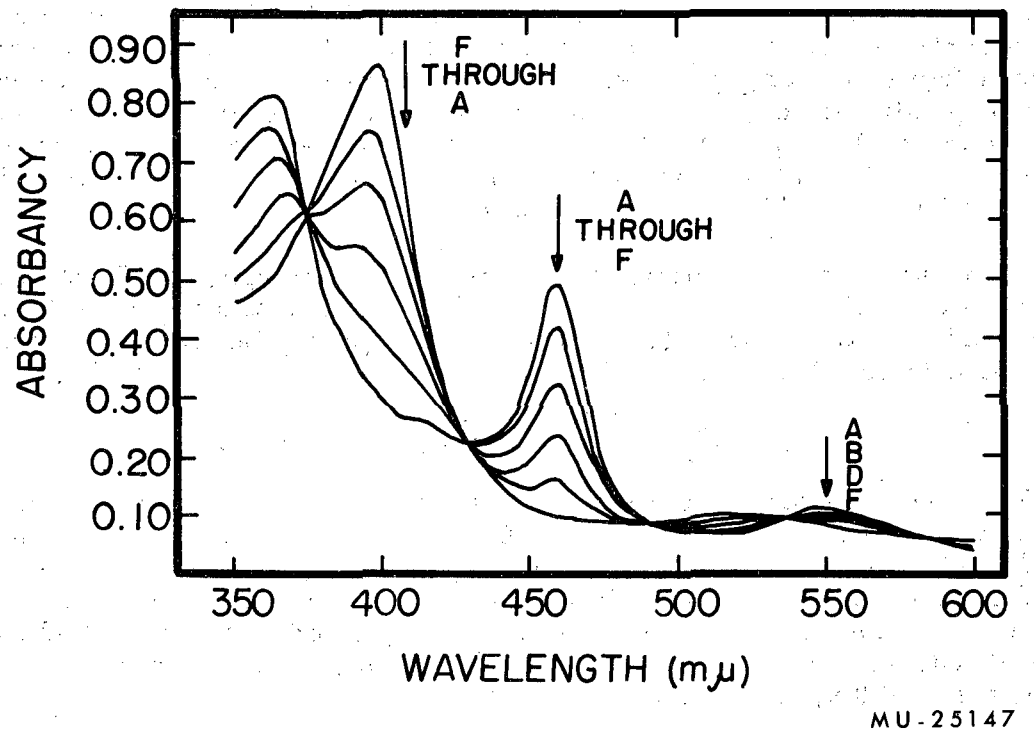

Fig. 3-9. Spectra of Mn^{III} hematoporphyrin IX recorded in the course of an oxidative titration. Mn^{III} hematoporphyrin IX, 1×10^{-5} M; pH 11.90; temp $22 \pm 2^{\circ}$ C; oxidizing agent, sodium hypochlorite. Percentage of oxidation: A, 0%, F, 100%.

Mn^{III} hematoporphyrin IX, since the same changes occur when the oxidizing agent is potassium ferricyanide instead of sodium hypochlorite. In addition, the gold-plated platinum electrodes being used do not always respond to changes in the state of oxidation of the pigment. This difficulty may be related to the formation of peroxides during the course of reduction of the higher oxidation state of manganese hematoporphyrin IX.

A few experiments have been carried out in which the change of the higher oxidation state to Mn^{III} hematoporphyrin IX was sufficiently slow and the electrodes responded sufficiently rapidly that equilibrium values of the reduction potential could be measured. Figure 3-10 shows the result of a plot of potentials corresponding to the percent reduction of the system as calculated from the absorption spectra. The results obtained agree well with those predicted for a reversible one-electron oxidation-reduction system represented by Eq. (1). The simplest interpretation consistent with the data at hand is that Mn^{III} hematoporphyrin IX is oxidized to Mn^{IV} hematoporphyrin IX by the addition of one equivalent of sodium hypochlorite.

Potentials for the system Mn^{IV}/Mn^{III} hematoporphyrin IX have been determined over a narrow range of pH, 11.0 to 13.5, and the results are summarized in Table 3-V. The simplest retaionship between E_m and pH consistent with the data at hand[12] is

$$E_m = E_x + \frac{RT}{F} \ln (H^+) [(H^+) + K_r'] , \qquad (4)$$

where K_r' is an apparent equilibrium constant for an oxidation-linked proton function in Mn^{III} hematoporphyrin IX, E_x is the potential which the half-reduced system would have at pH 0, were there no net oxidation-linked proton functions at values of pH below those covered in this study. In Fig. 3-11 the experimental values of E_m are plotted against pH and are compared with the curve described by Eq. (4) upon assignment of the constants $E = + 1.590$ v, $K_r' = 1.0 \times 10^{-12}$.

Once again the oxidation-linked proton function in Mn^{III} hematoporphyrin IX is apparent, and the presence of a slope of -0.120 v per pH unit for the E_m versus pH curve below pH 12 is consistent with the interpretation that a Mn^{IV} hematoporphyrin IX complex is formed by the addition of a strong oxidant to Mn^{III} hematoporphyrin IX. To explain the slope, it need only be assumed that the equilibrium*

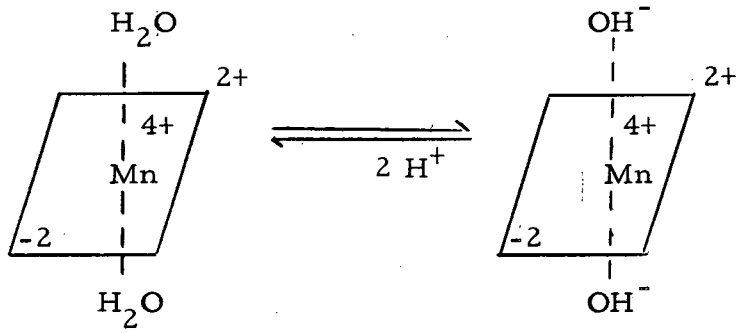

*The reaction is written as a concurrent loss of protons by two coordinated water molecules purely for the sake of simplicity of presentation.

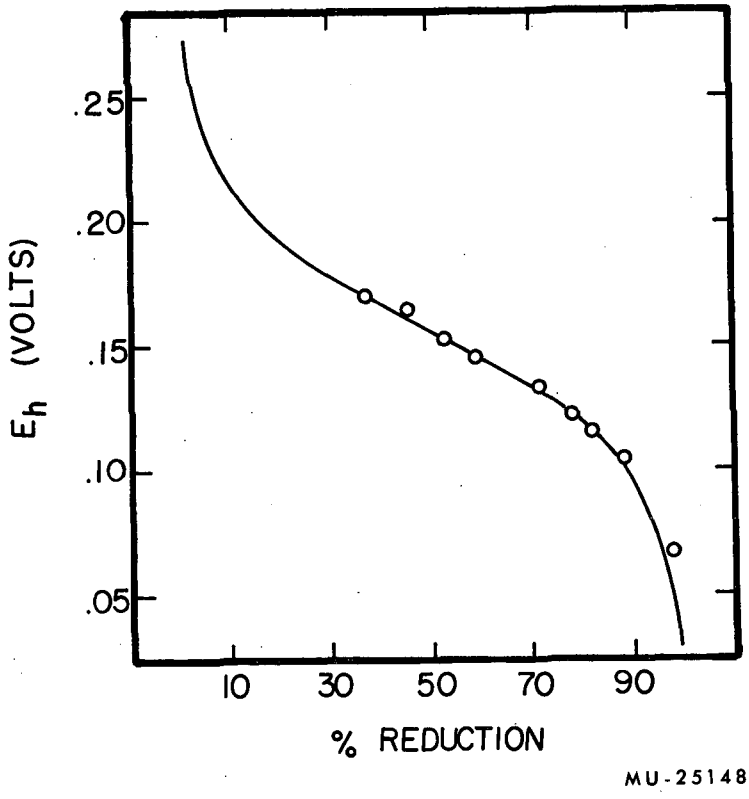

Fig. 3-10. Reductive titration of Mn^{IV} hematoporphyrin IX. Mn^{IV} hematoporphyrin IX, 1×10^{-5} M; pH 11.90; temp 22 ± 2° C; reducing agent, sodium dithionite. Solid line, theoretical curve for n = 1, E_m = +0.160 v; o, experimental points with percentage of reduction calculated from spectra.

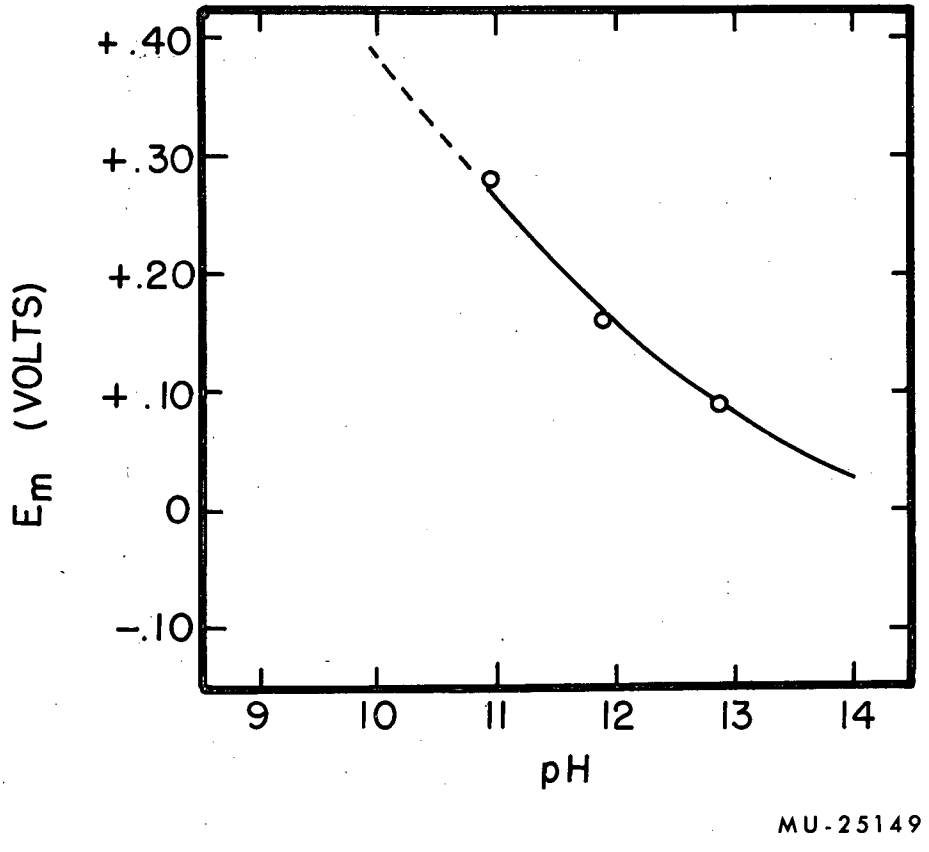

Fig. 3-11. pH- dependence of the oxidation-reduction potentials of half-reduced Mn^{IV} hematoporphyrin IX. Temp 22 ± 2° C; o, experimental values; the solid line represents Eq. 4 with $K_r' = 1.0 \times 10^{-12}$ and $E_x = +1.590$ volt.

occurs with a pK_0' below 10, a phenomenon in keeping with the fact that higher oxidation states of transition elements interact more strongly with hydroxide.

Table 3-V. E_m values for Mn^{IV}/Mn^{III} hematoporphyrin IX system.[a]

pH	Buffer[b]	Titrating agent[c]	E_m observed (v)	E_m calculated (v)	E_m observed $-E_m$ calculated (v)
10.95	II	A	+0.280	+0.271	+0.010
11.90	II	A	+0.160	+0.167	-0.007
12.88	II	A	+0.090	+0.091	-0.001

a. the temperature for these experiments was $22 \pm 2^{\circ}$ C.

b. same as for Table IV.

c. sodium dithionite.

Figure 3-12 summarizes the E_m-vs-pH relationships for the three oxidation states of manganese hematoporphyrin IX in aqueous solution. The equilibrium involved may be written schematically as shown on the following page. Rigorous extrapolation of the E_m versus pH curves of Fig. 3-12 to pH 7 is not warranted, since the values of other oxidation-linked proton functions in the range of pH below 10 has not been studied. However, it is apparent that Mn^{II} hematoporphyrin IX is a very strong reducing agent, strong enough to produce molecular hydrogen from water providing there is a mechanism for the reaction, whereas Mn^{IV} hematoporphyrin IX is a very strong oxidizing agent, possibly strong enough to produce molecular oxygen from water if there is mechanism for the reaction. Thus, such manganese porphyrin complexes are doubly interesting in terms of discovering the role of manganese in photosynthesis; a strong reducing agent is needed to reduce triphosphopyridine nucleotide, whereas a strong oxidizing agent is needed to produce molecular oxygen from water. After light energy is absorbed by chlorophyll, these latter two reactions, along with the formation of adenosine triphosphate, represent the next known products of the energy-capturing system.

The study of the properties of a stable Mn^{IV}-hematoporphyrin IX complex is the first to be made in which such a high oxidation state of the simple metalloporphyrin system has been examined under reversible conditions in aqueous solution. These data for manganese hematoporphyrin IX complexes are not of such great interest in the sense of leading one to expect to find this same complex in a living cell, but rather, they have their significance in helping to define the nature of metalloporphyrin systems in general and in extending our knowledge of their possible role in biological environments.

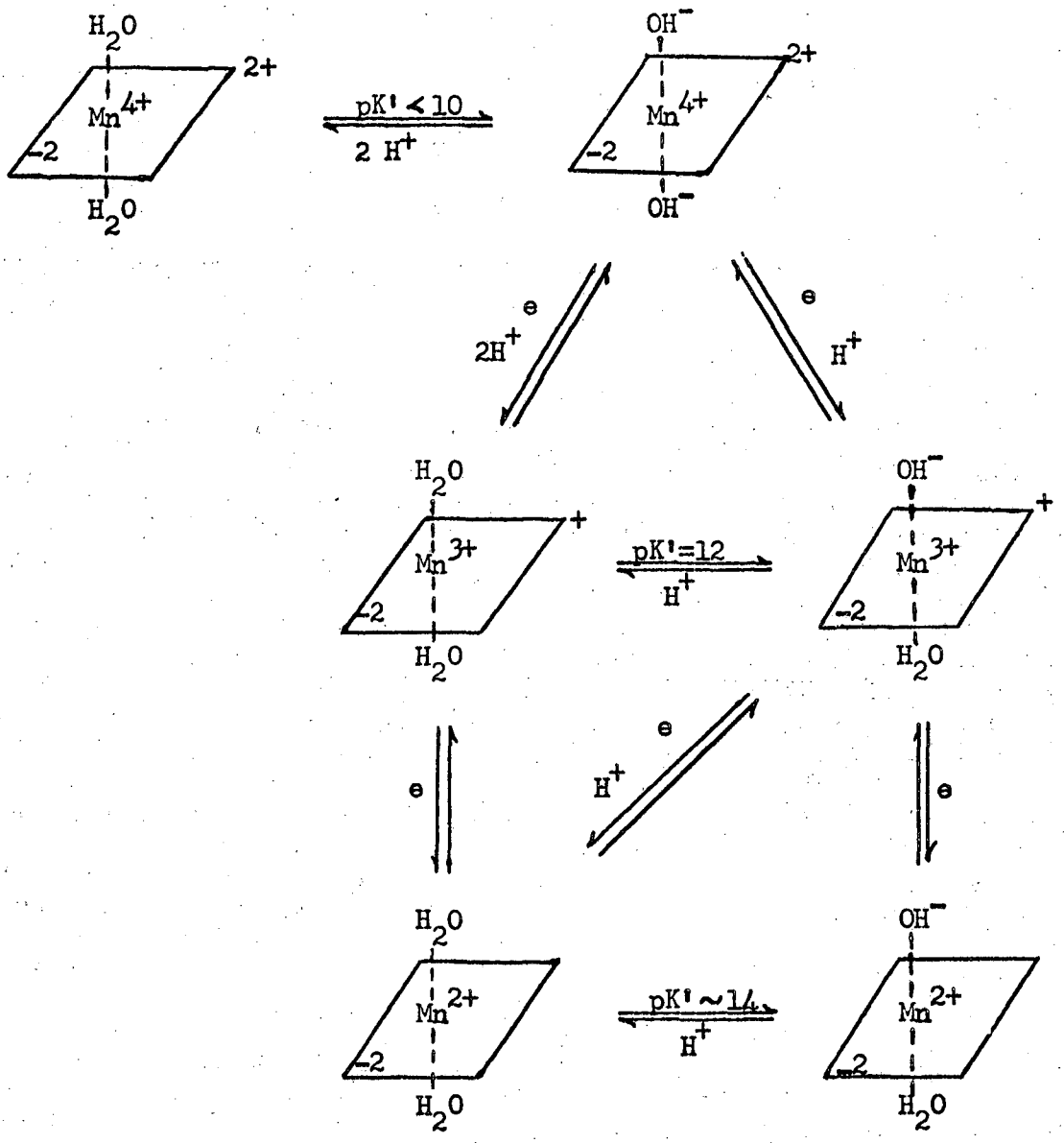
H2O
2+
Mn4+
-2
H2O
pK' < 10
2 H+
OH−
2+
Mn4+
-2
OH−
e
2H+
e
H+
H2O
+
Mn3+
-2
H2O
pK'=12
H+
OH−
+
Mn3+
-2
H2O
e
e
H+
e
H2O
Mn2+
-2
H2O
pK' ~ 14
H+
OH−
Mn2+
-2
H2O

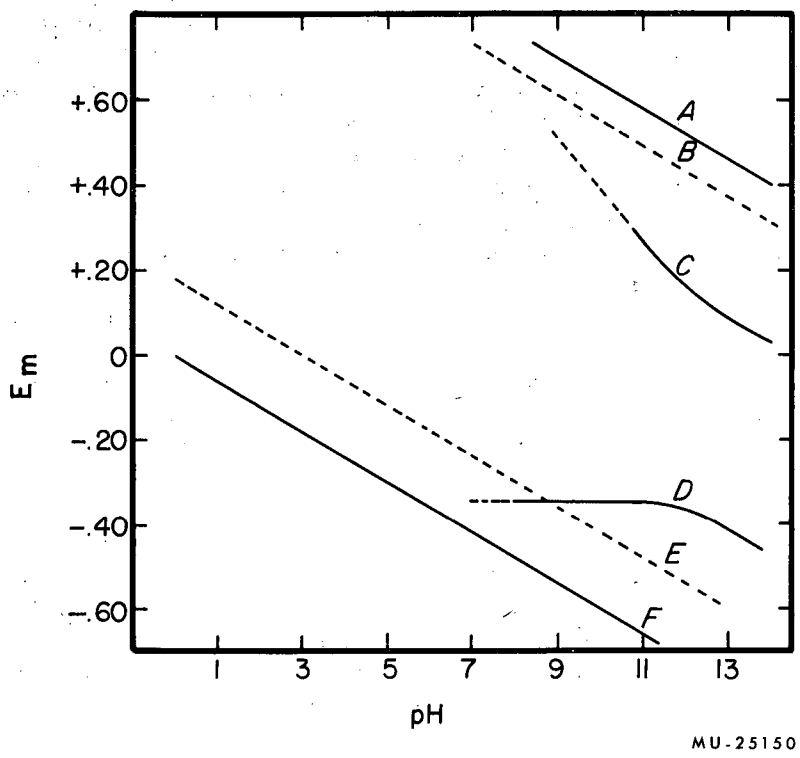

Fig. 3-12. E_m – pH curves. A, oxygen electrode, 1 atm oxygen; B, oxygen electrode, 10^{-6} atm oxygen; C, Mn^{IV}/Mn^{III} hematoporphyrin IX; D, Mn^{III}/Mn^{II} hematoporphyrin IX; E, hydrogen electrode, 10^{-6} atm hydrogen; F, hydrogen electrode, 1 atm hydrogen.

4. NUCLEAR MAGNETIC RESONANCE OF THE METHYL ESTERS OF THE FIRST- AND SECOND-ROW INORGANIC OXYACIDS

P. R. Hammond

This report is a continuation of an earlier one on this subject.[1] Knowledge of the π bonding between the oxygen and the heteroatom in the inorganic oxyacids, their anions, and their esters may be expected to be of value in interpreting the acid strengths and alkylating properties[2] of these compounds. This bonding has been proposed to explain the weak Lewis acidity of the borate esters in comparison with the trialkyl borons,[3] as well as to explain many other aspects of boron[4] and silicon[5] chemistry. Methods of estimating π bonding are therefore relevant as an aid to the understanding of the chemistry of the group. Bond-distance measurements on the ions have been given differing interpretations.[6] Changes in other physical properties have been attributed in part to changes in this bonding. Thus, variations have been observed in the basicity of the alkoxysilanes as demonstrated by hydrogen-bonding studies,[7] in the heteroatom-oxygen force constants,[8] and in the ultraviolet absorption spectra of a limited number of phenyl esters.[9]

A systematic study of the physical properties of the esters may provide answers to a number of problems. One such series of measurements--namely, nuclear magnetic resonance of hydrogen nuclei of the methyl esters--is reported here.

The position of resonance of the methyl protons in a given external magnetic field depends on the perturbation caused by the magnetic shielding due to the electron's environment, and on the net bulk magnetic susceptibility of the sample. The last effect may be eliminated[10,11] by comparing infinitely dilute solutions in inert, magnetically isotropic (spherical) solvents. Such a solvent, carbon tetrachloride, was used in this work.

---

[1] P. R. Hammond, in Bio-Organic Chemistry Quarterly Report, UCRL-9772, June 1961.

[2] M. Anbar, I. Dostrovsky, D. Samuel, and A. D. Yoffe, J. Chem. Soc. 1954, 3603.

[3] H. C. Brown and E. A. Fletcher, J. Am. Chem. Soc. 73, 2808 (1951).

[4] T. D. Coyle, S. L. Stafford, and F. G. A. Stone, J. Chem. Soc. 1961, 3103.

[5] F. G. A. Stone and D. Seyferth, J. Inorg. & Nuclear Chem. 1, 112 (1955).

[6] G. M. Phillips, J. S. Hunter, and L. E. Sutton, J. Chem. Soc. 1945, 146; A. F. Wells, ibid. 1949, 55.

[7] R. West, L. S. Whatley, and K. J. Lake, J. Am. Chem. Soc. 83, 761 (1961).

[8] H. Kriegsmann, Z. anorg. Chem. 299, 138 (1959); J. Goubeau, Angew. Chem. 69, 77 (1957); H. Siebert, Z. anorg. Chem. 275, 225 (1954).

[9] P. R. Hammond, in Bio-Organic Chemistry Quarterly Report, UCRL-9519, Jan. 1961.

[10] A. L. Allred and E. G. Rochow, J. Am. Chem. Soc. 79, 5361 (1957).

[11] A. A. Bothner-By and C. Naar-Colin, ibid. 80, 1728 (1958).

Experimental Procedure

Measurements of the NMR spectra were made in a spinning, cylindrical tube, 5 mm o. d., with a Varian spectrometer operating at 60 Mc. A fine capillary, 0.5 mm, containing water, was supported symmetrically in the sample by a plasticene seal at the top of the tube, and the positions of resonance from water were determined by measuring with respect to a 60-cycle/sec (cps) side band imposed on the spectra by an audio-oscillator. The same capillary and tube were used throughout the experiments.

Solutions were prepared in distilled reagent-grade carbon tetrachloride through which helium had been bubbled overnight. Commercial samples of all esters except methyl nitrate, nitrite, and perchlorate were fractionally distilled. Methyl nitrate was prepared by the method of Black and Babers[12] and was used without further purification. No lines were seen in the NMR spectrum that could be attributed to proton-containing impurities. Methyl nitrite[13] was passed over glass wool cooled to -15° and collected in carbon tetrachloride at this temperature. The solution was then slowly allowed to warm. When the change in weight showed that a predetermined concentration had been reached, standard samples were made immediately and were stored at -10°.

Methyl perchlorate solutions were prepared by the reaction of silver perchlorate and a small, known excess of methyl iodide in carbon tetrachloride. The mixture was shaken overnight in the dark, filtered from the yellow silver iodide through fine, sintered-glass funnels, and diluted to standard concentrations. The spectra showed two peaks about 150 and 30 cps from water. The ratio of the areas under the peaks was approximately in the proportion of excess methyl iodide to silver perchlorate, indicating nearly quantitative conversion of the salt to the ester.

Similar attempts to prepar methyl chlorate and chlorite from the silver salts were not successful. The reactions were tried at -15° in the absence of light the night before the measurement, and products were allowed to warm to room temperature in the NMR spectrometer tube. The chlorate showed no new lines in its spectrum although the chlorite showed two faint ones. Iodine color was very evident in both the chlorate and chlorite solutions, and only barely visible in the perchlorate. An attempt to extract methyl hypochlorite, by the method of Sandmeyer,[14] into cold carbon tetrachloride produced a solution having only a faint line in the spectrum.

Methyl phosphite solutions were prepared at room temperature (26°) an hour before the measurements, and no products of chemical reaction were seen in the spectra. Solutions with concentrations 2.0, 1.6, 0.8, 0.6, and 0.4 in methyl protium molarity were studied. All experimental values of positions of the resonance come from at least five measurements.

---

[12] A. P. Black and F. H. Babers, Organic Syntheses, Collected Volume II (John Wiley & Sons, Inc., New York, 1944) 412.

[13] W. H. Hartung and F. Crossley, Organic Syntheses, Collected Volume II, (John Wiley & Sons, Inc., New York, 1944) 363.

[14] T. Sandmeyer, Ber. deut. chem. Ges. 19, 857 (1886).

Results

Experimental values of the NMR chemical shift are shown in Table 4-I, where standard deviations of 0.5 cps are typical. The positions of resonance at infinite dilution, determined by using a linear graphical extrapolation, are shown in Table 4-II. Where these measurements and those of Allred and Rochow[10] overlap, close agreement is obtained except for the borate, where the shift is found to be 3.0 cps higher. Variations of position of resonance with concentration are found to be small. The positions for the methyl nitrate and methyl perchlorate are the lowest values for methyl-oxygen compounds yet recorded.

The spectra of the trimethyl phosphate and trimethyl phosphite always show two sharp peaks, and the frequency separation between them does not vary on dilution. This is attributed to coupling between the P^{31} and the proton nuclei. The coupling constants for the phosphate ($J = 11.4 \pm .2$ cps) and for the phosphite ($J = 11.9 \pm .5$ cps) are the same. The average values are shown in Table 4-II.

For increasing electronegativity of the heteroatom the methyl resonance appears at decreasing values of the applied field. Plots of the position of resonance for the borate, carbonate, nitrate, silicate, phosphate, sulfate, and perchlorate groups against the electronegativity of the heteroatom are shown in Fig. 4-1. These approximate two parallel straight lines. For sulfur and phosphorus, the resonance for an oxyacid of lower oxidation state occurs at a higher value of applied field. Variations in line width occur. In particular, methyl nitrate produces a broad line--broader, for example, than methyl nitrite (line half widths 4.8 cps compared with 2.2 cps).

Discussion

The variations in position of resonance may be considered to correspond to changes in a NMR parameter that closely resembles classical group electronegativity. In a number of publications[10, 15, 17] attention has been drawn to linear relationships between element electronegativity and the position of protium resonance of similar methyl compounds; yet the interpretation in some cases is not simple,[16] and a scale of values of this parameter may have limited application. However, Table 4-III shows values estimated from Table 4-II and from the work of Allred and Rochow[10] on the methyl halides. Huggins's electronegativity values were used for the halogens.[18]

---

[15] L. Pauling, The Nature of the Chemical Bond, Third Edition (Cornell University Press, New York, 1960), p. 93; H. O. Pritchard and H. A. Skinner, Chem. Revs. 55, 745 (1955); A. L. Allred and E. G. Rochow, J. Inorg. Nuclear Chem. 5, 264 (1958); A. L. Allred, J. Inorg. & Nuclear Chem. 17, 215 (1961).

[16] A. A. Bothner-By and C. Naar-Colin, Ann. N. Y. Acad. Sci. 70, 833 (1958).

[17] A. L. Allred and E. G. Rochow, J. Inorg. & Nuclear Chem. 5, 269 (1958).

[18] M. L. Huggins, J. Am. Chem. Soc. 75, 4123 (1953).

Table 4-I. NMR chemical shifts (from water, in cycles per second) of methyl esters in carbon tetrachloride at five different molarities.

	Molarity				
	2.0	1.6	0.8	0.6	0.4
Borate	78.9	78.4	79.2	78.8	78.5
Carbonate	62.6	62.8	62.3	62.3	62.9
Nitrate	40.2	39.7	39.9	40.0	40.1
Nitrite	48.4	46.2	47.7	46.3	46.4
Silicate	75.5	75.3	75.7	75.6	75.5
Phosphate	59.2 70.3	59.1 70.7	57.5 68.7	58.3 69.6	58.1 69.6
Phosphite	72.7 83.8	74.9 86.8	74.0 85.7	74.6 86.5	74.8 87.2
Sulfate	51.0	52.0	52.2	51.7	51.3
Sulfite	75.4	75.3	74.0	74.3	74.1
Perchlorate	31.0	31.1	30.5	31.1	31.1
Chlorite	69.5 96.4	73.2 95.8	-	-	-
Hypochlorite	53.8	57.7	-	-	-

Table 4-II. NMR chemical shifts (from water, in cycles per second) of methyl esters in carbon tetrachloride at infinite dilution.

Borate	Carbonate	Nitrate		
78.6	63.0	40.2		
		Nitrite		
		(45.6)		
	Silicate	Phosphate	Sulfate	Perchlorate
	75.6	57.6, 69.0 } 63.3, J = 11.4	51.6	31.2
		Phosphite	Sulfite	Chlorate
		75.0, 86.8 } 80.9, J = 11.8	73.8	-
				Chlorite
				(70.95)
				Hypochlorite
				(55)

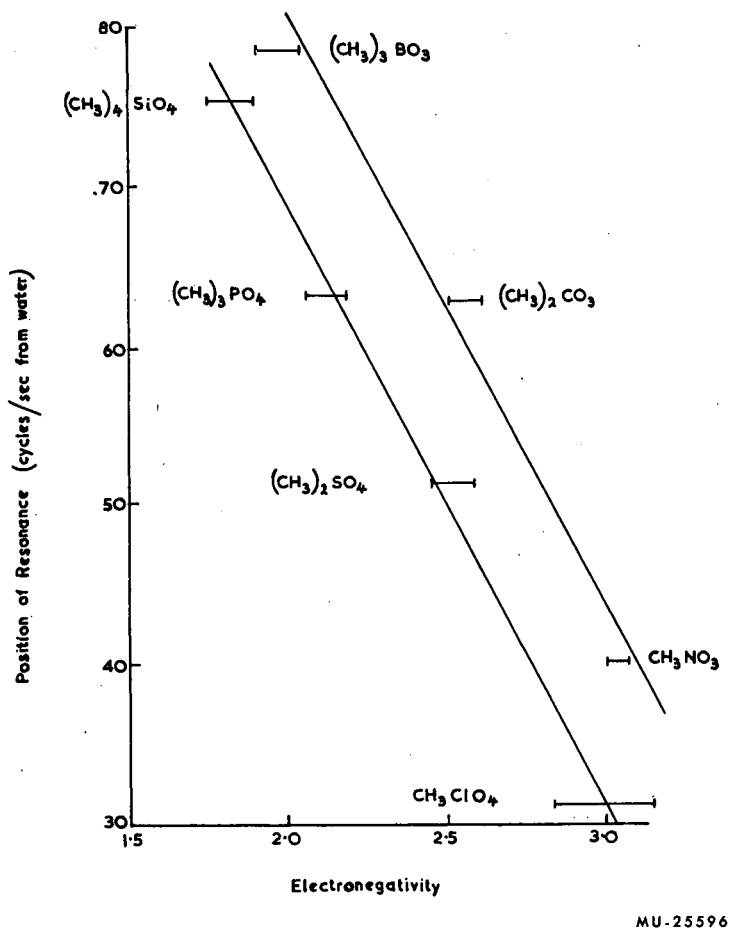

Fig. 4-1. Plots of the position of resonance for the methyl esters of inorganic oxyacids against electronegativity of the heteroatom. Range of electronegativity values comes from Refs. 15 and 18.

Table 4-III. Group electronegativity for the oxyacids from the NMR information of Table 4-II and the work of Allred and Rochow (Ref. 10) on the methyl halides.

Borate	Carbonate	Nitrate		
3.42	3.58	3.81		
	Silicate	Phosphate	Sulfate	Perchlorate
	3.45	3.58	3.70	3.90
		Phosphite[a]	Sulfite	
		3.40	3.47	

[a]As $P(OH)_3$

If the main influences on the position of resonance are considered to be those affecting electron density on the methyl hydrogens, shielding constants can be ascribed to contributions (a) from structures of the type $C-\overset{+}{O}=\overset{-}{X}$, and (b) from electronegativity differences between oxygen and the group containing the heteroatom. Changes in molecular geometry may affect the number of electronegative oxygen atoms neighboring the methyl groups, and therefore may also alter resonance positions. Thus, the interesting result involving electronegativity shown in the graph refers to molecules of similar geometry. Discrepancies may be introduced by anisotropy effects,[16] and these limit the interpretation at present, although the linear relations of the graph suggest that these are small. Case (b) contributes for acids of different oxidation states. It is also noteworthy that there is no simple correspondence between acid strength and position of resonance.

Geometrical isomerism has been observed in methyl nitrite.[19,20] At low temperatures this produces two lines in the NMR spectrum, and at room temperature the single line obtained represents an averaging effect for the two. The ratio of isomers at room temperature is about 1:1, although it is not known in carbon tetrachloride with the accuracy of the other measurements in Table 4-III. The separation of the doublet at low temperatures is in the order of a chemical shift, and this is comparable with the total spread of the values in Table 4-II. The broad line of the nitrate is probably associated with the quadrupole moment of the N^{14} nucleus. The sharper line for the nitrite implies that quadrupole relaxation occurs at a different rate than for nitrate, owing to the difference in electron environment of the nitrogen atom.

If there were a change of π bonding in the phosphate and phosphite esters, a redistribution of d-orbital electrons would be required. The fact that the hydrogen-phosphorus coupling constants are the same implies that the bonding is unaltered, or that the coupling is not sensitive to d-orbital bonding.

---

[19] P. Tarte, J. Chem. Phys. 20, 1570 (1952); R. N. Haszeldine and J. Jander, J. Chem. Soc. 1954, 691; P. Gray and L. W. Reeves, J. Chem. Phys. 32, 1878 (1960).

[20] L. H. Piette, J. D. Ray, and R. A. Ogg, J. Chem. Phys. 26, 1341 (1957).

5. SOME OBSERVATIONS ON RATES OF LABELING OF INTERMEDIATES OF THE CARBON-REDUCTION CYCLE DURING STEADY-STATE PHOTOSYNTHESIS WITH $C^{14}O_2$

Martha R. Kirk and J. A. Bassham

In several previous reports we have discussed experiments in which we studied the photosynthetic reduction of $C^{14}O_2$ by Chlorella under conditions appraoaching steady-state growth.[1, 2, 3] In our most recent quarterly report[3] on this subject, we described an improved steady-state apparatus in which we used separate automatic controls to maintain constant pH and density concurrently in the algal suspension. In that report we had found some variation in the rates of photosynthesis over a period of two days.

We have studied this variation further, and after elimination of some defects in the control system, we found that the algae underwent physiological changes when continuously exposed to the saturating light intensity we had been using. These changes resulted in decreased pigmentation of the cells and a progressively lower rate of photosynthesis, per given volume of algae. Also there appeared to be a decrease in the ratio of CO_2 uptake to O_2 evolved in most cases, indicating other shifts in the products of photosynthesis.

Since this variation with time clearly showed that we did not have completely steady-state conditions over a period of days, we have tried to find more suitable conditions. Various alterations of the concentration of one or more of the inorganic ions in the medium were made without improving the photosynthetic rate constancy. Reduction of the light intensity seemed to lead to more constant rates. Finally, a combination of reduced light intensity and increased algal concentration (to 2.5% packed volume/total suspension volume) gave rates that were approximately 1/3 those obtained before with the saturating light intensities. In some cases these rates remained reasonably constant for several days.

Several steady-state experiments have now been performed with these new conditions. Some of these experiments were carried out with both C^{14} and N^{15} as tracers, as described in our previous report. The resulting algal samples have been analyzed by paper chromatography and radioautography, and the C^{14} content of the compounds has been determined. Unfortunately, difficulties with the analysis of N^{15}, particularly in the mass spectrometer, have prevented us from obtaining the data on N fixation thus far. However, we have had a look at the rates of labeling of cycle intermediates with C^{14} and have noticed several differences, not unexpected, between these rates and those found under the earlier conditions with high light intensity. Also, we find the active reservoir sizes[1] different.

---

[1] J. A. Bassham and M. Kirk, Biochim. et Biophys. Acta 43, 447 (1960).

[2] D. C. Smith, J. A. Bassham, and M. Kirk, Biochim. et Biophys. Acta 48, 299 (1961).

[3] M. Kirk and J. A. Bassham, in Bio-Organic Chemistry Quarterly Report, UCRL-9772, June 1961, p. 97.

The reservoir sizes and rates from an earlier steady-state experiment (steady state 18) are compared in Table 5-I with those from two experiments (steady states 39 and 41) performed under the new conditions (including the lower light intensity). As can be seen there is a decrease not only in the rates of CO_2 uptake at the lower light intensities, but in the pool sizes of intermediates in the cycle as well. The decrease in the total carbon in all the pools in the cycle is nearly as great as the decrease in rate. The obvious conclusion is that decreasing the light intensity has more effect on the rate of introduction of CO_2 into the cycle than it has on the rates of utilization of the cycle intermediates for further biosynthetic pathways.

The point of incorporation of CO_2 into the cycle is the reaction of ribulose diphosphate with CO_2, and it is significant that the level of ribulose diphosphate is down by a factor of 6 to 10 in the experiments at lower light intensity while the level of the product of the carboxylation, phosphoglyceric acid (PGA), is down by a factor of 3. Other intermediates of the carbon-reduction cycle are also lowered, but none by as much as the ribulose diphosphate (RuDP). Thus the conversion of pentose monophosphates to RuDP, requiring ATP or a similar compound derived from the conversion of light energy to chemical energy, seems to be the point at which light intensity makes the greatest difference.

The reduction of PGA to sugar phosphates also requires ATP from the light, but in addition requires a reducing cofactor, presumed to be TPNH, also from the conversion of light energy to chemical energy. As noted above, the concentration of PGA falls at the lower light intensity, even though we know from earlier work that when the light is turned off entirely, following bright illumination in the presence of CO_2, the concentration of PGA goes up.[4] In the present experiments (steady-state at lowered light intensity) it appears that the light-limited reaction is RuDP formation, not PGA reduction, and the limiting cofactor is ATP (or a similar cofactor) not TPNH.

Another point to be noted is that reactions by which carbon-reduction-cycle intermediates are converted to secondary products outside the cycle are not as much slowed by lower light intensity as the primary carboxylation. This is probably because the intermediates derived from the cycle are for the most part reactive compounds, such as acetyl coenzyme A, phosphoenolpyruvic acid, etc., and do not require light-produced cofactors for the first step or so along the biosynthetic pathways leading from the carbon-reduction cycle to final products. Later steps in these pathways, for instance in the formation of fatty acids, do require light-produced cofactors. These later steps, however, do not necessarily reflect back strongly to the carbon-reduction cycle itself. Rather, there may be an increase in the concentrations of some of these intermediate compounds one or two steps removed from the cycle. In all likelihood, the changes in these secondary intermediate concentrations, coupled perhaps with a change in the ratio of steady-state levels of ATP and TPNH, produce changes in the composition of the end products of photosynthesis. One such change is the

[4] J. A. Bassham, K. Shibata, K. Steenberg, J. Bourdon, and M. Calvin, J. Am. Chem. Soc. 78, 4120 (1956).

Table 5-I. Amount of carbon in photosynthetic cycle intermediates found in several steady-state studies (expressed as μmoles of carbon per cc wet-packed algae).

Compound	Earlier high light condition	Present lower light condition	
	Steady-state Expt. 18	Steady-state Expt. 39	Steady-state Expt. 41
Phosphoglyceric acid	3.0	1.0	0.9
Hexose monophosphates	5.5	2.6	2.8
Heptose monophosphates	1.8	0.6	0.9
Pentose monophosphates	≈0.2	0.2	0.04
Triose monophosphates	≈0.8	0.3	≈0.3
Diphosphates (except RuDP)	≈0.54	0.4	≈0.2
Ribulose diphosphate	0.36	0.06	0.04
TOTAL (A)	12.2	5.2	5.2
Rate of est. CO_2 uptake (B) (μmoles C/min.)	15	5	5
Rate of CO_2 uptake through cycle (est.) (μmoles C/min)	12	4	4
Ratio $(\frac{\text{total pools}}{\text{rate}}) = \frac{A}{C}$	1	1.3	1.3
Time for 95% saturation (three changes)	3 min	4 min	4 min

level of pigment concentration, which is higher at lower light intensities. (We do not believe that the light intensities we used near saturation were high enough to cause bleaching.)

A final point of interest is the overall turnover rate of the cycle. From Tables 5-I we see that the total concentration of carbon in all intermediates of the cycle is about equal to one minute's carbon fixation via the cycle. Since about three "changes" of all the carbon in the cycle would be sufficient to reach 95% saturation of the intermediates with C^{14} of the same specific radioactivity as the entering $C^{14}O_2$, we would expect that the cycle intermediates would be "saturated" after about 4 to 5 minutes. This is just what we observe, within experimental error. The importance of this observation lies in the fact that it gives us more confidence in our kinetic arguments. For many of these arguments it is necessary to assume that carbon compounds are not passed from enzyme to enzyme without equilibration with their individual active reservoirs. That such equilibration does in fact take place is indicated by the fact that the pools saturate in the calculated time.

6. METHYL PHOSPHATE FORMATION IN MIXTURES OF P^{32}-PHOSPHATE, METHANOL, WATER, AND SONICALLY RUPTURED SPINACH CHLOROPLASTS

Johannes Ullrich*

E. Tyszkiewicz, in this Laboratory, found monomethyl phosphate when she killed suspensions of sonically ruptured spinach chloroplasts incubated in P^{32}-phosphate with 4 volumes of cold methanol.[1, 2] This and her observation that the incubated mixture could be heated for a short time and still yield some methyl phosphate upon the addition of methanol led to the assumption that the chloroplasts form, during the incubation, a high-energy phosphate donor, presumably able to transfer its phosphate group to alcohols or to water with comparable reaction rates.

As it was impossible to reproduce the experiment in which methyl phosphate was formed by a previously heated sample, the hypothesis is untenable. It was subsequently suggested that the methyl phosphate formation was due to a phosphatase.[3] In this report further data are provided in support of this latter mechanism.

Experimental Results

To establish the equilibrium of the reaction

$$CH_3OH + H_3PO_4 \rightleftharpoons CH_3OPO_2H_2 + HOH,$$

a series of experiments was done in the usual way in various concentrations of methanol in water only by adding very different quantities of methanol to a number of samples. Figure 6-1 shows the results. The curves obtained indicate clearly that the optimum concentration for the methyl phosphate formation is approximately 50% methanol (by volume) in water ($\gamma_{MeOH} = 0.31$). The left half of the curve (below 50% methanol) is dominated by the esterification equilibrium; above 50% methanol, the amount of methyl phosphate formed is cut down by the "killing effect" of the alcohol on the enzyme, the yield decreasing with increasing alcohol concentration. When methyl P^{32}-phosphate is used as the initial compound, the resulting curve corresponds to the one obtained with phosphate up to 50% methanol concentration; in higher alcohol concentrations the equilibrium cannot be approached because of the denaturation of the enzyme, so that most of the methyl phosphate is left unhydrolyzed. In methanol concentrations less than 10%, on the other

*NATO Fellow, 1961-2, on leave from Department of Chemistry, University of Bonn, Germany.

[1] Edwige Tyszkiewicz, in Bio-Organic Chemistry Quarterly Report, UCRL-9519, Jan. 1961, p. 58; UCRL-9652, April 1961, p. 117.

[2] E. Tyszkiewicz, G. Gingras and M. Calvin, Biochim. Biophys. Acta 50, 376 (1961).

[3] J. Ullrich, in Bio-Organic Chemistry Quarterly Report, UCRL-9900, Oct. 1961, p. 30.

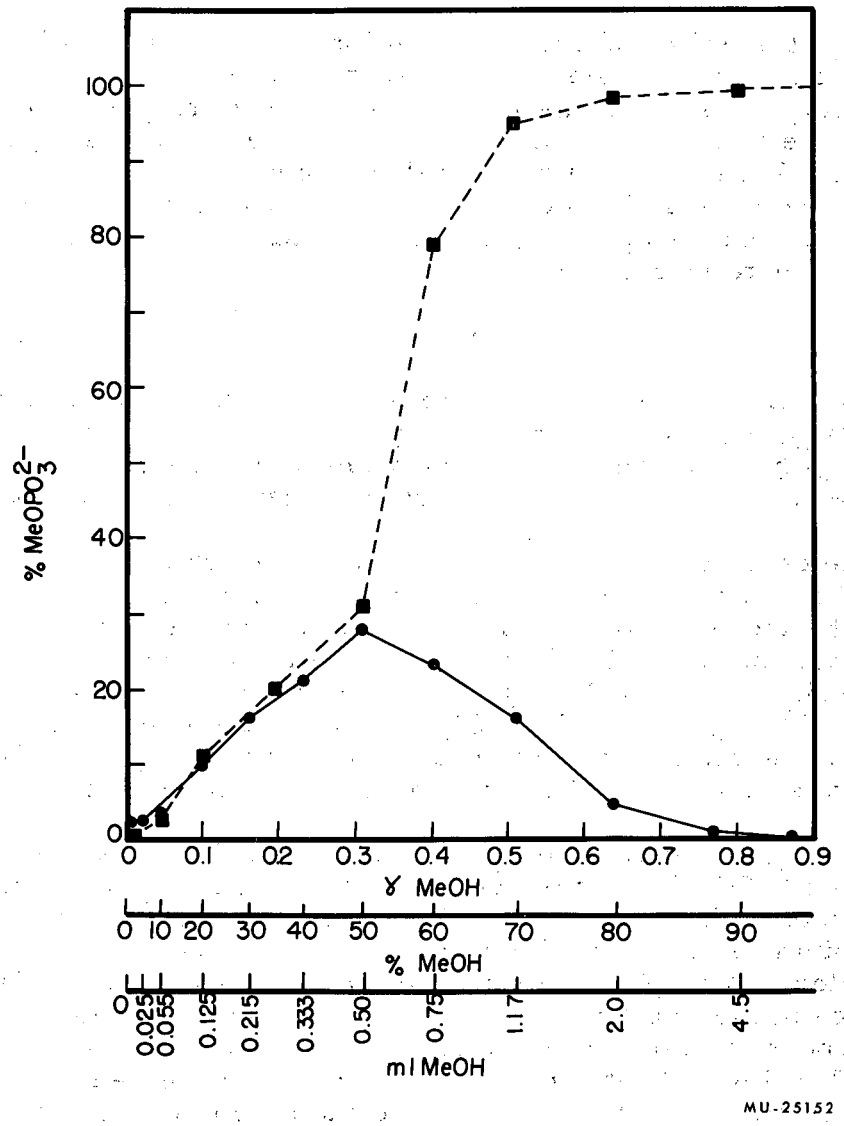

Fig. 6-1. Rate of methyl phosphate formation in % of total phosphate, dependent on the methanol concentration in water-methanol mixtures, with P^{32}-phosphate (solid curve) and $MeOP^{32}O_3^{=}$ (dashed curve) as substrates. Reaction time 4 days, temp 20 to 25°. The samples were killed by heating for 5 min in boiling water. Each reaction mixture contained 0.1 ml substrate solution, neutralized to pH=8.0, methanol as given in the figure, and 0.4 ml sonicated chloroplast suspension (1.3 mg chlorophyll/ml) in 10^{-3} M tris buffer pH=8.0.

hand, other esters of phosphoric acid appeared on the chromatograms in addition to the methyl phosphate. In mixtures containing less than 1% methanol, there was almost no methyl phosphate formed, but only a variety of other phosphates, and the origin contained most of the activity.

To study the effect of subsequent dilution, a sample with 50% methanol was stored 4 days at 0°, then divided into three parts. One of them (1), was killed by boiling the second one (2) was diluted with the same volume of methanol to give a final concentration of 75%, and the third (3) was diluted with an equal volume of water to a final methanol concentration of 25%. Parts 2 and 3 were stored under the same conditions for another 4 days, then heated and chromatographed simultaneously with Part 1. The yields of methyl phosphate were, respectively

1: 34.5%; 2: 36.8% 3: 16.1%.

This result shows that the phosphatase is still effective after 4 days in 50% methanol, but is killed rapidly by an increase of the methanol concentration, whereas it continues to function in 25% methanol to give the appropriate equilibrium yield of methyl phosphate (compare with Fig. 6-1).

In some other series of experiments, the methanol was partially replaced by different quantities of other organic solvents, which cannot react with phosphate and therefore do not disturb the equilibrium conditions, in order to always maintain the same total volume of organic solvent in the mixtures (50%). Figure 6-2 shows the results obtained with acetone-methanol mixtures and $P^{32}O_4^{---}$ or $MeOP^{32}O_4^{2-}$ as substrate; Fig. 6-3 shows the results with the acetone replaced by tetrahydrofurane or dioxane and $P^{32}O_4^{---}$ as the only substrate. The three different solvents gave similar results.

Another kinetic experiment was done with $P^{32}O_4^{---}$ as substrate in one mixture, $MeOP^{32}O_4^{--}$ in another one, and 50% methanol at 0° instead of 80% methanol at room temperature used in a previous similar experiment.[3] The final equilibrium percentage of methyl phosphate was approximately 34.5% in both samples. With phosphate as substrate, it took a considerably longer time to approach the equilibrium, probably because the substrate concentration was about 30 times as high as in the sample starting with methyl phosphate. The low activity in the methyl phosphate experiment caused large counting errors, but did not change the outcome of the experiment. Figure 6-4 shows both curves for the first 6 hours.

In some similar experiments the turnover rate at the beginning of the reaction varied considerably. This seemed to be due to the quality of the spinach and perhaps to some additional problems (which are uncontrollable) in the preparation of the chloroplasts. In order to exclude effects due to any impurity of the chloroplasts, some experiments were repeated with chloroplasts prepared by a completely different method and obtained as pure as possible. Frozen-dried spinach leaves were worked up in a non-aqueous procedure according to the method used by J. Biggins[4] in this Laboratory, who combined the methods described by U. Heber[5] and

[4] J. Biggins and R. Park, in Bio-Organic Chemistry Quarterly Report, UCRL-9900, Oct. 1961, p. 39.

[5] U. Heber, Ber. Dtsch. botan. Ges. 70, 371 (1957).

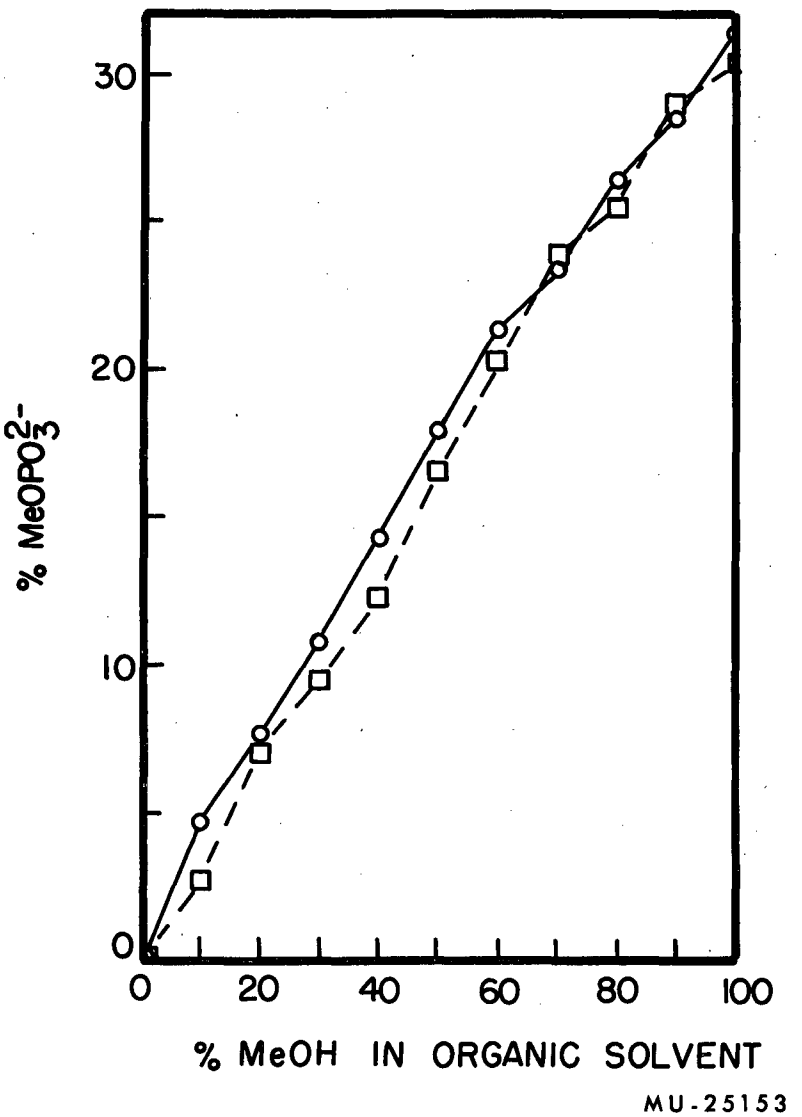

Fig. 6-2. Yield of methyl phosphate formed in 50% aqueous methanol-acetone mixtures. Reaction mixtures: 0.1 ml substrate solution (solid curve: phosphate; dashed curve: methyl phosphate), 0.5 ml acetone-methanol mixture, 0.4 ml sonicated chloroplast suspension (2.1 mg chlorophyll/ml) in 10^{-3} M tris buffer pH=8.0. Reaction time 4 days; temp 0°. The reactions were stopped by heating to 70° before they were put on the paper for chromatography.

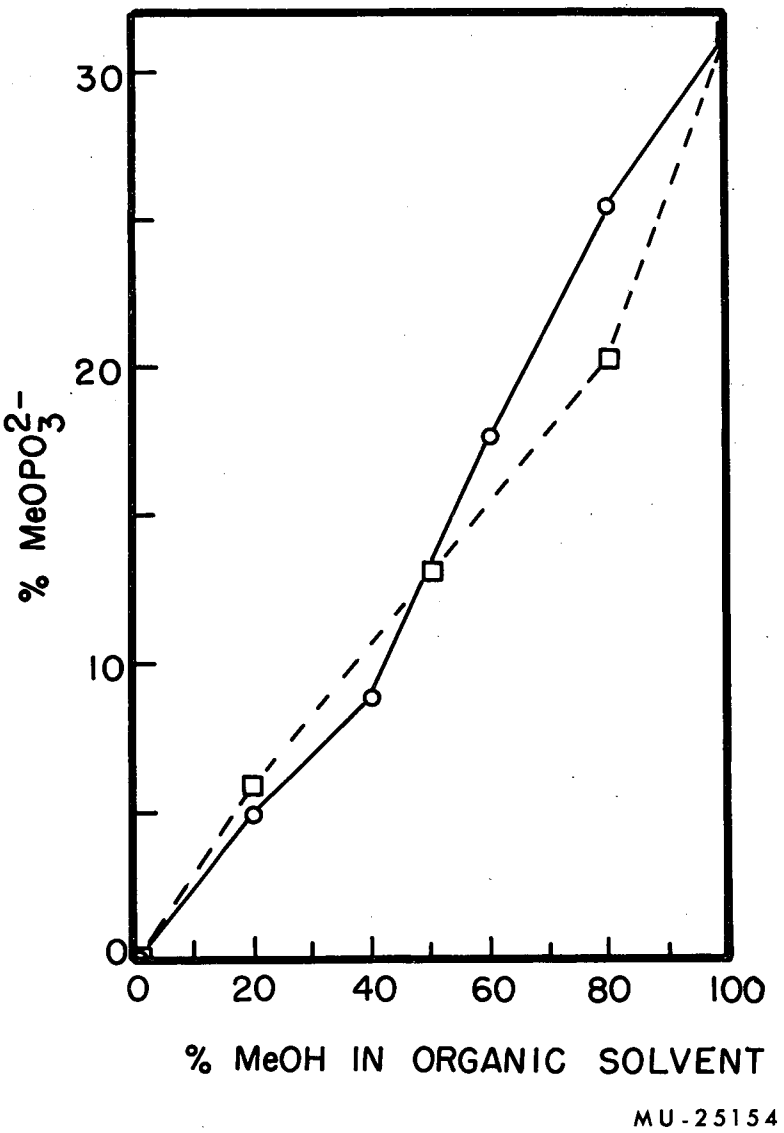

Fig. 6-3. Yield of methyl phosphate in mixtures of methanol-tetrahydrofurane (solid curve) and methanol-1, 4-dioxane (dashed curve) with 50% water. The conditions are the same as in Fig. 6-2. Inorganic phosphate was the only substrate used.

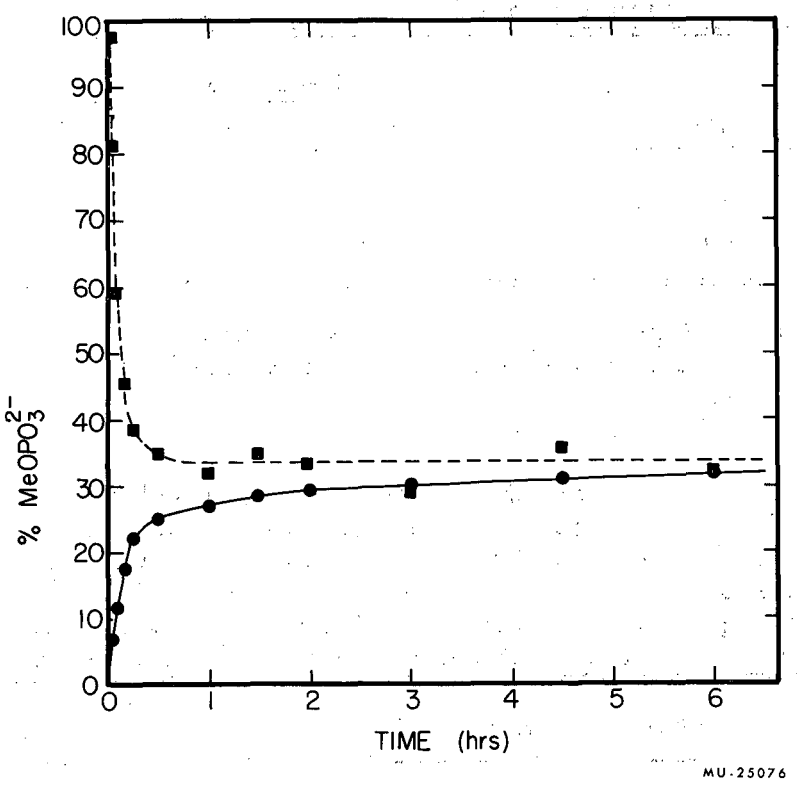

Fig. 6-4. The effect of the reaction time at 0° on the content of methyl phosphate in % of total phosphate, in 50 vol % aqueous methanol. Reaction mixture: 0.5 ml substrate solution pH=8.0 (solid curve: 30 μC $P^{32}O_4^{---}$; dashed curve: 1 μC $MeOP^{32}O_3^{--}$), 2.5 ml methanol, 2.0 ml chloroplast suspension (2.1 mg chlorophyll/ml) in 10^{-3} M tris buffer pH=8.0, previously sonicated for 90 sec. Samples were taken at different intervals and heated to 70° for at least 1 min, then chromatographed in the usual way.

C. R. STocking[6] to obtain dry chloroplasts of very high purity, which after resuspension in water still have some of their photosynthetic activity. In the phosphate equilibrium experiments, they worked as well as the chloroplasts isolated by the usual aqueous procedure (Table 6-I).

Table 6-I. Yield of methyl phosphate (in %) formed by chloroplasts isolated in a non-aqueous procedure from spinach.

	Temperature	
% MeOH	0°	20-25°
50	27.8	27.1
80	11.5	8.7

The experiment given in the previous report,[3] designed to yield higher alkyl phosphates, was repeated under different conditions, and gave the results in Table 6-II.

Table 6-II. Yield of alkyl phosphates (in % of total phosphate) formed by sonicated chloroplasts. Each sample contained 0.1 ml substrate ($P^{32}O_4^{=}$), 0.5 ml acetone, 0.5 ml R-OH (primary alcohol), and 0.4 ml chloroplast suspension (2.1 mg chlorophyll/ml). After 75 hr storage at 0°, the samples were heated to 70° and chromatographed. The solvent front did not reach the edge of the paper.

R	methyl	ethyl	n-propyl	alkyl	n-butyl	i-amyl
%	18.0	11.2	8.4	8.1	2.7	0.9

With respect to the observation by E. Tyszkiewicz that commercial phosphatases (alkaline and acidic) catalyze also the methyl phosphate formation,[7] a few experiments were run with some other biogenic materials as catalysts instead of the chloroplast fragments. The results are shown in Table 6-III.

An attempt to extend the experiment mentioned in the previous report,[3] in which some sugar phosphates were obtained from a mixture of 80% acetone and D-glucose or D-fructose, failed to yield any sugar phosphate when the mixture contained only 50% acetone and was stored at 0° for 4 days, then heated to 70°.

[6] C. R. Stocking, Plant Physiol. 34, 56 (1959).

[7] Edwige Tyszkiewicz, private communication, October 1961.

Table 6-III. Yield of methyl phosphate formed from $P^{32}O_4^{\equiv}$ by some biogenic materials. Each sample contained 0.1 ml substrate solution, if not otherwise stated, pH=0.8; 0.5 or 2.0 ml methanol; and 0.4 ml of a solution or suspension of the tested material. The samples were stopped after 4 days reaction time by heating to 70°. (No control experiments with boiled "enzymes" yielded any methyl phosphate.)

Tested material	50% MeOH		80% MeOH	
	0°	20-25°	0°	20-25°
Chlorella pyrenoidosa cells	25.4	16.0	3.6	4.0
Alkaline phosphatase, commercial	24.3	29.0	9.3	8.5
Acidic phosphatase, purified from commercial "Polidase," in acidic acetate buffer	25.1	25.5	9.5	31.2
Rat blood, fresh, containing some heparin to prevent coagulation	19.5[a]	17.4[b]	2.5	1.3
Bovine albumin, commercial	0	--	--	--

a. Three additional spots on the chromatogram

b. One additional spot

Discussion

The experimental results described in this report, coupled with those given in the previous one,[3] prove the nonexistence of a high-energy phosphate donor involved in the esterification reaction. There is also no doubt that a phosphatase catalyzes the reaction to approach an equilibrium, and that phosphatases with similar properties occur in other biogenic materials.

The position of the esterification equilibrium depends on the concentration of the reactants up to 50% alcohol in the mixture. If this concentration is too high (over 50%), the activity of the enzyme is reduced by denaturation before the reaction reaches equilibrium. This is the main reason for the quantitatively unreliable results obtained previously,[1,2,8] which led to the wrong conclusion.

In addition, there is a high probability that the phosphatase present in algae, due to this esterification (or this hydrolysis) has caused an uncontrolled number of errors and disturbances in, and sometimes even failures of, earlier photosynthesis experiments. When the incubation mixtures were "killed" only by the addition of cold methanol or ethanol to give 80% alcohol concentration, without heating of the sample, the surviving enzyme may have hydrolyzed some organic phosphates. These possible errors can now be avoided in future research.

[8] J. Ullrich, in Bio-Organic Chemistry Quarterly Report, UCRL-9772, June 1961, p. 95.

7. THE CHEMICAL EFFECT OF IONIZING RADIATION ON CYTOSINE

Cyril Ponnamperuma and Richard M. Lemmon

In a further study of the radiation chemistry of nucleic acid constituents,[1,2] we have examined the chemical effect of ionizing radiation on cytosine.

Several workers have described the formation of hydroxyhydroperoxides from pyrimidines under the influence of radiation. Sinsheimer and Hastings showed that the action of uv light on uracil in aqueous solutions produces a well-defined photoproduct, 4-dihydro, 5-hydroxy-dimethyluracil.[3] Scholes and Weiss have described the formation of hydroxyhydroperoxides when aqueous solutions of uracil and dimethyluracil were irradiated with Co^{60} γ rays or 200-kv x rays in the presence of air.[4,5,6] In the absence of oxygen, however, dimethyluracil gave 4-dihydro, 5-hydroxy-dimethyl uracil and the corresponding 4, 5-glycol. Ekert and Monier recently demonstrated the formation of glycol when a solution of cytosine was irradiated in the absence of oxygen.[7]

Our study of the chemical effects of ionizing radiation on cytosine is a continuation of earlier work on the purines adenine and guanine.[1,2] That work showed that the principal effects were the breakdown of the imidazole ring and deamination. We have continued our studies by looking for the same effects in the pyrimidine cytosine, that is, we have looked for (I) breakdown of the pyrimidine ring, and (II) deamination.

I. The Breakdown of the Pyrimidine Ring

Cytosine-2-C^{14} of specific activity 45.6 μC/mg was supplied by Schwarz BioResearch Inc., Mount Vernon, New York. The method of irradiation was the same as that described in an earlier report.[8] Two hundred and fifty microliters of a 0.1% solution of cytosine in water was sealed under vacuum after dissolved oxygen was expelled by bubbling nitrogen through the solution.

---

[1] Cyril Ponnamperuma and Richard M. Lemmon, in Bio-Organic Chemistry Quarterly Report UCRL-9652, April 1961, p. 50.

[2] Cyril Ponnamperuma and Richard M. Lemmon, in Bio-Organic Chemistry Quarterly Report, UCRL-9772, June 1961, p. 70.

[3] R. L. Sinsheimer and R. Hastings, Science 110, 525 (1949).

[4] G. Scholes and J. Weiss, Nature 185 305 (1960).

[5] G. Scholes, J. F. Ward, and J. J. Weiss, J. Mol. Biol. 2, 379 (1960).

[6] G. Scholes, J. F. Ward, and J. J. Weiss, Science 133, 2016 (1961).

[7] B. Ekert and R. Monier, Nature 188, 309 (1960).

[8] Cyril Ponnamperuma, Richard M. Lemmon, and Fritz H. Woeller, in Bio-Organic Chemistry Quarterly Report, UCRL-9408, Sept. 1960, p. 9.

A 1.5-kilocurie Co^{60} source was used for the irradiation. The intensity of radiation, determined by Fricke ferrous sulfate dosimetry,[9] was 5×10^6 rads per hour. The solutions were irradiated at different dose levels from 10^6 to 20×10^6 rads.

To estimate the amount of radioactivity lost on irradiation, probably volatile water-insoluble C^{14} compounds, 25 μl of each of the irradiated solutions was diluted to 5 ml. Aliquots (100 μl) of this solution were measured by liquid scintillation counting, by use of an internal standard.

The residual cytosine was separated from the radiation-decomposition products by two-dimensional paper chromatography on Whatman No. 4 paper washed with oxalic acid. Propanol-ammonia-water was used as a solvent in one direction, and butanol-propionic acid-water in the other.[10] Twenty-five μl of the irradiated solutions was spotted on each chromatogram. The distribution of radioactivity on the chromatogram was recorded by autoradiography with x-ray film. The amount of residual cytosine was estimated by measuring the activity on the cytosine spot by use of an end-window G-M counter. The results are shown in Table 7-I.

Table 7-I. Radiation decomposition of cytosine-2-C^{14}.

Experiment	Dose (rads)	Loss of radioactivity	Cytosine destroyed (%)	Uracil found (%)
Control	0	0	0	0
1	10^6	0	9.8	2.7
2	2×10^6	0	10.2	7.7
3	5×10^6	0	39.0	0.2
4	10×10^6	0	53.5	---
5	20×10^6	8.5	86.5	---

The effect of irradiation on the uv absorption of a 0.1% solution of cytosine is shown in Fig. 7-1. The measurements were made with a Cary recording spectrophotometer (Model 11) at a pH of 7. The optical density decreases with increasing radiation. This, however, is not an accurate indication of the breakdown of the pyrimidine ring, as some of the radiation products may absorb at this wavelength.

[9] J. Weiss, A. O. Allen, and H. A. Schwarz, in Proceedings of an International Conference on the Peaceful Uses of Atomic Energy, Geneva, 1955 (United Nations, New York, 1955), Vol. 14, p. 179.

[10] E. L. Bennett, Biochim. et Biophys. Acta 11, 487 (1953).

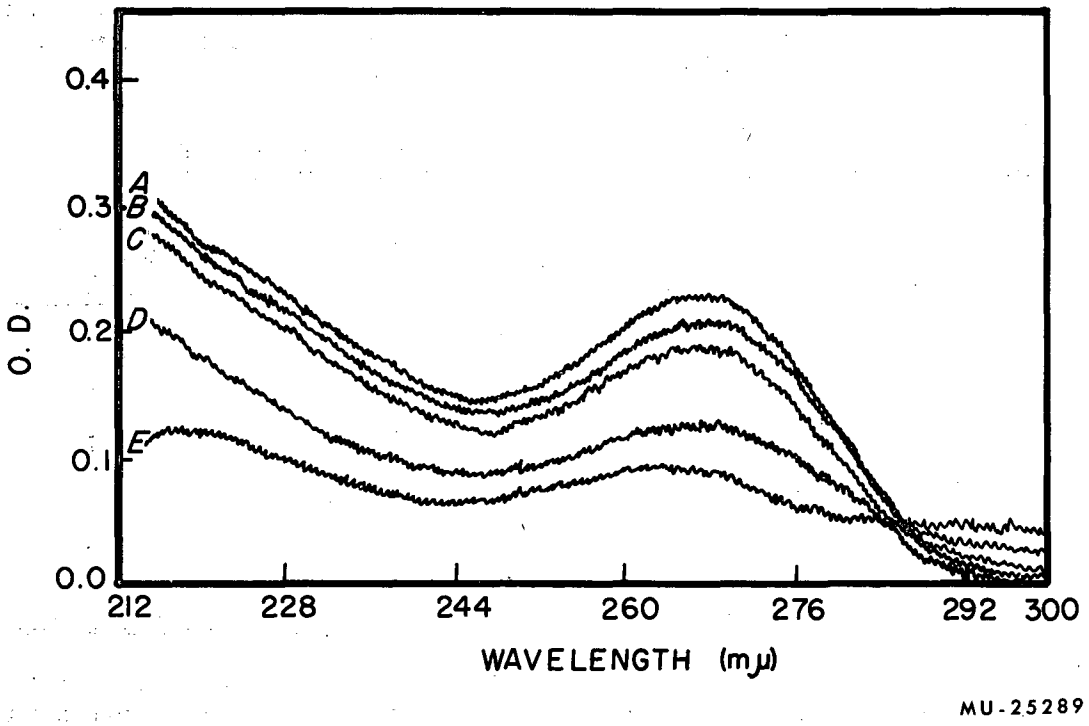

Fig. 7-1. Ultraviolet spectrum of irradiated cytosine at pH 7. A = unirradiated sample; B = 1×10^6 rads; C = 2×10^6 rads; D = 5×10^6 rads; E = 20×10^6 rads.

The results shown in Table 7-I indicate that cytosine is less sensitive to ionizing radiation than the purines adenine and guanine. At a dose level of 20×10^6 rads, adenine was completely destroyed,[1] and the loss of radioactivity as volatile material amounted to 46.8%. With cytosine, however, the loss of radioactivity as voltile compounds was only 8.5%, and 13.5% of the original material still remained intact.

II. Deamination of Cytosine

The deamination of adenine by ionizing radiation has already been reported.[11] In our present investigation, the conversion of cytosine to uracil has been observed.

The irradiation products of cytosine-2-C^{14} were cochromatographed with nonradioactive uracil as carrier. The uracil was detected in the chromatogram with the aid of shadowgrams.[12] These were prepared by laying the chromatogram over Kodagraph photographic paper (14×17 in.) and shining a uv source (G. E. Hanovia lamp - 115 watts) over it for 10 seconds. The uv-absorbing areas appeared as well-defined white spots on a dark background. The shadowgram was then matched with the autoradiograph of the same chromatogram. There was darkening of the x-ray film, corresponding to the uv-absorbing area of the shadowgram. This coincidence was obtained with four different solvent systems: butanol–propionic acid–water; propanol-ammonia-water; butanol–formic acid–water; and n-butanol. The radioactivity could have come only from the cytosine, establishing the conversion of cytosine to urasil. The maximum yield of uracil (Table 7-I) is 7.7% at 2×10^6 rads. This is significantly larger than the maximum of 1.9% at 5×10^6 rads observed in the deamination of adenine.[11]

The biological significance of the deamination of purines and pyrimidines has been widely recognized.[13, 14] Gierer and Mundry succeeded in demonstrating that nitrous acid treatment of tobacco mosaic virus RNA, or intact tobacco mosaic virus, actually results in the formation of mutants.[15, 16]

As cytosine occurs both in DNA and RNA, the conversion of cytosine to uracil may have more biological implications than the deamination of adenine. This change would give rise to an unnatural base in DNA. With RNA, it is conceivable that the altered nucleic acid undergoes identical replication.

---

[11] C. Ponnamperuma, R. M. Lemmon, E. L. Bennett, and M. Calvin, Science 134, 113 (1961).

[12] J. Smith and R. Markham, Biochem. J. 45, 294 (1949).

[13] H. Schuster, in The Nucleic Acids, Ed. E. Chargaff and J. N. Davidson (Academic Press, New York, 1960), Vol. III, p. 278.

[14] R. Lavalle, Compt. rend. 250, 1134 (1960).

[15] A. Gierer and K. W. Mundry, Nature 182, 1457 (1958).

[16] K. W. Mundry and A. Gierer, Z. Vererbungsforsch. 89, 614 (1958).

8. EXPERIMENTS ON WILZBACH TRITIUM LABELING ACCOMPANIED BY CHARCOAL ABSORPTION AND ELECTRIC DISCHARGE

Mohindra S. Chadha, Fritz H. Woeller, and Richard M. Lemmon

Since its discovery four years ago, considerable use has been made of the method of labeling organic compounds by the simple exposure of the compound to tritium gas (T_2 or HT).[1] The method depends upon the production of excited and ionized molecules in both the labeled hydrogen gas and the organic substitute. The labeling is then accomplished through such reactions as

$$RH^* + HT \rightarrow RT + H_2, \quad (1)$$

$$RH + HT^* \rightarrow RT + H_2, \quad (2)$$

$$HT^* \rightarrow H\cdot + T\cdot, \quad (3a)$$

$$RH + H\cdot \rightarrow R\cdot + H_2, \quad (3b)$$

$$R\cdot + HT \rightarrow RT + H\cdot. \quad (3c)$$

Nothing is known about the quantitative importance of the above reactions; however, probably each contributes to the resultant labeled organic compound.

The gas-exposure technique (often called "Wilzbach labeling," after its discoverer) is to expose the organic compound to several curies of tritium gas for about one week. Numerous attempts have been made recently, all with some measure of success, to decrease the amount of tritium needed and also to decrease the time. These attempts have involved putting some additional energy into the system during the time the organic compound is exposed to the tritium gas. Electric discharge,[2,3,4] gamma radiation,[3] and ultraviolet light[5] have been used as sources of additional energy.

A recent paper by Wenzel and Wollenberg indicated another way in which the efficiency of the Wilzbach method could be increased.[6] These authors reasoned that a very large increase in the surface area of the compound being exposed to the tritium gas should lead to an increase in the tritium incorporation. The tritium β has a range of only 0.7 mg/cm^2, and

---

[1] K. E. Wilzbach, J. Am. Chem. Soc. 79, 1013 (1957).

[2] L. M. Dorfman and K. E. Wilzbach, J. Phys. Chem. 63, 799 (1959).

[3] R. M. Lemmon et al., Science 129, 1740 (1959).

[4] F. L. Jackson et al., Nucleonics 18, No. 8, 102 (1960).

[5] P. Riez and K. E. Wilzbach, 134th Meeting American Chemical Society, Chicago, September 1958.

[6] M. Wenzel and H. Wollenberg, Paper No. TTS/66, IAEA-sponsored "Symposium on the Detection and Use of Tritium in the Physical and Biological Sciences," Vienna, May, 1961.

can penetrate an organic compound to a maximum distance of only about 10 microns. Wenzel and Wollenberg adsorbed several compounds separately onto charcoal, exposed the charcoal to tritium gas, and then measured the specific activities of their compounds compared to those obtained when no charcoal was used. All other conditions (time, amount of tritium, specific activity of the tritium, and temperature) were the same. The specific activities of their resultant labeled compounds were increased by the charcoal adsorption by factors ranging from 3 to 131.

The work described herein was undertaken to see whether a combination of electric discharge plus charcoal adsorption would have a particular advantage in Wilzbach labeling. It is desirable to achieve the same specific activities obtainable by the simple Wilzbach technique (1 to 100 mC/g) without having to use curie amounts of tritium, which is a considerable health hazard, and without having to wait so long (at least several days).

The compounds selected for this study were benzoic acid and salicylic acid. They were selected because, of the five compounds used by Wenzel and Wollenberg in their Wilzbach-charcoal studies, benzoic and salicylic acids showed the greatest increase in specific activity over that obtained by the simple Wilzbach technique. A second reason for using these particular compounds is that they offered facile quantitative determination by ultraviolet spectrophotometry. A third reason was that gas chromatography of their methyl esters appeared to be a powerful tool for guaranteeing the radiochemical purities of the tritium-containing products.

Experimental Procedure

Discharge Experiments

To a solution of 100 to 200 mg of benzoic or salicylic acid in 50% ethanol, 5 to 6 g of charcoal was added (Norite, 6-12 mesh, 600 m^2/g, American Norite Co., Jacksonville, Florida--water-washed and-vacuum dried). After 30 min the solution was decanted and the charcoal washed three or four times with water. The amount of unadsorbed acid (usually between 10 and 20 mg) was determined from the ultraviolet absorption in the decanted solution and washes. The charcoal was dried at 70° and 100 mm for 2 to 4 hr, and finally on a vacuum line until a pressure of about 70 μ was reached at room temperature. A known portion of the charcoal was put in the discharge cell (Fig. 8-1). The tritium gas was added from a metal container of UT_3 that was heated to 450°. This apparatus and the vacuum line used to transfer the tritium gas to the discharge cell were similar to those already described.[7]

The electric discharges were carried out in the simple cell shown in Fig. 8-1. The electric discharges were supplied by a Tesla coil rf generator. This device supplied pulses of 3 μsec duration (av current 1.5 amp, average voltage 5 kv) with an average time between pulses of 7 msec. The estimated

[7] Author unidentified, Nucleonics 16, No. 3, 62 (1958).

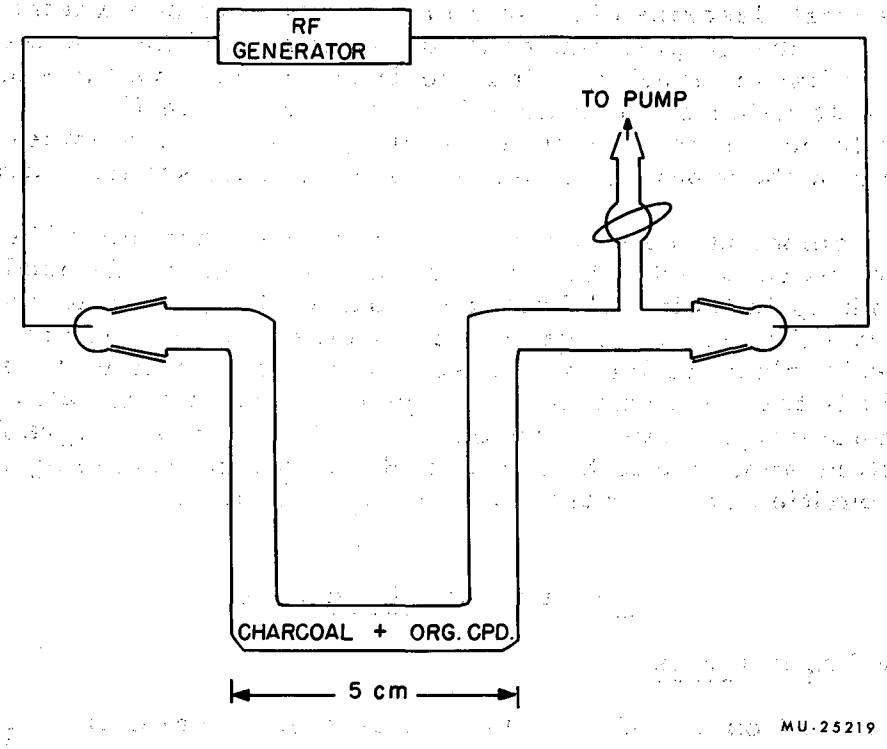

Fig. 8-1. Discharge cell.

maximum energy release in the charcoal for a 45-min discharge period (the usual time we used in this work) was 5×10^{10} ergs, or 3×10^{22} ev. The amount of energy dissipated by the tritium betas during this time was only about one-millionth of these figures.

After the discharge period, the cell was opened to the uranium tritide container and the bulk of the tritium gas reconverted to UT_3. The residual gas in the system was then pumped out until a pressure of about 70 mm was reached. The organic acids were extracted by shaking the charcoal with 50 to 80-ml portions of ammoniacal ethanol (30 ml conc NH_4OH diluted to 1 liter with absolute ethanol). This procedure was repeated six to eight times. The combined extracts were evaporated to dryness. The residue was dissolved in 10 to 20 ml of 0.1 N NaOH and then evaporated to dryness. This last procedure was repeated two or three times.

The residual solid was dissolved in water, the solution acidified, and the organic acid thoroughly extracted with ether. The ether solution was evaporated to dryness and the organic acid crystallized from an aqueous solution. (In two experiments, some formic acid was added to the water in order to eliminate the possibility that small amounts of highly labeled formic acid might be occluded in the benzoic acid or salicylic acid crystals.) The specific activity of the crystals was determined. The crystals were then dissolved in ether, and the acid was converted to its methyl ester on the addition of excess diazomethane in ether solution.

The methyl esters were purified by vapor-phase chromatography (VPC). The following columns (3/16 in. i.d.) were used:

(1) 20% castorwax on 60-80-mesh firebrick, 5 ft long,
(2) same column materials, but 2.5 ft long,
(3) 20% diethylene glycol succinate on 60-80 mesh firebrick, 5 ft.

The chromatographic instrument was a Model A-90 Aerograph (Wilkens Instrument Co.). This instrument was equipped with an internal-flow proportional counter that enabled us to detect radioactivity emerging from the VPC column. This counter has been described previously.[8] Specific activities of the trapped esters were determined by liquid scintillation counting and by the molar extinction.

Wilzbach Labeling

A solution of 100 mg of benzoic or salicylic acid in 5 ml of ethanol was placed in a 50-ml Pyrex bulb equipped with a standard taper joint and a break-off seal. The ethanol was evaporated in a rotating evaporator, whereby a fairly uniform layer of the acid with an average thickness of 15 μ was deposited (about twice the range of the tritium β particles in these compounds). The flasks were attached to the tritium line and, after the pressure was reduced to 70 μ, 3.5 mm of H_2^3 (containing 500 mC) was introduced. The bulb was then glass-sealed and allowed to stand for 10 days. The removal of the tritium gas, treatment with NaOH solutions, extraction

[8] Robert T. Mullen, The Chemical Interaction of Accelerated Carbon-14 Ions with Benzene (Thesis), UCRL-9603, March 14, 1961, pp. 58-65.

with ether, crystallization, esterification, and gas chromatography were all carried out as described in the previous section.

Results

The principal results of these investigations are summarized in Tables 8-I and 8-II.

Table 8-I. Tritium labeling of benzoic acid.

Experiment[a]	Duration of experiment	Sp act. of recryst. product (mC/g)	Sp act after 1st VPC (μC/g)	Sp act. after 2nd VPC (μC/g)
Charcoal plus discharge	45 min	5.5	540	547
Charcoal plus discharge	60 min	2.4	418	395
Charcoal --no discharge	45 min	0.015	---	---
Wilzbach --no charcoal	10 days	2.7[b]	681	653

a. The total tritium used in each experiment was 500 mC (the gas pressure varied from 3 to 5 mm).
b. Formic acid was added to the crystallizing solvent (H_2O).

Table 8-II. Tritium labeling of salicylic acid.

Experiment[a]	Time of experiment	Sp act. of recrystallized product (mC/g)	Sp act. after 1st VPC (μC/g)	Sp act. after 2nd VPC (μC/g)
Charcoal plus discharge	45 min	1.3	562	547
Charcoal plus discharge	60 min	1.6	570	576
Charcoal--no discharge	45 min	0.002	---	---
Wilzbach--no charcoal	10 days	2.1[b]	700	725

a. The total tritium used in each experiment was 500 mC (the gas pressure varied from 3 to 5 mm).
b. Formic acid was added to the crystallizing solvent (H_2O).

Discussion

Effectiveness of the Charcoal

The results of our experiments do not indicate any particular utility to the charcoal. The data of the tables allow us to compare the specific activities of the recrystallized products after the "charcoal-no discharge" experiments (3rd horizontal line of both tables) and the simple Wilzbach experiments (4th horizontal line). In all experiments the total tritium used was 500 mC. The time difference between these two types of experiments is the ratio of 45 min to 10 days, or 3×10^{-3}. Table 8-I shows that the Wilzbach experiment gave a specific activity in the recrystallized benzoic acid of 2.7 mC/g. Applying the above factor, we would expect in 45 min a specific activity of 8 μC/g. We actually measured 15 μC/g for the charcoal-adsorbed compound--an indication that the charcoal was helpful. On the other hand, the simple Wilzbach experiment on salicylic acid gave a specific activity of 2.1 mC/g, which gives an expected activity in 45 min of 6 μC/g. Instead, we actually measured only 2 μC/g for the charcoal-adsorbed compound. The Wenzel and Wollenberg results[6] are clearly in conflict with our findings. Their charcoal-adsorbed salicylic and benzoic acids were reported to have 131 and 27 times, respectively, the specific activity that they had after simple Wilzbach labeling. We can suggest no explanation for this conflict other than that the effective surface of the adsorbates used by the German workers may have been greater than ours.

Certain disadvantages of charcoal became evident in our experiments. In the cases of benzoic and salicylic acids it is most difficult to elute all the compound back from the charcoal. In general, we would expect that one would have to accept losses of at least 10% in order to make use of charcoal adsorption. In addition, one faces the trouble of removal of water from the charcoal after the adsorption and before the irradiation. This is difficult if the compounds, such as those used here, have an appreciable vapor pressure at room temperature. This trouble would be minimized if a more volatile solvent, such as methanol, were used. It could also have been minimized in our cases if we had irradiated the sodium salts instead of the free acids.

Achievement of Radiopurity

Our experiments reinforce the warning that has been made by nearly everyone who has studied the Wilzbach labeling technique--namely, that the achievement of radiopurity is both deceptive and difficult. A comparison of the data of the 3rd columns of both tables with those of the 4th and 5th columns shows that the specific activity after gas chromatography is about one-third to one-tenth that of the recrystallized material. By any ordinary chemical or physical test the recrystallized material would appear to be a single, or "pure" compound. However, when this material was esterified and put through VPC, the presence of large amounts of radioactive material (undetected by the mass detector--a thermal conductivity cell) was evident. It was only upon trapping our benzoic or salicylic acid peak, and then rechromatographing on a different substrate with no concomitant change in specific activity (within experimental error), that we were assured that our compounds were radiopure.

We do not know the identity of our radioactive impurities. One such suspected compound was formic acid. However, recrystallization from an aqueous formic acid solution gave specific activities essentially identical to those obtained when water alone was the recrystallizing solvent. Other possible radioactive impurities, which could have one atom of tritium per molecule, are benzene (from benzoic acid) and phenol (from salicylic acid). These possibilities were not tested.

In some of our gas chromatographic purifications of both the benzoic and salicylic acids we found that considerable amounts of radioactivity were left behind on the chromatographic columns. This activity appeared only when small amounts of water were injected into and eluted from the columns. The activity appeared right in the emerging water peak, and subsequent injections of water removed additional amounts of activity. It is extremely unlikely that any tritium in an easily exchangeable position would have survived all the water treatments (removal from charcoal, treatment with NaOH, crystallization). We are inclined to the idea that some decomposition of our compounds was occurring during the gas chromatography. This idea is reinforced by the observation that a reduction in our column temperature from 160° to 130° nearly completely eliminated the phenomenon of water-elutable radioactivity.

Utility of the Electric Discharge

There still remains the question of the value of the electric discharge compared with the simple Wilzbach treatment. There is no doubt that the activity reached in a given period of time, and at a given tritium exposure, is enormously greater in the presence of the discharge. It has been shown, in the case of Wilzbach-plus-discharge labeling of benzene, that the activity was 1.7×10^4 times as great as it would have been in the same time (1 hr) by exposure to the same amount of tritium (40 mC)[3]. In our work the time factor found for benzoic and salicylic acids appears much lower (about 240 instead of 1.7×10^4). However, no one has yet achieved a higher specific activity by using discharge procedures than has been obtained by the simple Wilzbach procedure, given adequate time.

Another question that remains unanswered is whether the electric discharge procedure causes more molecular destruction than the Wilzbach method for a given specific activity in the product. Our observations were obscured by the difficulties of removing our compounds from charcoal. However, the data we do have indicate that the electric discharge may cause the greatest damage. It appeared that only 50 to 70% of our compounds could be re-extracted from the charcoal after electric discharge. On the other hand, when our compounds were simply adsorbed onto charcoal, and then extracted (without subjection to tritium or to electric discharge), we could recover about 90%. Furthermore, some radioactive peaks were evident on our chromatograms after discharge experiments that were not visible after simple Wilzbach labeling procedures. In our Wilzbach experiments, where essentially the same specific activities were reached, we could detect no decomposition.

9. THERMAL TRANSIENTS IN ASCITES TUMOR SUSPENSIONS

Karl K. Lonberg-Holm

When glucose is fed to ascites cells in suspension, it causes them to undergo transient metabolic states before they can achieve a metabolic steady-state glycolysis. A variety of methods has been used to demonstrate this. Chance and Hess[1] and others in the same laboratory have measured transients in O_2 uptake, light absorption, glucose uptake, and acid production (this last work is unpublished). The concomitant changes in intracellular metabolite concentration were first described in this Laboratory[2, 3] and have recently been reconfirmed by somewhat more refined methods (unpublished). It is now possible to demonstrate transients in heat production following the feeding of glucose, and the method and some results are described below.

Methods

A microcalorimeter has been constructed to hold a 2.5-ml liquid reaction volume and about 4 ml gas phase. It consists of a teflon cup that can be screwed onto a teflon holder from which is suspended an insulated thermistor and a 75-ohm carbon resistor to serve as an internal heat supply. (See Figs. 9-1 and 9-2.) Also suspended from the holder is a stirring paddle on a glass fiber, and on another fiber a short length of tubing to hold substrate sugar (see figures). The cup and its holder (which is heavily greased) are inserted into a tight-fitting Dewar flask, and the flask is clamped inside a felt-lined box. A glass fiber from a 3-rps motor projects through the top of the box, and it is fastened to the stirring fiber with a bit of glass tape. Stirring is begun as soon as the cell suspension is placed in the box. Similarly another glass fiber projects through the top and is fastened to the substrate injector fiber with wax.

The leads from the thermistor are connected to a simple bridge circuit and recorder (Fig. 9-3). The recorder is modified by disconnecting the reference cell and calibrator, and replacing with a reference voltage from a 1.5-v dry cell in series with enough resistance to bring full scale from 1 mv down to about 0.3 mv. Full scale then represents about a 5-ohm change in the bridge circuit or about 50 m^{o}C at the thermistor. The leads to the heater are connected to a variable voltage.

In an experiment, 2.5 ml of a suspension of ascites cells is placed in the cup, which is then screwed to the holder with as little handling as possible. The cup and holder are insulated as described above, and 5 to 10 min are given for rapid temperature changes to occur. The temperature in the cup should then be equal to or as much as a degree higher than that in the box.

---

[1] B. Chance and B. Hess, Ann. N. Y. Acad. Sci. 63, 1008 (1956).

[2] Karl Lonberg-Holm, in Chemistry Division Quarterly Report, UCRL-8141, Dec. 1957, p. 49.

[3] K. Lonberg-Holm, Biochim. et Biophys. Acta 35, 464 (1959).

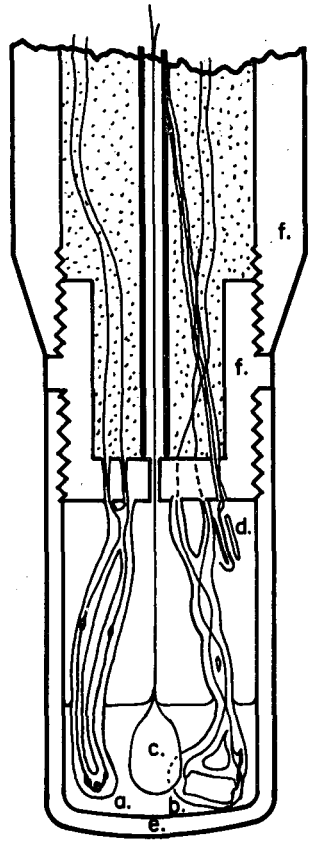

MU-26113

Fig. 9-1. Microcalorimeter vessel.
a. Thermistor soldered to lengths of 40-gauge copper wire (formvar-coated). These are soldered in turn to leads of 29-gauge copper wire. The projecting thermistor and wires are coated with "epon" and "glyptal."
b. 75-ohm carbon resistor soldered to 29-gauge copper wire, coated with epon and glyptal.
c. Stirring paddle suspended on glass fiber and freely rotated at a level where it will not touch a or b.
d. Substrate injector to hold 10 μl. This is a short length of open-ended polyethylene tubing concentric about the end of a glass fiber which is bent so that it can be pushed down the side of the cup into the liquid.
e. Teflon cup, 7/8-in. o.d. with 1/16-in. walls, 1-3/4-in. long.
f. Holder for cup filled with paraffin and cotton and through which wires, tubular bearing for stirrer, and hole for injector fiber pass. Not shown is a thin polyethylene tube leading into cup from outside.

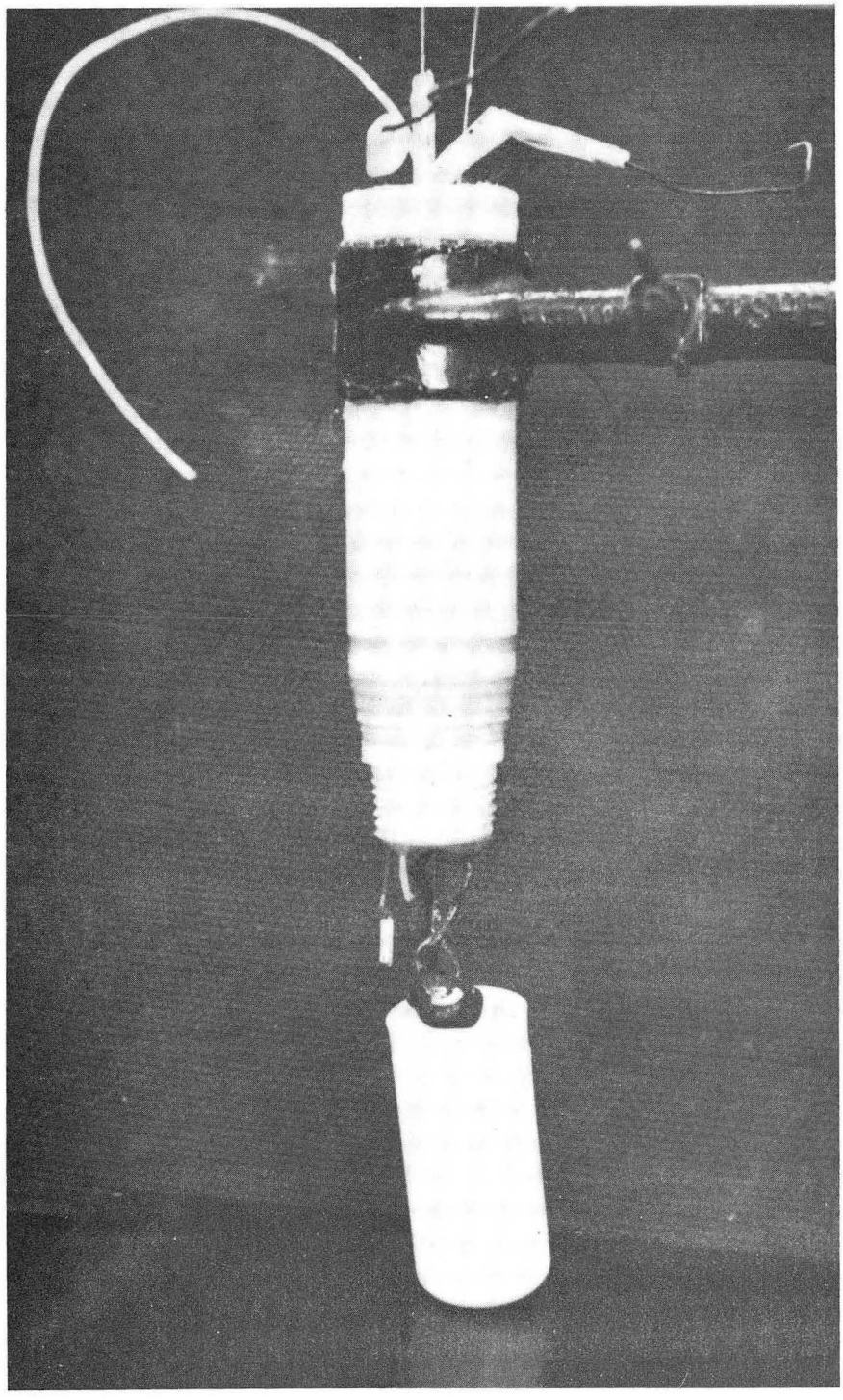

ZN-3033

Fig. 9-2. Arrangement of probes to fit into calorimeter cup. Substrate injector partly lowered.

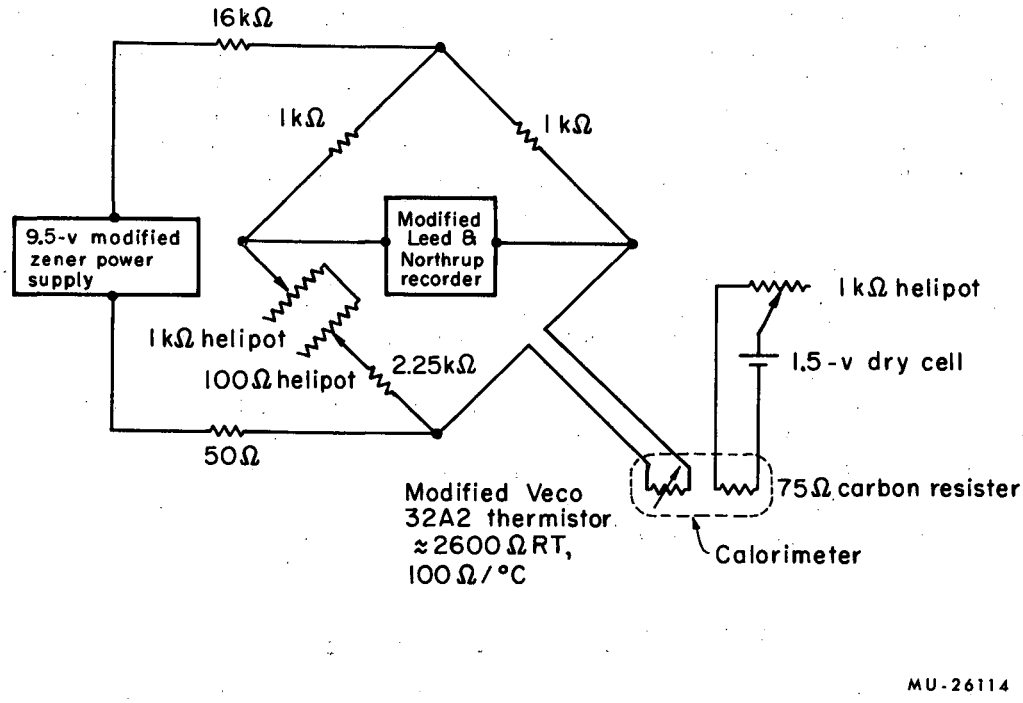

Fig. 9-3. Wiring diagram for bridge circuit and heater circuit.

Heat is then generated in the internal heater so that the rate of heat loss equals the rate of heat generation. It usually requires repeated adjustments for 10 to 30 min before a steady state can be achieved in which the temperature change is less than 0.3 m°/min. To get such a state with a 1° gradient between the cup and box it may be necessary to generate as much as 50 millicalories/min. The thermistor also generates heat, since current flows through it--the circuit is designed to keep this less than 3 millicalories/min. Because heat is produced in the detector, stirring must be kept constant. After the temperature is constant, the substrate is added by lowering and withdrawing the injector about six times repeatedly in rapid succession.

Two strains of tumors were used. Usually a "tetraploid" strain of the Ehrlich mouse ascites carcinoma, obtained from Dr. Sassenrath of the University of California Medical School in 1960, was employed ("Strain I"). Also a "hyperdiploid" strain, obtained from Dr. Cailleau of the University of California Medical School in 1961, was used ("Strain II"). The latter strain is probably cytologically similar to that which I used in all work before 1958. The tumor was harvested at 7 or 8 days, washed twice in unchilled Lockes buffer by brief centrifugation, and diluted to about 10% by volume* in Lockes buffer. Also, 5 to 8 μM lactate per ml was added to provide reserve substrate. The sugar substrates were made up in water or water and buffer so that the required amounts could be contained in 10 μl for injection.

A few experiments were made to measure to transient acid production by cells fed amounts of glucose similar to those used in the calorimeter experiments. A pH-Stat built by the International Instrument Company was outfitted with a cell to hold between 2.5 and 3.5 ml tumor suspension. The buffer strength was cut somewhat by substituting half of the phosphate in Lockes with iso-osmotic NaCl. The cells were washed and suspended in this in the same way as they had been in the calorimeter experiments. Usually lactate as lactic acid (5 to 10 μM) was given 3 to 10 min before glucose feeding. Glucose was injected in 150 μl of buffer at zero time.

Limitations and Corrections

It is necessary to review major limitations and corrections encountered in the use of this simple microcalorimeter.

(a) There is no reference cell to correct for thermal drift, and the cell is not isolated entirely from the environment. This means that temperature changes observed 6 to 10 min after the addition of substrate are often not meaningful, and thus that the total heat production for longer periods cannot be followed.[4]

---

*The volume of cells obtained in the second washing is divided by approximately 2.2 to give the volume that would be obtained by 15 min centrifugation. The latter procedure was on aliquots of cells from each experiment to give the cell volumes used in all calculations.

[4] R. Estabrook [Fed. Proc. 19, 39 (1960) (abstract)] has built a microcalorimeter employing two thermopiles, one in a reference cell. This can be used for slow reactions, but has not so far been used to follow transient heat production.

(b) The injection of substrate sometimes results in an addition artifact (usually negative) of as much as 2.5 m^{o}, which recovers (if no heat is produced by an immediate reaction) to a variable extent (45 to 75%) depending upon uncontrollable factors. Also there seems to be a small heat absorption from the mixing of concentrated sugars with the suspension. The evaluation of these two effects is difficult, but in most experiments the error from these artifacts is not greater than 10% of the initial temperature change.

(c) The resistance of the thermistor itself, as a function of temperature, seems to be constant: 1 ohm equals 10.0 m^{o} C. However, the sensitivity of the modified recorder changes, and the inches of pen displacement per ohm bridge circuit change, should be measured at each run.

(d) We do not start the experiment until there is a steady temperature inside the reaction vessel and endogenous heat production cannot be measured. Any increase in temperature is due to an increase in heat production above the endogenous.

(e) Another limitation is that the observed temperature changes in the liquid cannot be translated directly into calories by multiplying by the suspension volume or by some other constant. There is incomplete thermal isolation, and the higher the gradient between the cup and its immediate surroundings (the Dewar and the cup holder), the faster the heat flow out, and the lower the efficiency in raising the temperature.[5]

Equating the relation of the efficiency of the caloric input to the rise in the temperature was determined in two ways.

(a) With the in-series resistance in the heater circuit (R') set at zero, 7.76 millicalories/sec are generated. When the temperature is at equilibrium with R' at infinity, short pulses with R' = 0 (between 1 and 7 sec) produce linearly increasing maximal temperature changes. The maximum temperature increase occurs about 12 sec after the power is released, and is followed by a decrease as the heat diffuses out of the cup. The maximum temperature, observed on 16 separate occasions, corresponded to 69.3 ± 3.4% efficiency, where 100% corresponds to the hypothetical situation in which all heat goes to raise the temperature of the liquid.

(b) A more useful kind of efficiency to measure is that obtained when R' is decreased after dT is zero, so that there is excess power dissipation with an increase in temperature (dT') resulting. When this was done with a variety of rates of power dissipation initially needed to keep dT = 0, and with a variety of changes in R' thereafter, it was found that the rate of temperature change in the first minute after the introduction of an excess rate of power dissipation was greater than at later times. The first-minute slope was 67% efficient (73 to 60% range, av 9 determinations), and at 4 min the efficiency was 47% (31 to 52% range, av 7 determinations). Surprisingly, the efficiency did not seem to depend upon the rate of power dissipation needed initially to keep dT = 0 (the gradient between the box and the cup).

Results

Figure 9-4 illustrates the type of temperature changes caused by feeding glucose to a cell suspension. Looking from right to left, the first

[5] It may be possible to improve on this aspect by lining the Dewar with an insulating material.

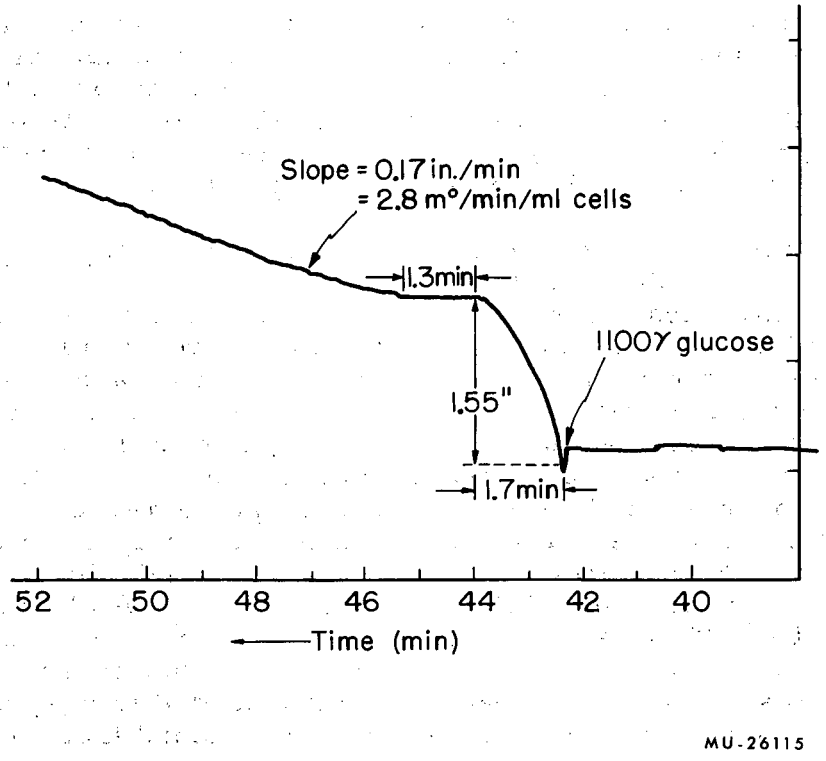

Fig. 9-4. 2.5 ml 12% cells at 26.35° C in 7 mM lactate given 1100 μg glucose. 1 m° C = 0.205 in. 1.55 in. corresponds to 25.3 m°/ml packed cells.

change is in initial negative addition artifact (the dotted line shows the estimated recovery). This is followed by a rapid transient increase to 1.7 min, which is followed by a lag of 1.3 min.[6] After the lag there follows a steady-state heat production. It should be further mentioned that in about one-half of such experiments, the initial transient heat burst is seen to be resolved into two components, the first and steeper portion lasting a few tenths of a minute only.

Table 9-I shows the results of similar experiments in which cells were fed glucose. The first section shows that there is considerable variation from mouse to mouse in the response of the tumor to glucose. The times required to attain the first transient, and the length of the following lag, suggest that the Strain I tumor may possibly have been altered in the early experiments (as a result of aureomycin treatments given the mice until mid-October) or that, possibly, Strain I responds more rapidly in its transients by nature of its smaller cell size or some other factor.

The initial transient heat burst is little affected by cutting the added glucose in half. Glucose reduced to 220 μg/2.5 ml suspension results in a lowered transient--this is to be expected, as all the 220 μg would be taken up by the cells during the initial burst of glycolysis, as seen at higher glucose concentrations. (This is based on pH-Stat and chemical work described elsewhere.)

The prior addition of fructose does not destroy the transient behavior resulting from glucose addition, even when small quantities of glucose are used. Further addition of glucose to cells already having glucose would result in altered transient behavior, and thus there must be some basic differences in the control mechanisms for glucose and fructose fermentation. Two successful experiments were made to measure the temperature effect of added fructose alone to the cells. One of these is shown in Fig. 9-5. Fructose caused no rapid transient heat production, but only a steady slope of 3.0 and 1.6 m^{o}/min/ml packed cells in the two runs.

Iodoacetate (IAA) decreases the transient heat production by two-thirds and lowers the steady-state heat production so much that it is impossible to detect any temperature rise after 4 min.

The effect of methylene blue on heat production was also investigated. Table 9-II shows four experiments, and Fig. 9-6 shows the shape of the curves obtained. Methylene blue uncouples respiration and speeds glycolysis so that the entire amount of added glucose is used up in a short enough time to afford a good estimate of the total temperature change. The maximum rate of temperature change after feeding 1100 μg glucose is comparable to that obtained in the absence of methylene blue, but occurs after an initial lag of about a minute. The slope at 6 min is 2 to 3 times that obtained without methylene blue. There is no evidence for the delay that is observed in unpoisoned cells after the initial rapid production of heat; the steady state

[6] This lag is in part due to a tendency for the initial rapid transient increase to be lost as outward heat flow. Mock experiments made by adjustment of R' show that this lag is, in part at least, a real transient lag in heat production.

Table 9-I. Results of feeding glucose to 2.5 ml of about 10% tumor cells; 5 to 8 μM/ml lactic acid present in all cases.

Date	Glucose added (μg)	Strain of tumor	Age (days)	Temp of cells (°C)	Initial displacement (m°/ml packed cells)	Time of maximum (min)	Duration of lag following maximum (min)	Slope at 4 or 6 min (m°/min/ml packed cells)
9/25	1100	I	8	(~29.0)	20.9	1.6	1.4	2.2
10/24	1100	I	7	28.7	23.4	2.5	1.1	2.8
10/25	1100	I	8	27.2	20.6	2.2	1.2	3.3
10/31	1100	I	7	28.9	29.7	2.2	1.0	3.5
11/21	1100	I	7	27.3	19.4	1.1	1.1	2.8
10/28	1100	III	7	26.4	25.3	1.7	1.3	2.8
11/5	1100	III	8	28.0	26.2	1.6	0.0	3.7
11/13	1100	III	8	30.4	24.1	1.3	0.3	4.1
11/13	1100	III	8	29.2	24.1	0.8	1.3	3.6
11/13	1100	III	8	29.0	23.8	1.5	0.0	4.0
Average	1100	-	-	(28.4)	23.8	1.6	0.9	(3.3)
10/18	550	I	8	(~28.0)	20.9	1.8	1.1	2.3
10/21	550	I	8	26.0	20.7	1.6	2.0	1.0
10/21	550	III	8	25.3	23.2	1.3	3.8	1.1
Average	550	-	-	-	21.6	1.6	-	-
10/13	220	I	8	31.9	10.5	0.7	1.0	3.1
10/17	110	I	7	28.1	2.3	0.3	-	-
10/18	110	I	8	27.2	3.9	0.4	1.0	1.4
10/25	1100[a]	I	8	28.5	20.6	1.3	1.4	2.0
11/14	1100[b]	I	8	28.0	17.3	0.7	0.8	2.4
10/29	110[c]	I	8	26.7	5.1	0.6	1.3	0.7
10/31	110[d]	I	7	28.6	2.7	0.4	0.7	2.1
11/6	1100[e]	I	8	28.2	9.6	0.6	-	-
11/6	1100[f]	I	8	29.4	5.3	0.7	-	-

a. 1.1 mg fructose 9 min before glucose. b. 2.75 mg fructose 12 min before glucose.
c. 2.75 mg fructose 8 min before glucose. d. 2.75 mg fructose 6 min before glucose.
e. Cells in 1.2×10^{-4} M IAA. f. Cells in 1.2×10^{-4} M IAA.

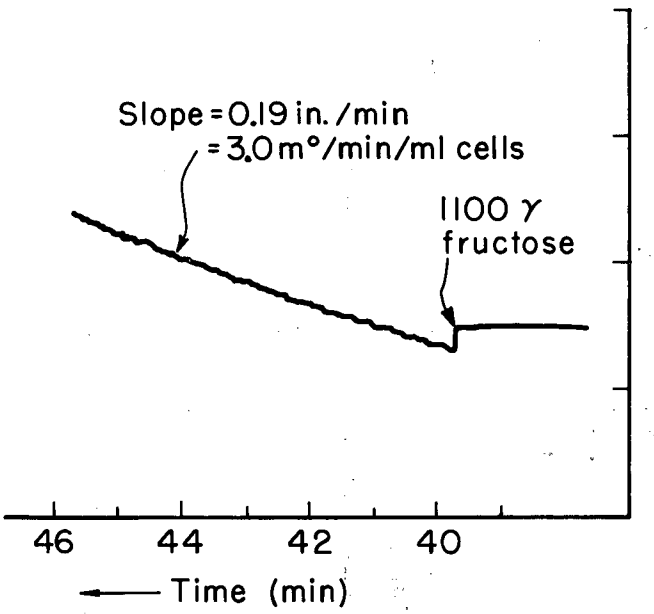

MU-26116

Fig. 9-5. 2.5 ml 11.6% cells at 27.5° C, 8 mM lactate, given 1100 μg fructose.

Table 9-II. Temperature changes resulting from feeding methylene-blue-poisoned ascites cells glucose. 2.5 ml Strain I tumor suspension at about 10%. Cells washed twice and suspended in 0.33 μM/ml methylene blue in Lockes, except on 11/14/61, when methylene blue was added after washing to bring its concentration to 0.31 μM/ml. Lactate present in each experiment.

Date	Glucose added (μg)	Temp cells (°C)	Maximum slope[a]	Slope at 6 min[a]	Total temp change (m°)	Time to completion (min)
11/8	1100	28.9	20.9	9.2	26.8	11
11/14	1100	29.1	25.0	6.8	27.4	12
11/8	550	28.0	13.5	-	15.5	7
11/8	110	29.7	-	-	3.3	1.5

a. Slopes as m°/min/ml packed cells.

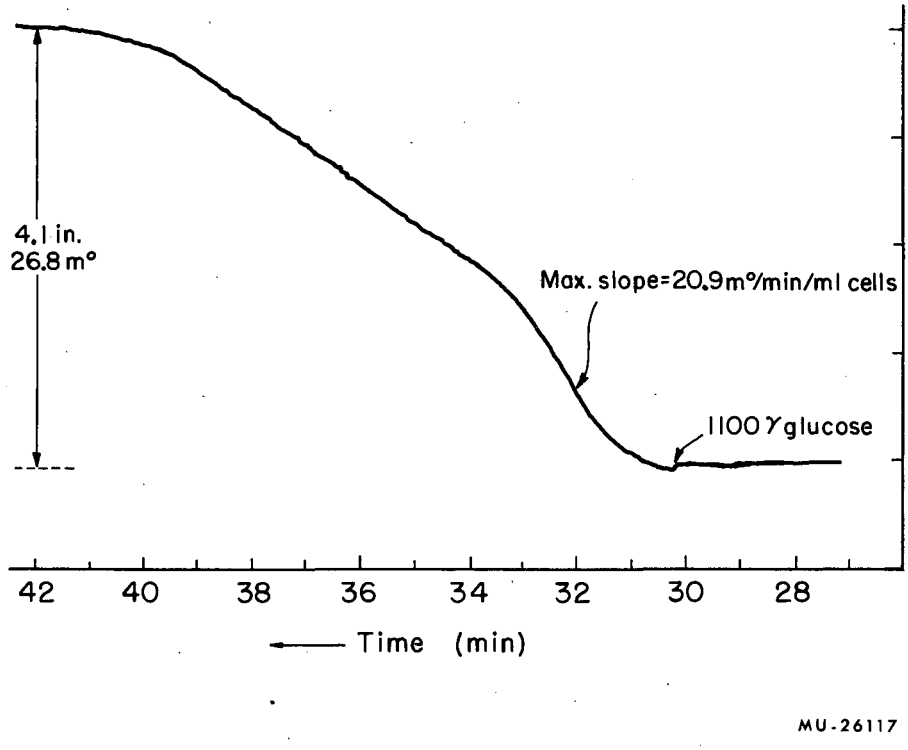

Fig. 9-6. 2.5 ml 10% cells at 28.9° C, 7 mM lactate, washed and suspended in 0.33 mM methylene blue and given 1100 μg glucose.

follows soon after the rapid period of heat production. Methylene blue has no striking effect on the pattern of heat production that follows fructose feeding.

The acid production by ascites cell suspensions has been measured in the pH-Stat. A typical curve of alkali addition required to maintain the cells at pH 7.3 is shown in Fig. 9-7. First, there is a complete lag in acid production lasting a few tenths of a minute. Then acid production increase to a maximum rate, and then decreases again to a steady state. Often there is evidence that a slightly slower rate exists between the initial transient and the ultimate steady state. The time at which the lowest rate occurs after the initial transient is designated as t'. The steady-state rates were all measured about 6 min after feeding, and these rates continue with little abatement until most of the sugar is used up. If each mole of sugar gives 2 moles of (lactic) acid, the reaction is 95 to 100% complete, based on the total acid production. It should be pointed out that the acid-production curves are similar to the temperature-change curves, but that the behavior is displaced; thus the initial transient acid production is initiated after the temperature transient is well under way, and t' occurs at the end of the lag in heat production that follows the initial temperature transient. Table 9-III summarizes some of the pH-stat results.

Discussion

The initial temperature change caused by glycolysis can be used to calculate the heat produced to cause this change, if the calorimeter is assumed to be 67% efficient in this time (see discussion of Limitations and Corrections). The average change in the 2.5 ml suspension is 23.8 m°/ml packed cells 1.6 min after feeding of 1100 μg glucose. Thus $2.5 \times 23.8/0.67$ equals 89 millicalories/ml cells. In this initial 1.6-min period roughly 3.6 μM of glucose has been converted to lactic acid (as based on pH-stat experiments), splitting 1 mole glucose to 2 moles lactic acid, and formation of 2 moles ATP produced 26.9 kcal in an aqueous buffer.[7] Glycolysis of 3.6 μM glucose to 7.2 μM ATP should liberate 97 millicalories, a figure close to the calculated heat production. There is chemical evidence,[3] however, that the cells do not store as much APT as is produced in the first 1.6 min. Thus the net reaction does not include ATP production, and much more heat could be expected. Also we have neglected the heat production from the exothermic phosphorylation of the intermediates that remain in the cell at 1.6 min, and which may be about 1 μM/ml packed cells. Thus the net observed heat production as calculated from the temperature change is lower than that to be expected on the basis of the expected rates of reaction and the known enthalpy changes. Therefore, the endogenous heat production from other than glycolytic sources must be reduced, even during the initial period following glucose feeding.

Similarly, we can compare the heat production in the steady state with that expected on the basis of the steady-state glycolytic rate and the known

[7] H. A. Krebs and H. L. Kornberg, Energy Transformations in Living Matter (Springer-Verlag, Berlin, 1957), p. 250.

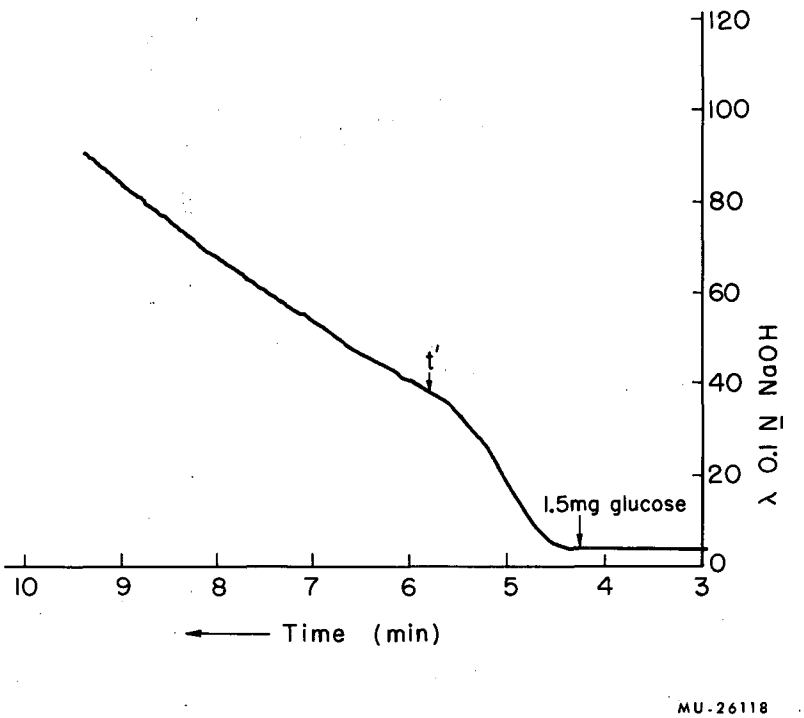

Fig. 9-7. Acid production by ascites cells given glucose. 3.0 ml suspension containing 11.6% cells was given 1.5 mg glucose in 150 μl buffer. Strain I, 8-day cells were twice washed before use. The buffer was phosphate-Lockes with half the phosphate replaced with iso-osmotic saline. Temperature-jacketed at 36.5°.

Table 9-III. Acid production by ascites cell suspensions given glucose. 2.5 to 3.5 ml cells (about 10%) given glucose at zero time. Full scale on pH-stat recorder equivalent to 200 μl of 0.1 N NaOH. Lactate present as reserve substrate. All runs except 49-C are Strain I tumor. Tumors are 7 to 8 days old and have been washed twice in buffer. The buffer used is Lockes with half of the Phosphates replaced with iso-osmotic saline.

#	Methylene blue (mM/liter)	Glucose (micromoles/ml suspension)	Temperature (°C)	Maximum rate acid production[a]	t'	Steady rate acid production at 6 min[a]
48'-A	-	2.3	25.3	4.9	2.2	1.1
47	-	2.3	28-27	>5.5	2.6	1.8
48'-D	-	2.6	28.7	6.0	2.7	2.4
48'-B	-	2.3	29.3	6.6	2.3	2.2
48'-E	-	2.6	35.2	8.7	1.1	2.7
49-C	-	2.6	36.4	10.7	1.1	-
49-A	-	2.6	36.5	10.0	1.6	4.9
48'-C	0.30	3.2	29.4	10.6	3.1	5.9
49-B	0.33	2.6	36.5	14.8	2.2	6.7

a. Rates given in μM acid/min/ml packed cells. (Note: 47, 48'-D, and 48'-B averaged 7.2-μM lactic acid production per ml cells at 1.6 min. This indicates 3.6 μM glucose has been used up at this particular time. See discussion.

enthlpy change. When 1 mole of glucose is split to 2 moles of lactic acid without net ATP production in an aqueous buffer, 50 kcal/mole is released as heat.[8] Glucose uptake to lactic acid at 6 min is roughly 1.1 μM glucose per min per ml packed cells (average of 47, 48'-D, and 48'-B in Table 9-III), and the heat expected is 55 millicalories/min/ml packed cells. We observe a steady-state temperature change averaging 3.3 m°/min/ml packed cells at an average temperature of 28.4°, and with 47% efficiency (see above) the heat production should be 18 millicalories/min/ml packed cells. Therefore, the actual net heat production is lower than the enthalpy change of the glycolysis, and the endogenous sources of heat production that existed before the glucose was fed must have been decreased correspondingly. This is a thermal equivalent of the Crabtree effect in which oxygen uptake is cut appreciably when tumor cells are fed glucose.

In the methylene-blue-poisoned cells fed 1100 μg glucose, we can also assume roughly 47% efficiency and calculate that an average of 144 millicalories is produced during the entire period of glycolysis (av Table 9-II, first two). Here 305 millicalories would be expected from theory, and again it is evident that the heat of glycolysis is partly masked by a decrease in heat from other sources.

The lag in the heat production after feeding of glucose to methylene-blue-poisoned cells is probably the length of time needed to build up the ATP concentration inside the cell to a level at which phosphorylation can proceed at a high or maximal rate. In unpoisoned cells, the initial ATP concentration is high enough to permit maximal rates of phosphorylation. In the normal cells the heat production falls drastically after the initial high period when the intracellular ratio of ATP/ADP gets too high; the possible mechanism of this control is discussed in previous papers.[2,3]

Conclusion

A simple microcalorimeter has been built and used to measure thermal transients that correspond to chemical transients inside ascites tumor cells fed glucose. The effects of two cell poisons on this thermal behavior have been investigated. Fructose given alone produces no transient effects, and given before glucose does not interfere with the typical glucose pattern of heat production. The observed additional heat after feeding of glucose is lower than the heat expected on the basis of the known enthalpy change by 1/2 and 2/3, indicating that other heat-generating reactions inside the cell are slowed during glycolysis.

I wish to thank Frank Upham and John Mendes for their valuable advice and help in constructing the electronic equipment used in this investigation.

[8] H. A. Krebs and H. L. Kornberg, op. cit., p. 234.

10. FURTHER STUDIES OF THE EFFECTS OF DEUTERIUM AND TRITIUM ON DROSOPHILA

Ann M. Hughes

(In collaboration with Philip Hildreth
Department of Biomedical Research)

In a continuation of the study of the genetic effects of D_2O on Drosophila melanogaster we have consistently found a statistically significant increase in the number of unusual progeny from D_2O-treated males over control males. In a previous Quarterly Report[1] it was suggested that part of the "D_2O effect" might be due to the relatively high tritium content of some of the D_2O stock solutions. Repeated experiments in which controlled amounts of tritium were added to the D_2O have not substantiated this hypothesis. We are therefore forced to conclude that the D_2O effect is due only to the D_2O. However, tritium alone has caused the occurrence of a mutant in two consecutive experiments.

The results of a typical D_2O experiment, in which males of the stock y/sc^8. Y. B^s were grown on 19% D_2O or H_2O media and then mated with y females grown on H_2O media, are given in Table 10-I.

Table 10-I. Effect of D_2O on the occurrence of unusual Drosophila

	Normal females	Normal males	Unusual flies per 1000
Control	7900	7228	2.12
D_2O	6128	5836	5.68

Although it seemed probable that the unusual flies were caused by crossing-over between the X and Y chromosomes in the male or by male nondisjunction, other genetic events could not be ruled out as the causative factors. Therefore, two experiments have been done with a female stock which would permit more definite identification of the cause of unusual flies. This stock is an attached XY stock, Y^s. car f v y. Y^L(Ins(1) EN, dl 49). The same male stock (y/sc^8. Y. B. ^{s}) was used as in the previous experiment. The results of these experiments substantiate our hypothesis that the unusual progeny obtained from male drosophila grown on D_2O are caused by (a) crossing-over between the X and Y chromosome, and (b) male nondisjunction.

In an experiment in which the male stock y/sc^8. Y. B^s was grown on media containing 0.1 μC H^3/g (which gives a maximum of 0.5 r/fly) and mated to females grown on normal media, two mutations producing the same phenotype were recovered independently (four mutant flies from one male and one mutant from another). These male flies had yellow bodies, B^s eyes, and wild-type wings. (Normal males of this type of mating would have had an all-wild-type body and B^s eyes.)

[1] Ann M. Hughes, in Bio-Organic Chemistry Quarterly Report, UCRL-9408, Sept. 1960, p. 5.

A replication of the experiment produced another of these mutants from the tritium-fed males. No such mutant has ever been seen in our control flies.

The mutant stock (mated to yellow females) has, at this time, bred true for several generations.

11. VARIATION IN ENVIRONMENTAL COMPLEXITY AND BRAIN MEASURES*

Edward L. Bennett, Hiromi Morimoto, and Marie Hebert

(In collaboration with Mark R. Rosenzweig, David Krech, and James F. Zolman
Department of Psychology, University of California, Berkeley)

This report is one in a series of studies investigating the effects of exposure to environmental complexity and training (ECT) upon brain biochemistry and anatomy. The data reported here replicate and extend two generalizations from previous studies reported.[1,2,3] First, there is a monotonic relation between complexity of environment and terminal cerebral measures. Second, the cerebral effects of an early period in an impoverished environment can be reversed, in part at least, by a succeeding period in an enriched environment.

Method

The subjects were eleven sets of male triplets drawn from nine litters of our S_1 strain of rats. At weaning (23 to 25 days of age), one animal of each set was assigned at random to one of the three following conditions:
(a) exposure to a complex environment for 81 days, during the latter part of which formal training in three types of mazes was given (ECT group);
(b) isolation in an individual cage for 81 days (IC group);
(c) isolation in an individual cage for 33 days, then exposure for 48 days to a complex environment including the entire program of formal training (IC-ECT group).
All animals were sacrificed on the same day (ages 103 to 105 days). The ECT and IC conditions have been described in detail in our previous reports.[1,3]

For each animal, the wet weight and cholinesterase (ChE) activity were determined for five sections into which the total brain had been dissected. From these samples we derived three increasingly inclusive cortical measures and two subcortical measures. In addition, two ratios of cortical to subcortical measures are reported. These are all measures and ratios that we have employed in previous publications. The cortical measures are

*This investigation was supported by a research grant, MY-1292, from the National Institute of Mental Health, United States Public Health Service.

[1] D. Krech, M. R. Rosenzweig, and E. L. Bennett, J. Comp. and Physiol. Psychol. 53, 509-519 (1960).

[2] D. Krech, M. R. Rosenzweig, and E. L. Bennett, Relations Between Brain Chemistry and Problem Solving Among Rats Raised in Enriched and Impoverished Environments, J. Comp. and Physiol. Psychol. (in press).

[3] M. R. Rosenzweig, D. Krech, E. L. Bennett, and M. C. Diamond, Effects of Environmental Complexity and Training on Brain Chemistry and Anatomy: a Replication and Extension, J. Comp. and Physiol. Psychol. (in press).

(a) sensory cortex, composed of the samples from the visual and somesthetic regions; (b) total dorsal cortex, composed of sensory cortex plus the remaining dorsal cortex; and (c) total cortex, composed of total dorsal cortex plus ventral cortex. The subcortical measures are (a) subcortex I, all of the brain remaining after total dorsal cortex is removed; and (b) subcortex II, all of the brain remaining after total cortex is removed. The cortical/subcortical ratios are (a) the value for sensory cortex divided by the value for subcortex I (called, as in previous papers, the CS ratio); (b) the value for total cortex divided by the value for subcortex II (called TC/SII).

The method of chemical analysis has been described in detail by Rosenzweig, Krech, and Bennett[4] and the delineation of the brain sections by Rosenzweig et al.[3] A laboratory accident during chemical analysis caused the loss of the remaining dorsal cortex of one animal and of subcortex II of another animal. The corresponding samples of littermates are therefore also eliminated from the results. This accounts for the differing N's shown in Tables 11-II and 11-III for the various brain measures.

Results

Cortical Values

The ECT group shows greater weight of cerebral cortex than the IC-ECT group, and this group in turn shows greater cortical weights than the IC group. This is true for all three cortical measures--sensory cortex, total dorsal cortex, and total cortex (see Table 11-I). In general, the intermediate group, IC-ECT, shows cortical weights about 2% less than the ECT values and about 3% more than the IC values. The data of all three groups were subjected to analyses of variance which demonstrated statistical significance at better than the .05 level for sensory cortex and total cortex and at better than the .01 level for total dorsal cortex. To determine which differences between any two groups were significant we applied Duncan's Multiple Range Test.[5] For sensory cortex, the ECT group differed from the IC group at better than the .05 level of confidence; the intermediate IC-ECT group did not differ significantly from the others. For total dorsal cortex, the ECT and IC groups differed at better than the .01 level; the IC-ECT differed from the ECT group at better than the .05 level but did not differ significantly from the IC group. For total cortex, the extreme groups again differed at better than the .01 level; the intermediate IC-ECT group differed from the IC group at better than the .05 level but did not differ significantly from the ECT group.

The results for total activity of ChE conform in general with those observed for cortical weight. Seven of the nine differences between groups are in the expected direction--i.e., with ECT the greatest, IC-ECT intermediate, and IC the least (see Table 11-II). For sensory cortex, all three

[4] K. R. Rosenzweig, D. Krech, and E. L. Bennett, Brain Enzymes and Adaptive Behaviour, in Ciba Foundation Symposium on the Neurological Basis of Behaviour, 1958, London (J. & A. Churchill, London, 1958) 337-355.

[5] A. L. Edwards, Experimental Design in Psychological Research (Rinehart & Company, Inc., New York 1960), p. 137-138.

Table 11-I. Weights of brain sections.

	Mean weights (mg)						Cortical-to-subcortical ratios	
Group	Sensory cortex (V+S)	Total dorsal cortex	Total cortex	Sub-cortex I	Sub-cortex II	Total brain	CS ratio	TC/SII
ECT	100.0	410.9	682.3	1242.7	971.3	1653.6	0.0806	0.703
IC-ECT	98.8	394.6	672.4	1261.4	983.7	1656.1	0.0786	0.683
IC	95.5	385.0	644.9	1252.3	992.4	1637.3	0.0763	0.650
P	< 0.05	< 0.01	< 0.05	N. S.	N. S.	N. S.	N. S.	<0.001
N	11	11	11	11	11	11	11	11

Table 11-II. Total activity of cholinesterase of brain sections.

	Acetylcholine hydrolyzed per minute (10^{-8} mole)						Cortical-to-subcortical ratios	
Group	Sensory cortex (V+S)	Total dorsal cortex	Total cortex	Sub-cortex I	Sub-cortex II	Total brain	CS ratio	TC/SII
ECT	64.4	294.2	629.9	2150.4	1810.9	2436.5	0.0299	0.3479
IC-ECT	63.9	284.8	631.5	2163.9	1819.6	2439.9	0.0297	0.3471
IC	63.4	284.9	614.0	2111.2	1781.1	2400.6	0.0302	0.3428
N	11	10	10	10	10	10	10	9

Table 11-III. Specific activity of cholinesterase of brain sections.

	Acetylcholine hydrolyzed per minute per mg tissue (10^{-10} mole)						Cortical-to-subcortical ratios	
Group	Sensory cortex (V+S)	Total dorsal cortex	Total cortex	Sub-cortex I	Sub-cortex II	Total brain	CS ratio ($\times 10^2$)	TS/SII ($\times 10^2$)
ECT	64.9	72.0	93.0	173.7	187.2	148.9	37.3	49.4
IC-ECT	65.0	72.8	94.9	172.1	185.2	148.9	38.0	51.2
IC	66.7	73.6	95.5	168.6	179.1	146.8	39.7	53.0
N	11	10	10	10	10	10	10	9

values are in the expected order. For total dorsal cortex there is one inversion, the IC value being slightly larger than the IC-ECT value; and for total cortex, there is one inversion, the IC-ECT value being greater than the ECT value. The differences in total ChE activity tend to be smaller than those for weight and are not statistically significant.

The values for specific activity of ChE (i.e., activity per unit of tissue weight) show inverse monotonic relations with environmental complexity for all three cortical measures; in each case the ECT value is the lowest and the IC value is the highest, but the differences are not statistically significant. In our first report of this series[1] we observed that specific acitvity of ChE in the cortex was significantly lower in the ECT than in the IC animals. In the second report[3] we replicated this significant relation and we also found that environmental complexity led to a greater increase in cortical weight than in total activity of ChE in the cortex. We suggested there that the fall in specific activity with ECT was a consequence of the differential rates of increase of weight and total enzymic activity in the cortex. In this experiment, comparing Tables 11-I and 11-II, we again see that for each of the three cortical measures, environmental complexity is followed by greater increases in cortical weight than in total activity of ChE in the cortex.

Subcortical Values

In general, the two subcortical measures yield similar results (which should be expected, since subcortex II makes up about four-fifths of subcortex I). As we have observed consistently in our previous studies on effects of environmental complexity, we again find the weight of the subcortex to be slightly lower in the ECT than in the IC animals (Table 11-I). While in no experiment have we found this decrease to be significant, the consistency with which it appears suggests that this subcortical effect may be a real one.

Again, as we have reported previously, total activity of ChE in the subcortex is greater in the ECT than in the IC animals. The IC-ECT group shows an inversion here; its total activity is slightly greater than that of the ECT group (Table 11-II).

Specific activity of ChE decreases regularly from the ECT, through the IC-ECT, to the IC value, but the differences are not significant (Table 11-III).

Thus, the effects of enriched environment on tissue weight and on specific activity of ChE are opposite for cortical and subcortical measures; e.g., with ECT, weight of the cortex goes up and weight of the subcortex goes down.

Cortical/Subcortical Ratios

The opposed cortical and subcortical effects can be combined into a single index value by using a cortical/subcortical ratio. The two ratios used in previous reports are given in Tables 11-I, 11-II, and 11-III as CS (Sensory Cortex/Subcortex I) and TC/SII (Total Cortex/Subcortex II).

For tissue weight, each ratio shows a monotonic relation increasing from IC through ECT (Table 11-I). Although this effect does not reach statistical significance for the CS ratio, it is significant at better than the 0.001 level for TC/SII, as tested by an analysis of variance. The Multiple Range Test reveals that for TC/SII the ECT and the IC-ECT groups do not differ significantly from each other, but each of them differs at better than the 0.01 level from the IC group.

For total activity of ChE, neither ratio yields a significant effect (Table 11-II).

For specific activity of ChE, each ratio again shows a monotonic relation, this time decreasing from IC through ECT (Table 11-III). Differences among groups on the CS ratio are significant at better than the 0.001 level, but those for TC/SII do not attain statistical significance. For the CS ratio, the ECT and IC-ECT groups do not differ significantly, but each differs at better than the 0.01 level from the IC group.

Total Brain

Consistent with our previous reports, the values for total brain in Tables 11-I, 11-II, and 11-III do not differ significantly among the three experimental groups. Thus the opposed changes that we have observed in the cortex and the subcortex tend to cancel each other out when undifferentiated total brain measures are used. As McIlwain has pointed out, "A major limitation in present knowledge of metabolic events in the brain is that the majority of biochemical investigations have been carried out with the organ as a whole or with preparations from relatively large portions of it."[6] The same need for differentiation of the brain occurs in studies relating behavior to cerebral measures.

Conclusions

Animals first subjected to isolation for 33 days after weaning and then immersed for 48 days in an enriched environment (the IC-ECT group) were compared with littermates which were kept in isolation for 81 days (the IC group) and with littermates maintained in the enriched environment for 81 days (the ECT group). The total experience of the IC-ECT group was thus considered to be intermediate in complexity between those of the IC and ECT groups. For cortex and subcortex, measures were taken of tissue weight, total activity of cholinesterase (ChE), and specific activity of ChE. The group with intermediate experience (IC-ECT) was found in general to have intermediate values on the cerebral measures.

[6] H. McIlwain, Brain Metabolism and Activity, Brit. med. Bull. 1950, No. 6, 301-3.

These results support and extend two conclusions from our previous reports:

a. In a previous experiment in which an intermediate group was maintained throughout under "social control" conditions and in which only specific activity of ChE was analyzed, we found "a statistically significant monotonic relationship with environmental complexity." [1] The experiment described here replicates this result and extends it by demonstrating a similar significant monotonic effect of environmental complexity on the cortical-subcortical ratio of tissue weights.

b. Zolman and Morimoto[7] and Krech et al.[2] have indicated that the effects of an early period of isolation on specific activity of ChE could be compensated by later exposure to a complex environment or to intensive training. The design of those experiments did not, however, permit comparison of the IC-ECT group with both an IC and an ECT group. Comparison of the results of the three groups in the present experiment gives fuller support for our earlier suggestion and extends it to the cortical-subcortical ratio of tissue weights.

[7] J. F. Zolman and H. Morimoto, Effects of Age of Training on Cholinesterase Activity in the Brains of Maze-Bright Rats, J. Comp. and Physiol. Psychol (in press).

Information Division
sa

This report was prepared as an account of Government sponsored work. Neither the United States, nor the Commission, nor any person acting on behalf of the Commission:

A. Makes any warranty or representation, expressed or implied, with respect to the accuracy, completeness, or usefulness of the information contained in this report, or that the use of any information, apparatus, method, or process disclosed in this report may not infringe privately owned rights; or

B. Assumes any liabilities with respect to the use of, or for damages resulting from the use of any information, apparatus, method, or process disclosed in this report.

As used in the above, "person acting on behalf of the Commission" includes any employee or contractor of the Commission, or employee of such contractor, to the extent that such employee or contractor of the Commission, or employee of such contractor prepares, disseminates, or provides access to, any information pursuant to his employment or contract with the Commission, or his employment with such contractor.